OPTIMIZATION OF GREEN DERIVED SILVER NANOPARTICLES AND ANTIMICROBIAL EFFECT ON *Escherichia coli* AND *Pseudomonas aeruginosa*

BY
EKAJI FRANKLIN ANGBOJI
REG. NO: 20154941188

A THESIS SUBMITTED TO THE POSTGRADUATE SCHOOL, FEDERAL UNIVERSITY OF TECHNOLOGY, OWERRI, IMO STATE, NIGERIA

IN PARTIAL FULFILMENT OF THE REQUIREMENTS FOR THE AWARD OF MASTER OF SCIENCE (M.Sc.) DEGREE IN MEDICAL MICROBIOLOGY.

MAY, 2021

CERTIFICATION

This is to certify that this study of OPTIMIZATION OF GREEN DERIVED SILVER NANOPARTICLES AND ANTIMICROBIAL EFFECT ON *Escherichia coli* and *Pseudomonas aeruginosa written* by Ekaji Franklin Angboji was formally approved as Postgraduate project from Department of Microbiology, Federal University of Technology, Owerri, Imo State.

Dr. Campbel Akujobi (Supervisor)	27/06/2021 Date
Dr. (Mrs) S. I. Umeh (Co-Supervisor)	28/06/2021 Date
Prof. C. E. Nwanyanwu (HOD, Microbiology)	19/08/2021 Date
Prof. F.O.U. Osuala (Dean of Biological Science)	25/05/21 Date
Prof. C. C. EZE (Dean of Postgraduate)	Date
Prof. D. Arutopin (External Examiner)	19/05/2021 Date

DEDICATION

This thesis work is dedicated to God Almighty for his love, protection and guidance.

ACKNOWLEDGEMENT

I am very grateful to God Almighty for his marvellous deeds towards me.

My profound gratitude goes to my Head of Department Prof. C. Nwayanwu, my supervisor Dr. C. O Akujobi, Dr. Mrs. S. I. Umeh.Also I appreciate the succinct contribution of my Lecturers Prof Braide Wesley, Dr. Adieze, Mr Henry Anuforo of BTC for their guidance which led to a successful completion of this work, despite his tight schedule made out time to follow up my progress step by step during my research work in the laboratory, and to Prof. W. Brade for his professional counsel.

My deepest appreciation goes to my lovely wife Mrs. Grace Franklin for her moral support, her unending commitment to my progress and also to my son Master Franklin Jnr for his prayers and understanding, my daughter Felista Franklin for her sacrifices, I love you all. I also appreciate the contribution of Mrs Lilian Ndubuisi for painstakingly typesetting this work.

May God bless you all.

TABLE OF CONTENTS

LIST OF TABLES

LIST OF FIGURES

ABSTRACT

Nanoparticles can be synthesized using various approaches including chemical, physical, and biological. Chemicals used for nanoparticles synthesis and stabilization are toxic and lead to generation of non-ecofriendly by-products. The need for environmental non-toxic synthetic protocols for nanoparticles synthesis leads to increasing demand for green nanotechnology. The major advantage of using plant extracts for silver nanoparticle synthesis is that they are available, safe, and non-toxic. The leaves of ten (10) selected plants were washed several times with distilled water to remove the dust particles and air-dried to remove the residual moisture. The dried leaves were crushed using mechanical method and 10 gram of dried powder boiled in 100 ml of deionized water for 20 minutes. The aqueous extracts were separated by filtration with Whatman No. 1 filter paper and centrifuged at 1200 rpm for 5 minutes to remove heavy biomaterials. The extract were stored at 4°C until further use. The biochemical screening and identification of the isolates in the stock culture from the extract were carried out according to microbiological guidelines and standards. The colour change of the solution from yellow to dark green was indicative of the reduction process silver ion to silver-nanoparticles. The Box-benken design was adopted for the optimization of the silver nanoparticle production in a 3 x 3 design. Also, extracellular synthesis of silver nanoparticles from green plant was carried out to determine nanoparticle production. Synthesized silver nanoparticles were scanned by Ultra violet visible ray is spectrophotometer at the wavelength of 340 – 820 nm. Antibacterial effect was determined *invitro* using Kirby-Bauer method. The optimal conditions for the production of goatweed nanoparticle (GwNP) were (pH 8.0, temperature 35^0C and Time of 24 hours) which was different from the optimum conditions for Independence leaf (XXYNP) production at pH 8.0, temperature of 35 degree celsius and a time of 72 hours. Similar effects were observed in the experiment with all the samples. The antimicrobial activities of these samples demonstrated that the nanoparticles had antimicrobial properties which vary depending on the isolate and condition (temperature, pH and time).

Keywords: Antimicrobial, Extracellular, Nanoparticles, Spectrophotometer, Biomaterials.

CHAPTER ONE

1.0 INTRODUCTION

1.1 Overview of the Study

Materials in the nano dimensions (1-100 nm) have remarkable difference in the properties compared to the same material in the bulk. These differences lie in the physical and structural properties of atoms, molecules and bulk materials of the element due to difference in physiochemical properties and surface to volume ratio (Abhishek *et al*., 2013). Due to swift industrialization and urbanization, our environment is undergoing huge smash up and a large amount of perilous and superfluous chemical, gases or substances are released into the environment. There is need to learn about the secrets that are present in the nature and its products which leads to the growth of advancements in the synthesis processes of nanoparticles. Nanotechnology applications are highly suitable for biological molecules, because of their exclusive properties (Abhishek *et al*., 2013). The biological molecules undergo highly controlled assembly for making them suitable for the metal nanoparticle synthesis which was found to be reliable and eco-friendly (Harekrishna *et al*., 2009).

As a matter of fact with advancement in nanotechnology, a large number of nanomaterials are appearing with unique properties, opening spectrum of applications and research opportunities (Sharma *et al*., 2009). About 5000 years ago, many Greeks, Romans, Persians and Egyptians used silver in one form or other to store food products (Srikar et al., 2016). Use of silver ware during ancient period by various dynasties was common across the globe utensils for drinking and eating and storing various drinkable and eatable items probably due to the knowledge of antimicrobial action (Srikar et al., 2016). There are records regarding therapeutic application of silver in literature as earlier as 300 BC. In the Hindu religion, till date silver utensils are

preferred for the “panchamrit” preparation using curd, *Ocimum sanctum* and other ingredients (Srikar et al., 2016). The therapeutic potentials of various metals are mentioned in ancient Indian ‘Aurvedic’ medicine book medicinal literature named “Charak Samhita” (Duran *et al*., 2011). Until the discovery of antibiotics by Alexzander Flemming, silver was commonly used as antimicrobial agent (Srikar et al., 2016). In the recent past, silver nano particles (AgNPs) have received enormous attention of the researchers due to their extraordinary defence against wide range of microorganisms and also due to the appearance of drug resistance against commonly used antibiotics (Sharma *et al*., 2009). The exceptional characteristics of AgNPs have made them applicable in various fields like biomedical, drug delivery, water treatment, agricultural and so on (Catauro *et al*., 2005). Silver nanoparticles are applied in inks, adhesives, electronic devises, pastes and so on due to high conductivity (Kaviya & Viswanathan, 2011). Silver nanoparticles have been synthesized by physio-chemical techniques such as chemical reduction, gamma ray radiation, micro emulsion, electrochemical method, laser ablation, autoclave, microwave and photochemical reduction. These methods have effective yield, but they are associated with the limitations like use of toxic chemicals and high operational cost and energy needs (Srikar et al., 2016). Considering the drawbacks of physio-chemical methods, cost-effective and energy efficient new alternative for Silver nanoparticles synthesis using microorganisms (Sharma *et al*., 2009), plant extracts ((Morones *et al*., 2005a) and natural polymers as reducing and capping agents are emerging very fast. The association of nanotechnology and green chemistry will unfold the range of biologically and cytologically compatible metallic nanoparticles (Mohamed, 2010).

Nanoparticles can be synthesized using various approaches including chemical, physical, and biological. Although chemical method of synthesis requires short period of time for synthesis

of large quantity of nanoparticles, this method requires capping agents for size stabilization of the nanoparticles. Chemicals used for nanoparticles synthesis and stabilization are toxic and lead to non-eco-friendly by-products. The need for environmental non-toxic synthetic protocols for nanoparticles synthesis leads to developing interest in biological approaches which are free from the use of toxic chemicals as by-products. Thus, there is an increasing demand for green nanotechnology (Garima *et al*., 2011). Many biological approaches for both extracellular and intracellular nanoparticles synthesis have been reported till date using microorganisms including bacteria, fungi and plants (Mukherjee *et al*., 2001).

1.2 Statement of problem

Antibacterial resistance is a global concern and the quest to combat these phenomenon of great feat is still ongoing (Roe *et al*., 2008). Nanoparticles have been found to be promising in combating antimicrobial resistance (Gupter, 2003). However, most industrially applied nanoparticles are synthesized by chemical methods. The chemical reduction method is widely used to synthesize AgNP because AgNP could be synthesized under a mild as well as on a large scale (Roe *et al*., 2008). However, the use of environmentally benign materials like plant leaf extracts and fungi for the synthesis of silver nanoparticles is more acceptable as they offer several benefits over chemical methods like conditions of high temperature, pressure, and toxic chemicals which are not required in the synthesis protocol (Zewede *et al*., 2016). Therefore, preparation of AgNP by a green synthesis approach and its optimization has compatibility for pharmaceutical and biomedical applications. Plant extracts (Antagonistic) in combination with silver nitrate, to form nanoparticles can be a lifeline and a broad spectrum antimicrobial (Zewede *et al*., 2016). Despite this fact, optimization studies for the production of these important

metabolites are limiting. As a result, in this thesis, Goatweed, Ugwu leaf, Bitter leaf, Neem leaf, Uziza leaf, Sweet Potato leaf, Comelina leaf, Cassava leaf, Moringa leaf and an Independence leaf (*Chromolaena odorata*) were used as bio-machineries for the synthesis of silver nanoparticles. The production of the nanoparticles were optimized using Response Surface (RS) modelling.

1.3 Aim of the project

The aim of this project is to optimize the production of silver nanoparticle (AgNPs) using ten plants.

1.4 Objectives of the project

The objectives of this work are:

a) To produce silver nanoparticles of green origin using ten plants.
b) To determine the effects of pH, temperature and time on the product of AgNPs to identify the optimum AgNPs production condition.
c) To test the activity of the optimized product on two bacteria isolates.

CHAPTER TWO

2.0 LITERATURE REVIEW

2.1 Nanotechnology

Nanotechnology has overtime proved to be an important field of modern research dealing with design, synthesis, and manipulation of particles structure ranging from approximately 1-100 nm in one dimension. Remarkable growth in this up-and-coming technology has opened novel fundamental and applied frontiers, including the synthesis of nanoscale materials and exploration or utilization of their exotic physicochemical and optoelectronic properties that has hitherto seemed non-approachable. Nanotechnology is rapidly gaining importance in a number of areas which include health care, cosmetics, food and feed, environmental health, mechanics, optics, biomedical sciences, chemical industries, electronics, space industries, drug-gene delivery, energy science, optoelectronics, catalysis, reorograpHy, single electron transistors, light emitters, nonlinear optical devices, and photoelectrochemical applications (Colvin and Alivisatos, 1994). Nanomaterials are seen as probably the best solution to many technological and environmental challenges in the field of solar energy conversion, catalysis, medicine, microbial optimization and water treatment. In the context of global efforts to reduce hazardous waste, the continuously increasing demand of nanomaterials must be accompanied by green synthesis methods.

Nanotechnology is fundamentally changing the way in which materials are synthesized and devices are produced. Incorporation of nanoscale building blocks into functional assemblies and further into multifunctional devices can be achieved through a “bottom-up approach”. Research on the synthesis of nanosized material is of great interest because of their unique properties like optoelectronic, magnetic, and mechanical, which differs from bulk (Atul *et al*., 2010).

2.2 Nanoparticles

The term “nanoparticles” is used to describe a particle with size in the range of 1nm-100nm, at least in one of the three possible dimensions. In this size range, the physical, chemical and biological properties of the nanoparticles changes in fundamental ways from the properties of both individual atoms/molecules and of the corresponding bulk materials. Nanoparticles can be made of materials of diverse chemical nature, the most common being metals, metal oxides, silicates, non-oxide ceramics, polymers, organics, carbon and biomolecules. Nanoparticles exist in several different morphologies such as spheres, cylinders, platelets, tubes etc. Generally the nanoparticles are designed with surface modifications tailored to meet the needs of specific applications they are going to be used for. The enormous diversity of the nanoparticles (Figure. 2.1) arising from their wide chemical nature, shape and morphologies, the medium in which the particles are present, the state of dispersion of the particles and most importantly, the numerous possible surface modifications the nanoparticles can be subjected to make this an important active field of science now-a-days.

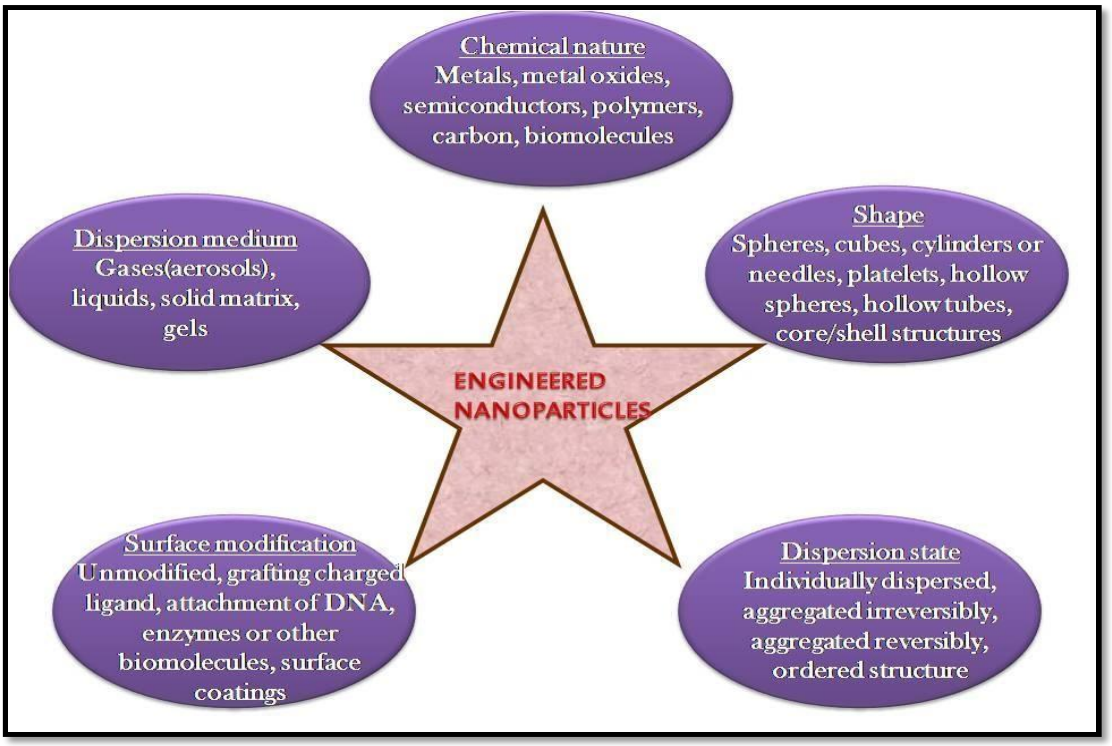

Figure. 2.1: Various features contributing to the diversity of engineered nanoparticles. The same chemical can generate a wide variety of nanoparticles.

Source: Atul *et al.*, 2010.

2.3 Types of Nanoparticles

There are two known groups of nanoparticles namely; organic nanoparticles comprising of carbon nanoparticles (fullerenes) and the inorganic nanoparticles which include magnetic nanoparticles, noble metal nanoparticles (like gold and silver) and semiconductor nanoparticles (like titanium oxide and zinc oxide). The interest in inorganic nanoparticles is growing rapidly i.e. of noble metal nanoparticles (Gold and silver) as they provide superior material properties with functional versatility. Due to their size features and advantages over available chemical imaging drug agents and drugs, inorganic particles have been examined as potential tools for medical imaging as well as for treating diseases. Inorganic nonmaterial have been widely used for cellular delivery due to their versatile features like wide availability, rich functionality, good compatibility, and capability of targeted drug delivery and controlled release of drugs (Xu *et al*., 2006).

2.4 Gold Nanoparticles

With the advances in various analytical technologies in the 20th century, studies on gold nanoparticles have accelerated. Advanced microscopy methods, such as atomic force microscopy and electron microscopy, have contributed the most to nanoparticle research. Due to their comparably easy synthesis and high stability, various old particles have been studied for their practical uses. Different types of gold nanoparticles are already used in many industries, such as medicine and electronics. For example, several FDA-approved gold nanoparticles are currently used in drug delivery (Hurst, 2011).

2.5 Silver Nanoparticles

the unique properties of silver nanoparticles (e.g., size and shape depending optical, electrical, and magnetic properties) which can be incorporated into antimicrobial applications, biosensor materials, composite fibres, cryogenic superconducting materials, cosmetic products, and electronic components make them an area of interest. Physical and chemical methods have been used for synthesizing and stabilizing silver nanoparticles (Senapati, 2005). Popular chemical approaches, including chemical reduction using a variety of organic and inorganic reducing agents, electrochemical techniques, physicochemical reduction, and radiolysis are widely used for the synthesis of silver nanoparticles. Lately, nanoparticle synthesis is among the most interesting scientific areas of inquiry, and there are growing attention to produce nanoparticles using environmentally friendly methods (green chemistry). Green synthesis approaches include mixed-valence polyoxometalates, polysaccharides, Tollens, biological, and irradiation method which have advantages over conventional methods involving chemical agents associated with environmental toxicity.

2.6 Synthesis of Nanoparticles

In the synthesis of nanoparticles, three approaches are mainly employed. These approaches include: chemical, physical and biological methods.

2.6.1 Chemical Methods

Of all the available nanoparticle synthesis methods, the most common approach for synthesis of silver nanoparticles is chemical reduction by organic and inorganic reducing agents. Generally, various reducing agents such as sodium citrate, ascorbate, sodium borohydride

($NaBH_4$), elemental hydrogen, polyol process, Tollens reagent, N, N-dimethylformamide (DMF), and poly (ethylene glycol) block copolymers are used for reduction of silver ions (Ag^+) in aqueous or non-aqueous solutions. The aforementioned reducing agents reduce silver ions (Ag^+) and lead to the formation of metallic silver (Ag), which is followed by agglomeration into oligomeric clusters. These clusters eventually lead to formation of metallic colloidal silver particles. It is important to use protective agents to stabilize dispersive nanoparticles during the course of metal nanoparticle preparation, and protect the nanoparticles that can be absorbed on or bind onto nanoparticle surfaces, avoiding their agglomeration (Oliveira *et al*., 2005). The presence of surfactants comprising functionalities (e.g., thiols, amines, acids, and alcohols) for interactions with particle surfaces can stabilize particle growth, and protect particles from sedimentation, agglomeration, or losing their surface properties. A simple one-step process, Tollens method, has also been used for the synthesis of silver nanoparticles with a controlled size. In the modified Tollens procedure, silver ions are reduced by saccharides in the presence of ammonia, yielding silver nanoparticle films (50-20 nm), silver hydrosols (20-50 nm) and silver nanoparticles of different shapes (Yin *et al*., 2002).

2.6.2 Physical Method

Physical approaches include evaporation-condensation and laser ablation. Various metal nanoparticles such as silver, gold, lead sulphide, cadmium sulphide, and fullerene have previously been synthesized using the evaporation-condensation method. The advantages of physical approaches in comparison with chemical processes include the absence of solvent contamination in the prepared thin films and the uniformity of nanoparticles distribution. Also, silver nanoparticles could be synthesized via a small ceramic heater with a local

heating source (Jung *et al*., 2006). The evaporated vapour can cool at a suitable rapid rate, because the temperature gradient in the vicinity of the heater surface is very steep in comparison with that of a tube furnace. This makes possible the formation of small nanoparticles in high concentration. This physical method can be useful as a nanoparticle generator for long-term experiments for inhalation toxicity studies, and as a calibration device for nanoparticle measurement equipment (Jung *et al*., 2006). Silver nanoparticles could be synthesized by laser ablation of metallic bulk materials in solution. The ablation efficiency and the characteristics of produced nanosilver particles depend upon many factors such as the wavelength of the laser impinging the metallic target, the duration of the laser pulses (in the femto-, pico- and nanosecond regime), the laser influence the ablation time duration and the effective liquid medium, with or without the presence of surfactants. One important advantage of laser ablation technique compared to other methods for production of metal colloids is the absence of chemical reagents in solutions. Therefore, pure and uncontaminated metal colloids for further applications can be prepared by this technique (Tsuji *et al*., 2002).

2.6.3 Biological Methods

The development of efficient green chemistry methods employing natural reducing, capping, and stabilizing agents to prepare silver nanoparticles with desired morphology and size have become a major focus of researchers. Biological methods can be used to synthesize silver nanoparticles without the use of any harsh, toxic and expensive chemical substances . The bioreduction of metal ions by combinations of biomolecules found in the extracts of certain organisms (*e.g.*, enzymes/proteins, amino acids, polysaccharides, and vitamins) is environmentally benign, yet chemically complex. Many

studies have reported successful synthesis of silver nanoparticle using organisms (microorganisms and biological systems) (Hurst, 2011).

2.7 Synthesis of Nanoparticles From Plants

The major advantage of using plant extracts for silver nanoparticle synthesis is that they are easily available, safe, and nontoxic. In most cases, they have a broad variety of metabolites that can aid in the reduction of silver ions, and are quicker than microbes in nanoparticles synthesis. The mechanism employed for this process is the plant-assisted reduction due to phytochemicals. The major phytochemicals involved are terpenoids, flavones, ketones, aldehydes, amides, and carboxylic acids. Flavones, organic acids, and quinones are water-soluble phytochemicals that are responsible for the immediate reduction of the ions. Studies have revealed that xerophytes contain emodin, an anthraquinone that undergoes tautomerization, leading to the formation of the silver nanoparticles. In the case of mesopHytes, it was found that they contain three types of benzoquinones: cyperoquinone, dietchequinone, and remirin. It was suggested that the phytochemicals are involved directly in the reduction of the ions and formation of silver nanoparticles (Jha *et al*., 2009).

2.8 Synthesis of Nanoparticles from Microorganisms

Microorganisms have shown that they can synthesize nanoparticles as discussed below:

2.8.1 Bacterial Synthesis of Silver Nanoparticles

The first evidence of bacteria synthesizing silver nanoparticles was established using the *Pseudomonas stutzeri* AG259 strain that was isolated from silver mine. There are some microorganisms that can survive metal ion concentrations and can also grow under those

conditions, and this phenomenon is due to their resistance to that metal. The mechanisms involved in the resistance are efflux systems, alteration of solubility and toxicity via reduction or oxidation, biosorption, bioaccumulation, extracellular complex formation or precipitation of metals, and lack of specific metal transport systems (Husseiny *et al.*, 2006). There is also another aspect that though these organisms can grow at lower concentrations, their exposure to higher concentrations of metal ions can induce toxicity.

The most widely accepted mechanism of silver biosynthesis is the presence of the nitrate reductase enzyme. The enzyme converts nitrate into nitrite. In in-vitro synthesis of silver using bacteria, the presence of alpha-nicotinamide adenine dinucleotide phosphate reduced form (NADPH)- dependent nitrate reductase would remove the downstream processing step that is required in other cases (Vaidyanathan *et al*., 2011).

2.8.2 Fungal Synthesis of Silver Nanoparticles

When in comparison with bacteria, fungi can produce larger amounts of nanoparticles because they can secrete larger amounts of proteins which directly translate to higher productivity of nanoparticles. The mechanism of silver nanoparticle production by fungi is achieved through the following steps: trapping of Ag^{+} ions at the surface of the fungal cells and the subsequent reduction of the silver ions by the enzymes present in the fungal system. The extracellular enzymes like naphthoquinones and anthraquinones are said to facilitate the reduction. Considering the example of *F. oxysporum*, it is believed that the NADPH-dependent nitrate reductase and a shuttle quinine extracellular process are responsible for nanoparticle formation (Ahmad *et al*., 2003). Though the exact mechanism involved in silver nanoparticle production by fungi is not fully deciphered, it is believed that the above mentioned phenomenon is responsible for the process. A major drawback of

using microbes to synthesize silver nanoparticles is that it is a very slow process when in comparison with plant extracts. Hence, the use of plant extracts to synthesize silver nanoparticles becomes an option that is feasible.

2.9 Green Synthesis of Nanoparticles

The need for biosynthesis of nanoparticles rose as the physical and chemical processes were costly. Biosynthesis of nanoparticles is a kind of bottom up approach where the main reaction occurring is reduction/oxidation. Often, chemical synthesis method leads to presence of some of the toxic chemical absorbed on the surface that may have adverse effect in the medical applications (Parashar and Sharmah, 2009). This is not an issue when it comes to biosynthesized nanoparticles via green synthesis route. So, in the search of cheaper pathways for nanoparticles synthesis, scientist used microbial enzymes and plant extracts (phytochemicals). With their antioxidant or reducing properties they are usually responsible for the reduction of metal compounds into their respective nanoparticles. Green synthesis provides advancement over chemical and physical method as it is cost effective, environment friendly, easily scaled up for large scale synthesis and in this method there is no need to use high pressure, energy, temperature and toxic chemicals (Parashar and Sharmah, 2009).

2.10 Concept of Nanosilver

Silver is one of the substances used in nano-formulation (nanosilver). Due to its antimicrobial properties, silver has also been incorporated into filters during the purification drinking water and clean swimming pool water. To generate nanosilver, metallic silver has been engineered into ultrafine particles by several methods; include spark discharging,

electrochemical reduction, solution irradiation and cryo-chemical synthesis (Ju-Nam and Lead, 2008). Nanosilver particles are mostly smaller than 100 nm and consist of about 20-15,000 silver atoms (Ju-Nam and Lead, 2008). In addition, nanostructures can be produced as tubes, wires, multifactes or films. At the nano-level, the silver particles exhibit deviating physico-chemical properties (like pH dependent partitioning to solid and dissolved particulate matters) and biological activities compared with the regular metal. This is due to the higher surface area per mass, allowing a larger amount of atoms to interact with their surroundings. Due to the properties of silver at the nanoscale, nanosilver is nowadays used in an increasing number of consumer and medical products. Because, silver is a soft white lustrous element, an important use of silver nanoparticles is to give a products a silver finish. Still, the remarkably strong antimicrobial activity is the major direction for development of nano-silver products. Examples are food packaging materials and food supplements, odour-resistant textiles, electronics, household appliances, cosmetics and medical advices, water disinfectants and room sprays.

2.10.1 Quality Advantage of Silver

Silver is one of the basic element that makes up our planet. It is a rare, but naturally occurring element, slightly harder than gold and very ductile and malleable. Pure silver has the highest electrical and thermal conductivity of all metals and has the lowest contact resistance. Silver is present in four different oxidation states: Ag^0, Ag^{1+}, Ag^{2+}, Ag^{3+}. The former two are the most abundant ones, the latter are unstable in the aquatic environment (Ramya and Sylvia, 2012). Metallic silver itself is insoluble in water, but metallic salts such as $AgNO_3$ and Silver chloride are soluble in water. Metallic silver is used for the surgical prosthesis and splints, fungicides and coinage. Soluble silver

compounds such as silver slats, have been used in treating mental illness, epilepsy, nicotine addition, gastroenteritis and infectious diseases including syphilis and gonorrhoea (Ramya and Sylvia, 2012). Although acute toxicity of silver in the environment is dependent on the availability of free silver ions, investigations have shown that these concentrations of Ag+ ions are too low to lead toxicity. Metallic silver appears to pose minimal risk to health, whereas soluble silver compounds are more readily absorbed and have the potential to produce adverse effects. The wide variety of uses of silver allows exposure through various routes of entry into the body. Ingestion is the primary route for entry for silver compounds and colloidal silver proteins. Dietary intake of silver is estimated at 7090μg/day. Since silver in any form is not thought to be toxic to the immune , cardiovascular, nervous or reproductive system and it is not considered to be carcinogenic, therefore silver is relatively non-toxic. Silver demand will likely to rise as silver find new uses, particularly in textiles, plastics and medical industries, changing the pattern of silver emission as these technologies and products diffuse through the global economy (Ramya and Sylvia, 2012).

2.10.2 Antimicrobial Characteristics of Silver Nanoparticles

The exact mechanism which silver nanoparticles employ to cause antimicrobial effect is not clearly known and is a debated topic. There are however various theories on the action of silver nanoparticles on microbes to cause the microbicidal effect. Silver nanoparticles have the ability to anchor to the bacterial cell wall and subsequently penetrate it, thereby causing structural changes in the cell membrane like the permeability of the cell membrane and death of the cell. There is formation of “pits” on the cell surface, and there is accumulation of the nanoparticles on the cell surface (Sondi and

Salopek-Sondi, 2004). The formation of free radicals by the silver nanoparticles may be considered to be another mechanism by which the cells die. There have been electron spin resonance spectroscopy studies that suggested that there is formation of free radicals by the silver nanoparticles when in contact with the bacteria, and these free radicals have the ability to damage the cell membrane and make it porous which can ultimately lead to cell death. It has also been proposed that there can be release of silver ions by the nanoparticles, and these ions can interact with the thiol groups of many vital enzymes and inactivate them. The bacterial cells in contact with silver take in silver ions, which inhibit several functions in the cell and damage the cells. Then, there is the generation of reactive oxygen species, which are produced possibly through the inhibition of a respiratory enzyme by silver ions and attack the cell itself. Silver is a soft acid, and there is a natural tendency of an acid to react with a base, in this case, a soft acid to react with a soft base . The cells are majorly made up of sulphur and phosphorus which are soft bases. The action of these nanoparticles on the cell can cause the reaction to take place and subsequently lead to cell death. Another fact is that the DNA has sulphur and phosphorus as its major components; the nanoparticles can act on these soft bases and destroy the DNA which would definitely lead to cell death (Morones *et al*., 2005b). The interaction of the silver nanoparticles with the sulphur and phosphorus of the DNA can lead to problems in the DNA replication of the bacteria and thus terminate the microbes. It has also been found that the nanoparticles can modulate the signal transduction in bacteria. It is a well-established fact that phosphorylation of protein substrates in bacteria influences bacterial signal transduction. Dephosphorylation is noted only in the tyrosine residues of gram-negative bacteria. The phosphotyrosine profile of

bacterial peptides is altered by the nanoparticles. It was found that the nanoparticles dephosphorylate the peptide substrates on tyrosine residues, which leads to signal transduction inhibition and thus the stoppage of growth. It is however necessary to understand that further research is required on the topic to thoroughly establish the claims. (Figure 2.2).

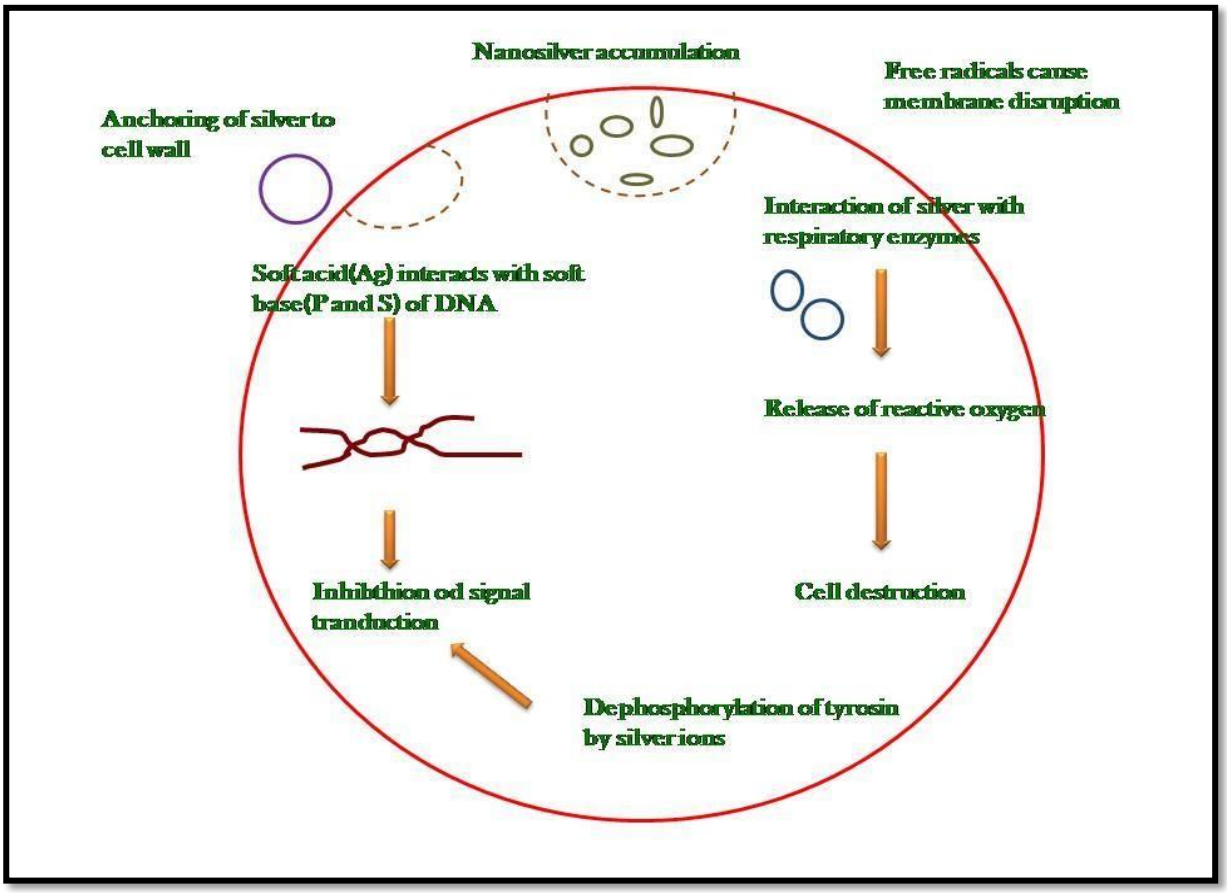

Figure 2.2. Various modes of action of silver nanoparticles on bacteria.
Source: Atul *et al.*, 2010

2.11 Applications of Silver Nanoparticles

Nanoparticles are of great interest due to their extremely small size and large surface to volume ratio, which lead to both chemical and physical differences in their properties compared to bulk of the same chemical composition, such as mechanical, biological and stearic properties, catalytic activity, thermal and electrical conductivity, optical absorption and melting point (Lee *et al*., 2008). Therefore, designing and production of materials with novel applications can be resulted by controlling shape and size at nanometer scale. Nanoparticles exhibit size and shape-dependent properties which are of interest for applications ranging from biosensing and catalysts to optics, antimicrobial activity, computer transistors, electrometers, chemical sensors, and wireless electronic logic and memory schemes. These particles also have many applications in different fields such as medical imaging, nano-composites, filters, drug delivery, and hyperthermia of tumours. Silver nanoparticles have drawn the attention of researchers because of their extensive applications in areas such as integrated circuits, sensors, bio-labelling ,filters , antimicrobial deodorant fibres, cell electrodes, low-cost paper batteries (silver nano-wires) and antimicrobials (Lee *et al*., 2008). Silver nanoparticles have been used extensively as antimicrobial agents in health industry, food storage, textile coatings and a number of environmental applications. Antimicrobial properties of silver nanoparticles caused the use of these nano-metals in different fields of medicine, various industries, animal husbandry, packaging, accessories, cosmetics, health and military. For instance, it was shown that silver nanoparticles mainly in the range of 1-10 nm attached to the surface of *E. coli* cell membrane, and disturbed its proper function such as respiration and permeability (Lee *et al*., 2008) **(Figure. 2.3)**.

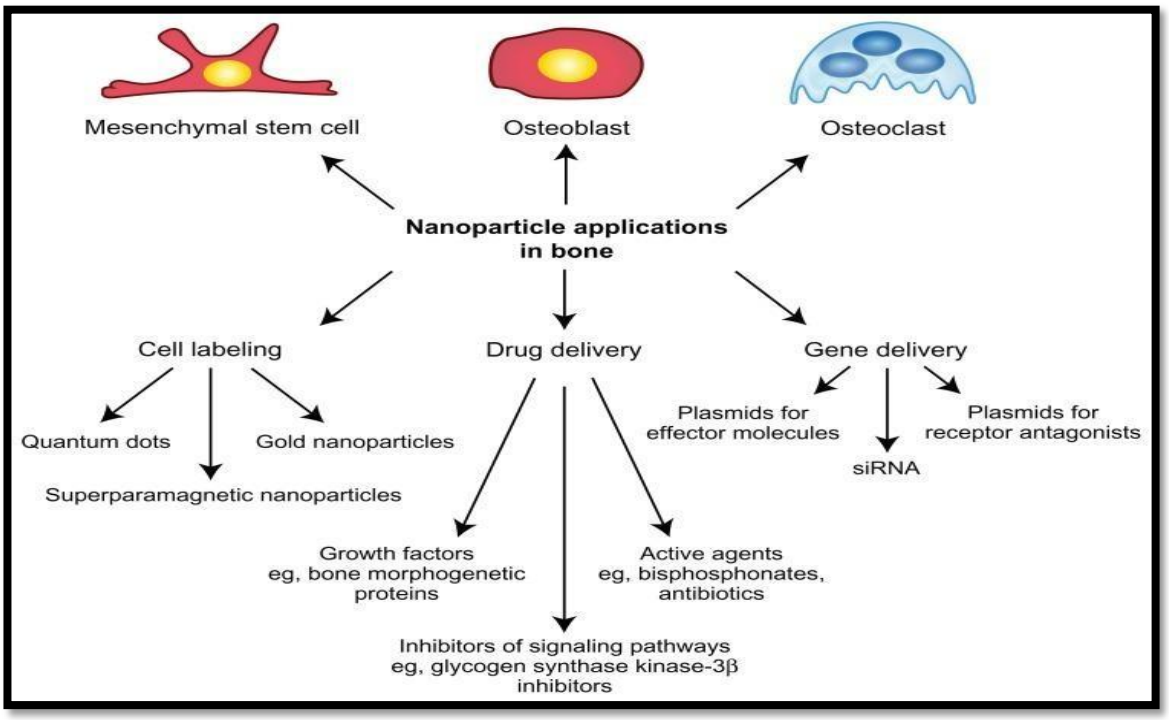

Figure 2.3**:** Diagrammatic overview of nanoparticle applications **(**Liu**,** 2009)

In general, therapeutic effects of silver particles (in suspension form) depend on important aspects, including particle size (surface area and energy), particle shape (catalytic activity), particle concentration (therapeutic index) and particle charge (oligodynamic quality). Mechanisms of antimicrobial effects of silver nanoparticles are still not fully understood, but several studies have revealed that silver nanoparticles may attach to the negatively charged bacterial cell wall and rupture it, which leads to denaturation of protein and finally cell death **(**Table 2.1**)**. Fluorescent bacteria were used to study antibacterial effects of silver nanoparticles. Green fluorescent proteins were adapted to these investigations. It was found that silver nanoparticles attached to sulphur-containing proteins of bacteria, and caused death. Moreover, fluorescent measurements of cell-free supernatants showed the effect of silver nanoparticles on recombination of bacteria. The attachment of silver ions or nanoparticles to the cell wall caused accumulation of envelope protein precursors resulting in immediate dissipation of the proton motive force **(**Liu, 2009). Catalytic mechanism of silver nanoparticle composites and their damage to the cell by interaction with phosphorous- and sulphur-containing compounds such as DNA have been also investigated (Sharma *et al*., 2009). Furthermore, silver nanoparticles exhibited destabilization of the outer membrane and rupture of the plasma membrane, thereby causing depletion of intracellular ATP. Another mechanism involves the association of silver with oxygen and its reaction with sulfhydryl groups on the cell wall to form R-S-S-R bonds, thereby blocking respiration and causing cell death **(**Table 2.2**)** (Sharma *et al*., 2009).

Table 2.1: Applications of silver nanoparticles in pHarmaceutics, medicine, and dentistry

Applications of silver nanoparticles in pharmaceutics, medicine, and dentistry	
Pharmaceutics and Medicines	Treatment of dermatitis; inhibition of HIV-1 replication. Treatment of ulcerative colitis and acne. Antimicrobial effects against infectious organisms Remote laser light-induced opening of microcapsules Silver/dendrimer nanocomposite for cell labelling. Molecular imaging of cancer cells. Enhanced Raman Scattering (SERS) spectroscopy Detection of viral structures (SERS and Silver nanorods) Coating of hospital textile (surgical gowns, face mask) Additive in bone cement Implantable material using clay-layers with starch stabilized Ag NPs Orthopaedic stocking. Hydrogel for wound dressing.
Dentistry	Additive in polymerizable dental materials Patent Silver-loaded SiO_2 nanocomposite resin filler (Dental resin composite). Polyethylene tubes filled with fibrin sponge embedded with Ag NPs dispersion.

Source: Sharma *et al*., 2009

Table 2.2: Mechanisms of antibacterial effects of silver nanoparticles

Mechanisms of Antibacterial Effects of Ag NPs
Cell death due to uncoupling of oxidative phosphorylation
Cell death due to induction of free radical formation
Interference with respiratory chain at Cyt C level
Interference with components of microbial ETS
Interactions with protein thiol groups and membrane bound enzymes
Interaction with pHospHorous- and sulfur-containing compounds such as DNA

Source: Sharma *et al*., 2009

2.12 Toxicity of Silver Nanoparticles

The unique physical and chemical properties of silver nanoparticles make them excellent candidates for a number of day-to-day activities, and also the antimicrobial and anti-inflammatory properties make them excellent candidates for many purposes in the medical field. However, there are studies and reports that suggest that nanosilver can allegedly cause adverse effects on humans as well as the environment. It is estimated that tonnes of silver are released into the environment from industrial wastes, and it is believed that the toxicity of silver in the environment is majorly due to free silver ions in the aqueous phase. The adverse effects of these free silver ions on humans and all living beings include permanent bluish-gray discoloration of the skin (argyria) or the eyes (argyrosis), and exposure to soluble silver compounds may produce toxic effects like liver and kidney damage; eye, skin, respiratory, and intestinal tract irritations; and untoward changes in blood cells (Panyala *et al*., 2008).

Since the beginning of the twenty-first century, nanosilver has been gaining popularity and is now being used in almost every field, most importantly the medical field. However, there have been reports of how nanosilver cannot discriminate between different strains of bacteria and can hence destroy microbes beneficial to the ecology. There are only very few studies conducted to assess the toxicity of nanosilver. In one study, in vitro toxicity assay of silver nanoparticles in rat liver cells has shown that even low-level exposure to silver nanoparticles resulted in oxidative stress and impaired mitochondrial function. Silver nanoparticles also proved to be toxic to in vitro mouse germ line stem cells as they impaired mitochondrial function and caused leakage through the cell membranes. Nanosilver aggregates are said to be more cytotoxic than asbestos. There is evidence that shows that silver ions cause changes in the permeability of the cell membrane to potassium and sodium ions at concentrations that do not even limit sodium, potassium, ATP, or mitochondrial activity. The literature also proves that nanosilver can induce toxic effects on the proliferation and cytokine expression by peripheral blood mononuclear cells. Nanosilver is also known to show severe toxic effects on the male reproductive system. Research shows that nanosilver can cross the blood-testes barrier and be deposited in the testes where they adversely affect the sperm cells (McAuliffe and Perry, 2007). Even commercially available silver-based dressings have been proved to have cytotoxic effects on various experimental models. In vivo studies on the oral toxicity of nanosilver on rats have indicated that the target organ in mouse for the nanosilver was the liver. It was also found from histopathological studies that there was a higher incidence of bile duct hyperplasia, with or without necrosis, fibrosis, and pigmentation in the study animals (Kim *et al*., 2010).

Studies have also suggested that there is release of silver when the nanoparticles are stored over a period of time. Hence, it has to be said that aged nanosilver is more toxic than new nanosilver. Nanosilver with its antimicrobial activity can hinder the growth of many „friendly" bacteria in the soil. By showing toxic effects on denitrifying bacteria, silver can disrupt the denitrification process, which involves the conversion of nitrates into nitrogen gas which is essential for the plants. Loss of environmental denitrification through reduction of plant productivity can lead to eutrophication of rivers, lakes, and marine ecosystems and destroy the ecosystem. Nanosilver also has toxic effects on aquatic animals because silver ions can interact with the gills of fish and inhibit basolateral Na^+-K^+-ATPase activity, which can in turn inhibit osmoregulation in the fish. To understand the toxic potential nanosilver has on the freshwater environment, the Daphnia magna 48-h immobilization test was conducted, and the results showed that the silver nanoparticles have to be classified under „category acute 1 "as per the Globally Harmonized System of Classification and Labelling of Chemicals, suggesting that the release of nanosilver into the environment has to be carefully considered (Asghari *et al*., 2012). Though these studies tend to suggest that nanosilver can induce toxicity to living beings, it has to be understood that the studies on nanosilver toxicity were done in in vitro conditions which are drastically different from in vivo conditions and at quite high concentrations of nanosilver particles. Hence, it is imperative that more studies be carried out to assess the toxicity effect nanosilver has in vivo before a conclusion on its toxicity is reached.

CHAPTER THREE

3.0 MATERIALS AND METHODS

3.1 Preparation of Plant Materials

Fresh and healthy leaves of Goat weed (*Ageratum conyzoid*), Ugwu leaf (*Telferia accidentali*), Bitter leaf (*Vernonia amygdelina*), Neem leaf (*Azadirata indica*), Uziza leaf (*Piper gineansis*), Sweet Potato leaf (*Ipeomea Botata*), Comelina leaf (*Comelina benghalensis*), Cassava leaf (*Manihot esculentu*), Moringa leaf (*Moringa oleifera*) and Independence leaf (*Chromolaena Odorata*) (XXY) were collected and separately washed three times with running tap water to remove dust particles. They were then air-dried to remove residual moisture. The dried leaves were crushed using mortar and pestle. For each powder, 10 g was boiled in 100 ml distilled water for 20 minutes and filtered with Whatman No. 1 filter paper. The filtrates were centrifuged at 4,000 rpm for 5 minutes using S-P digital Centrifuge to remove heavy biomaterials and then stored at 4°C for further use.

3.2 Qualitative Phytochemical Analysis of Plant Extracts

Qualitative phytochemical analysis of plant extracts was done as follows;

3.2.1. Test for Phlobatannins

Analytical method was according to Ejikeme *et al.* (2014). To each sample (0.30 g) weighed into a beaker was added 30ml of distilled water. After 24 hours of extraction, aqueous extract (10 cm^3) of each wood sample was boiled with 5 cm^3 of 1% aqueous hydrochloric acid. Deposit of red precipitate showed positive test.

3.2.2. Test for Saponin

Methodology is as reported by Ejikeme *et al.* (2014). Distilled water (30 cm^3) was added to wood powder samples (0.30 g) and boiled for 10 minutes in water bath and filtered using Whatman filter paper number 42 (125 mm). A mixture of distilled water (5 cm^3) and filtrate (10 cm^3) was agitated vigorously for a stable persistent froth. The formation of emulsion on addition of three drops of olive oil showed positive result.

3.2.3. Wagner's test for Alkaloids

A few drops of Wagner's reagent are added to few ml of plant extract along the sides of test tube. A reddish- brown precipitate confirms the test as positive (Wagner, 1993, Banu *et al.*, 2015).

3.2.4. Benedict's test for Carbohydrates

To 0.5 ml of filtrate, 0.5 cm^3 of Benedict"s reagent is added. The mixture is heated on a boiling water bath for 2 minutes. A characteristic coloured precipitate indicates the presence of sugar (Raaman, 2006).

3.2.5. Test for Sterols and Triterpenoids

Methodology is as reported by Ejikeme *et al.* (2014). Each wood powder sample (0.30 g) was weighed into a beaker and extracted with 30 cm^3 and component extracted for 2 hours. A mixture of chloroform (2 cm^3) and concentrated tetraoxosulphate (VI) acid (3 cm^3) was added to 5 cm^3 of each extract to form a layer. Red colored lower layer indicates presence of Sterols and yellow colored layer indicates presence of Triterpenoids.

3.2.6. Ferric chloride test for Tannins

To 1 cm^3 of the plant extract was added few drops of 5% ferric chloride ($FeCl_3$) solution. Greenish black colour indicates the presence of catecholic Tannins; blue colour (gallic Tannins); and greenish brown colour (condensed tannins) (Raaman, 2006).

3.2.7. Million's test for proteins and amino acids

The plant extract is dissolved in 10 ml of distilled water and then filtered. A few drops of Million's reagent is added to 2 cm^3 of filtrate. The white precipitate proves the presence of proteins (Raaman, 2006).

3.2.8. Alkaline reagent test for Flavonoids

A small amount of the extract is treated with few drops of sodium hydroxide and if the intense yellow colour solution becomes colourless on addition of dilute acid proves the presence of flavonoids (Saxena *et al.,* 2013).

3.2.9. Spot test for fixed oils and fats

A small quantity of extract was pressed between two filter papers. Oil stain on the paper indicates the presence of fixed oils (Banu and Cathrine, 2015).

3.2.10. Borntrager's Test for Anthraquinone glycosides

To 3 cm^3 extract, dilute sulphuric acid was added, boiled and filtered. To the cold filtrate equal volume chloroform was added. The organic layer was separated and ammonia was added. Ammonical layer turns pink or red.

3.2.11. Lead acetate test phenolic compounds

One cm^3 of the plant extract was treated with 0.1ml of lead acetate (10%) solution. Occurrence of white precipitate indicates the presence of phenolic compounds.

3.2.12. Keller-Killani test for Cardiac glycoside

To 2 ml of extract, glacial acetic acid, one drop 5 % ferric chloride and concentrated sulphuric acid were added. Appearance /of reddish brown colour at the junction of the two liquid layers indicates the presence of cardiac glycosides.

3.3 Synthesis of Siver Nanoparticle under Un-Optimized Conditions

Ten milliliter (10 ml) of leaf extract was mixed with 90 ml of 1 mM $AgNO_3$ solution. Each mixture was left under ambient conditions and colour change from yellow to dark green which indicated reduction of Ag^+ to Ag^0 nanoparticles (NPs) was visually monitored. After 6 hours of incubation, the absorbance of each solution was determined at 400 nm using LANMAN Spectrophotometer at a resolution of 1 nm. The mixture centrifuged at 4000 rpm for 20 minutes. After discarding the supernatants, the AgNPs were redispersed in distilled water and washed. They were then stored at 4^oC until used.

3.4 Synthesis Of Siver Nanoparticle Under Optimized Conditions

The 3 x 3 factors Box-Benken design (Minitab® 17) was adopted for optimization of synthesis of silver nanoparticles. The effects of temperatures (25, 30 and 35^oC), pH (6, 7 and 8), and time of incubations (2, 4 and 6 hours) on the yield and activity of AgNPs were studied, which gave a total of 15 non-randomized runs as shown in Table 3.1. For each of the 10 plant extracts, fifteen conical flasks were labeled 1 – 15. After mixing 90 ml of 1 mM silver nitrate and 10 ml plant extract in each test tube. The pH was adjusted using either 0.1M HCl or 0.1M NaOH solution

(Christopher *et al.*, 2015) and then buffered with 10ml 0.1M phosphate buffer. Each mixture was left to synthesize AgNPs for a period defined in Table 3.1. After which, the absorbance was read at 400 nm using LABMAN Spectrophotometer at a resolution of 1 nm and results recorded.

Table 3.1: Design of experiment for non-randomized 15 runs in Box-Benken

StdOrder	RunOrder	PtType	Blocks	pH	Temperature	Time
1	1	2	1	6	25	4
2	2	2	1	8	25	4
3	3	2	1	6	35	4
4	4	2	1	8	35	4
5	5	2	1	6	30	2
6	6	2	1	8	30	2
7	7	2	1	6	30	6
8	8	2	1	8	30	6
9	9	2	1	7	25	2
10	10	2	1	7	35	2
11	11	2	1	7	25	6
12	12	2	1	7	35	6
13	13	0	1	7	30	4
14	14	0	1	7	30	4
15	15	0	1	7	30	4

Using Response Optimizer (Minitab® 17), the absorbance recorded from the 15 setups were optimized for each plant extract. The resulting optimized pH, temperatures and times of incubation were used to synthesize AgNPs. The absorbance was read at 400 nm at a resolution of 1 nm, before centrifuging at 4,000 rpm for 20 minutes. The AgNPs were washed and stored at 4^{o}C in the refrigerator till used.

3.5 Characterization of Synthesized Siver Nanoparticles

Ultraviolet – visible spectrophotometer was used to characterize the silver nanoparticles synthesized under optimized and un-optimized conditions at wavelength range of 340 - 820 nm using LABMAN Spectrophotometer at a resolution of 1 nm. Noble metal particles possess strong surface plasmon resonance (SPR) absorption in the visible region and are highly sensitive to the surface modification (Yousaf et al., 2020).

3.6 Collection of Isolates

Clinical isolates of *Escherichia coli* and *Pseudomonas aeruginosa* used as test microorganisms were obtained from Anthony Van Leuwenhoek's Research Centre, Nekede, Owerri West Local Government Area., Imo State, Nigeria. The viability and identities of the isolates were confirmed using routine biochemical screening and identification methods described by Cheesbrough (2009).

3.7 Antimicrobial Activity Assay For Siver Nanaparticles

The antibacterial activity of AgNPs synthesized under optimized and un-optimized conditions was studied following the Kirby-Bauer disc diffusion method described by Cheesbrough (2009) with slight modifications. The plates were prepared by dissolving 11.4 g of Mueller Hinton agar (MHA) powder in 300 ml distilled water and autoclaving at 121^{o}C for 15 minutes. After cooling,

it was poured into sterile petri dishes and left to solidify. The turbidity of each inoculum in nutrient broth was adjusted to 0.5ml McFarland's standard (1.5×10^8 CFU/ml) and aliquot of each isolate was collected with sterile swab stick and inoculated onto 20 Mueller Hinton agar (MHA) plates. The 0.5 ml McFarland standard was prepared by mixing 0.05ml 1% $BaCl_2$ and 9.95 ml 1% H_2SO_4. For each extract, paper discs, about 5 mm in diameter were punched out, labeled 1 – 5 and soaked with raw extract, AgNps synthesized under un-optimized conditions, AgNps synthesized under optimized conditions, 1 nm $AgNO_3$ and distilled water respectively. The discs were then deposited at equidistance on the plates which were incubated at 37^{o}C for 24 hrs. The diameters of zones of inhibition were measured to the nearest millimeter.

CHAPTER FOUR

4.0 RESULTS

4.1 Main Effect and Interaction Plots for the Production of Goatweed(Gw) Synthesized Nanoparticle (GwNP)

Figure 4.1 shows the main effects plot for the production of plant based Nanoparticles using Goatweed (GwNP). Findings show that the production of the nanoparticle was decreasing at approximately the first 40 hours and continued to decrease over time till the end of the experiment. At pH 7-8 an increase in the production of the nanoparticle (NP) was observed with a yield of 13.5 ml. However, a sharp decrease was observed between pH 6-7 with a yield of 11.8 ml. Increase in temperature from 25-35 degree Celsius resulted in an increase in the production of GwNP.

The interactions of these factors are displayed in figure 4.2. Findings had it that at constant time, that is time - pH, there appeared to be similitude in the activity of pH 6 and 7 as indicated by their interaction but pH 8 had no interaction with the activity of the other pH ranges. The interaction resulted in an overall decrease in the production of GwNP. In the case of the interaction between time - temperature, dissimilar results of pH 7 and 8 was recorded at temperatures of 30 and 35 ^{0}C, the interaction was very brief between temperatures 30 and 35 ^{0}C. The interaction between time temperature did not result in an overall increase or decrease in the production of GwNP. At a temperature of 25 ^{0}C, the production of GwNP had no interaction with other effects at other temperatures. Also, at constant pH, that is pH - temperature Interaction, the temperatures of 25, 30 and 35 ^{0}C had no interaction but eventually led to an overall increase in GwNP production.

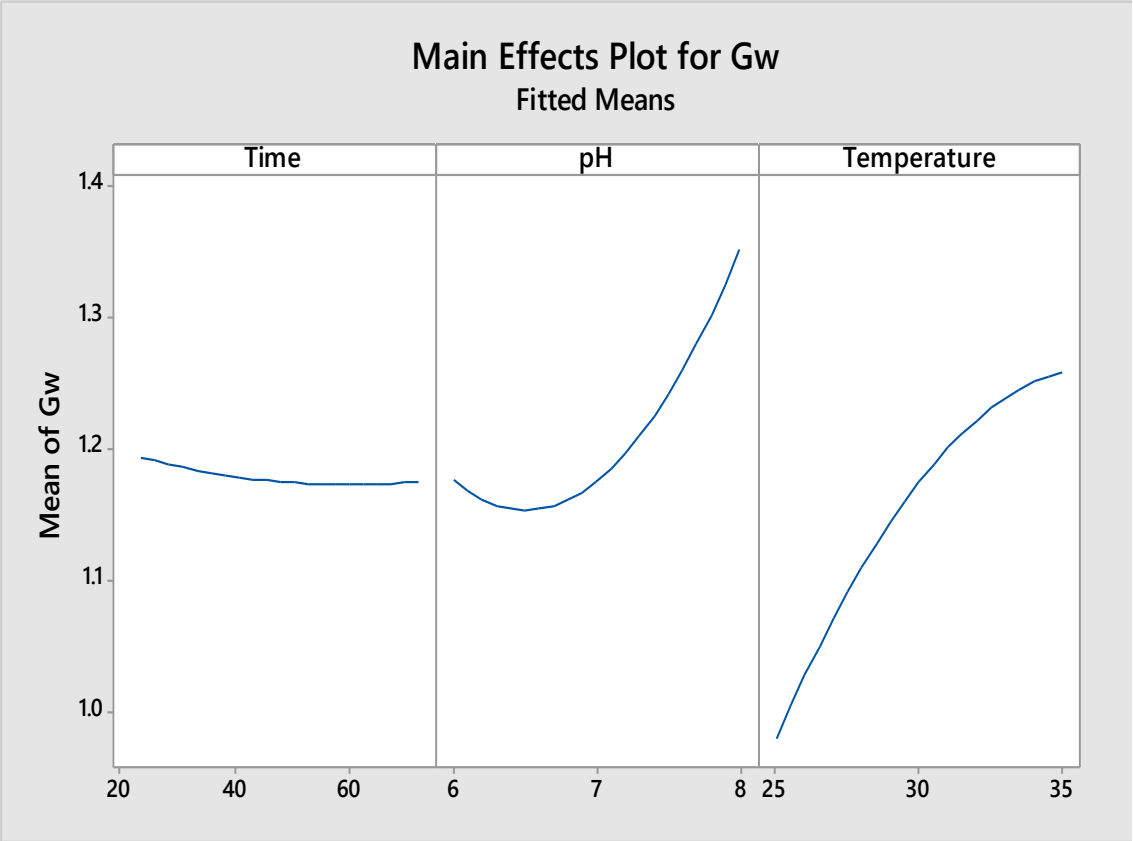

Figure 4.1: Main effect plot for the production of GwNP

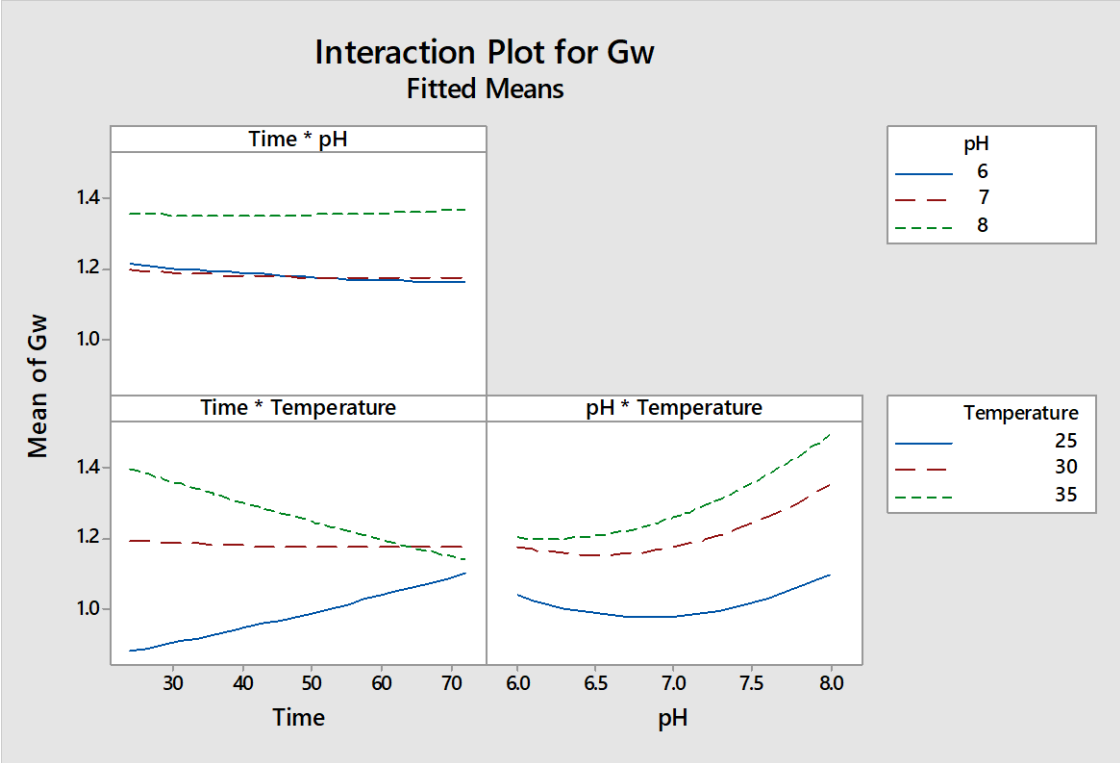

Figure 4.2**:** Interaction plots for Gw production (Temperature in Degrees Celsius)

4.2 Response Surface Plots for the Production of Goat Weed

The response surface plots aids in the comprehension of the main effects (to examine differences between level means for one or more factors) and interaction plots (a visual representation of the interaction between the effects of two factors) by analysing each interaction separately. At constant holding values or constant values of temperature of 30 ^{0}C, the production of Gw decreased with increase in time but, increased initially with increase in pH before a decrease as the pH approaches pH 8. This is shown in Figure 4.3.

On the other hand, Figure 4.4 holds it that at a constant holding pH value, the production of Gw increased with increase in time and the production continued to increase as the temperature approaches 35 ^{0}C. This can be observed in figure 4.4.

At a constant holding time, the production of the Gw increased with an increase in temperature and continued to increase as the temperature approached 35 ^{0}C. On the other hand, the pH increase resulted in an initial decrease in Gw production but the production increased as the pH approached pH 8 as shown in figure 4.5

The observations of the response surface regression shows that only time had significant effect on the production of the Gw at $P<0.05$ as shown in the appendix A. the regression had an r^2 value of 82.90% indicating that about 14% of the results occurred by chance.

The Regression Equation in Units is given as

$$
\begin{aligned}
Gw - Response \\
&= 3.33 + 0.0235\,Time(hrs) - 1.527\,pH \\
&+ 0.127\,Temperature + 0.000016\,Time(hrs) * Time(hrs) \\
&+ 0.0882\,pH * pH - 0.00222\,Temperature * Temperature \\
&+ 0.00064\,Time(hrs) * pH - 0.000996\,Time(hrs) \\
&* Temperature + 0.0117\,pH * Temperature
\end{aligned}
$$

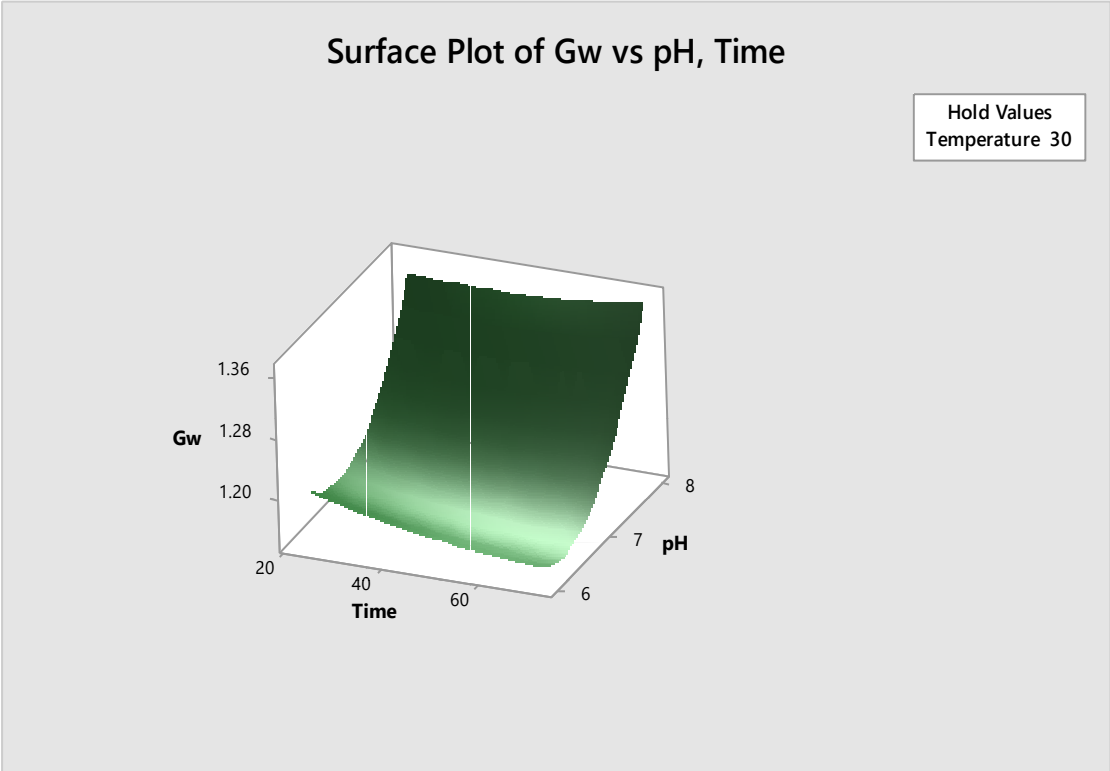

Figure 4.3: Response Surface Plot of Gw-Response vs pH, Time (hrs)

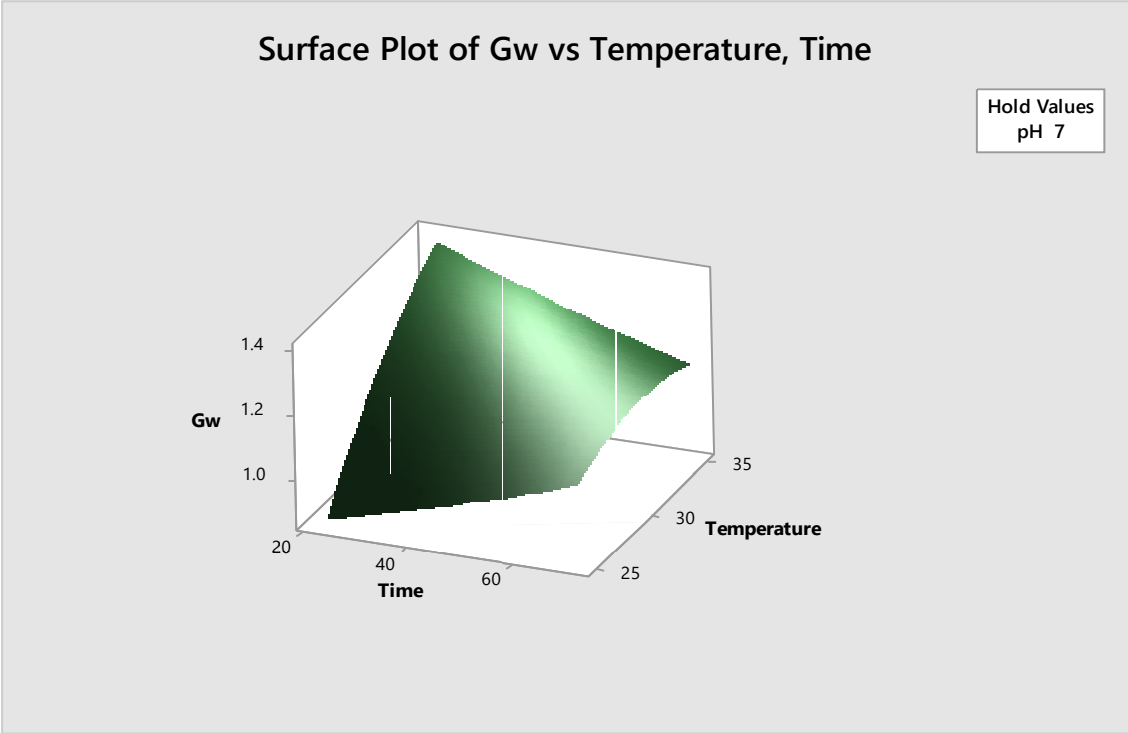

Figure 4.4: Response Surface Plot of Gw-Response vs Temperature, Time (hrs)

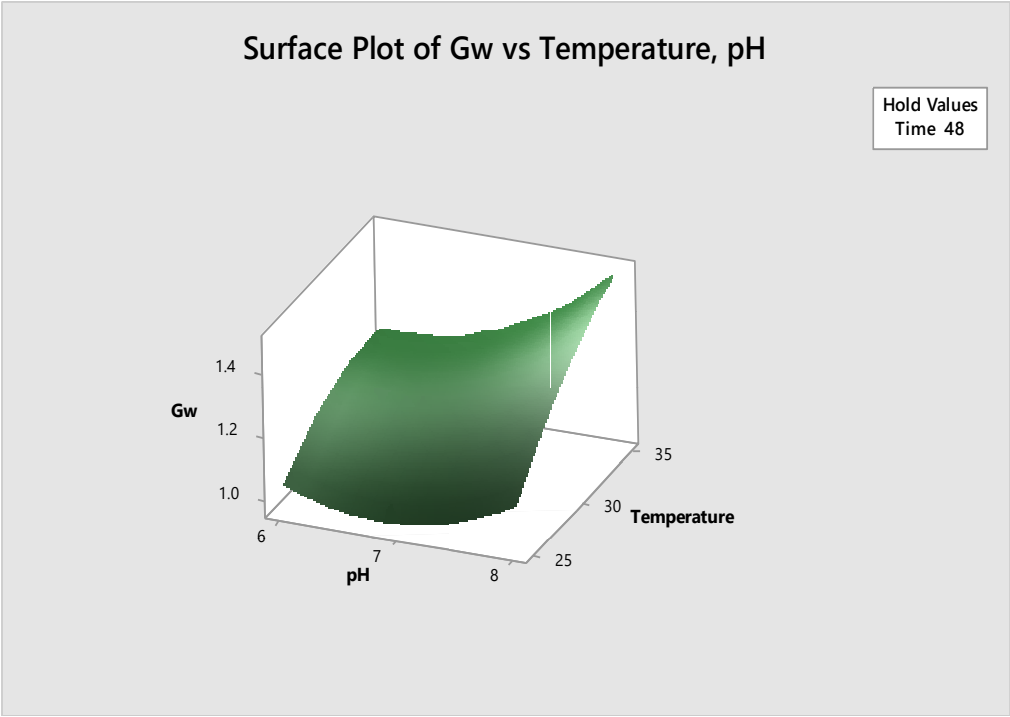

Figure 4.5: Response Surface Plot of Gw-Response vs Temperature, pH

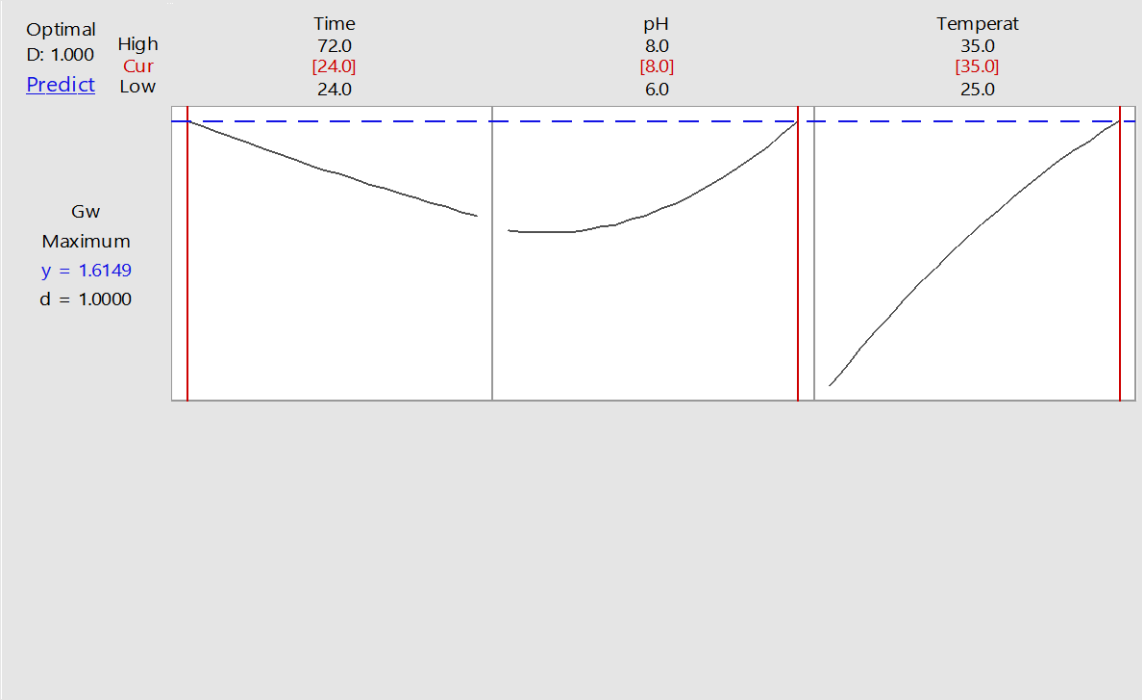

Figure 4.6: Optimization Plots of the Production of Goatweed.

4.3 Optimization of the production of Goatweed

Figure 4.6 shows the optimization plots for the production of Gw. Findings show that the optimum conditions for the production of Gw were pH 8.0, temperature of 35 degree Celsius and a time of 24 hours. At these conditions the maximum yield that would be achieved had a response of 1.6149.

4.4 Main Effect and Interaction Plots for the Production of Moringa Leaf Synthesized Silver Nanoparticle (MoNP)

Figure 4.7 shows the main effects plots for the production of Moringa leaf synthesized silver nanoparticle (MoNP). Findings displays that there was a considerable increase in the production of MoNP with increase in time following an initial decrease in production. This signifies that time is an essential component in the production of the nanoparticle. On the other hand, an increase in pH resulted in a steady increase in production of MoNP as the pH approached pH 8. Increase in temperature resulted in an initial increase in production. However, a gradual decrease in production of MoNP was observed as the temperature approached 30 degrees Celsius as indicated in the negative slope shown.

Observations of the interaction plots of the production of MoNP (Figure 4.8) shows that at constant time, time - pH, there was no interaction. On the other hand, Temperature, time - temperature recorded an interaction between 25 and 35 Degrees Celsius, albeit briefly. At all three measured temperatures. The findings of this interaction probably resulted in an increase in the production of MoNP. pH - Temperature interaction at pH 6.5, resulted in a considerable increase in the production of MoNP as the pH approached pH 8.

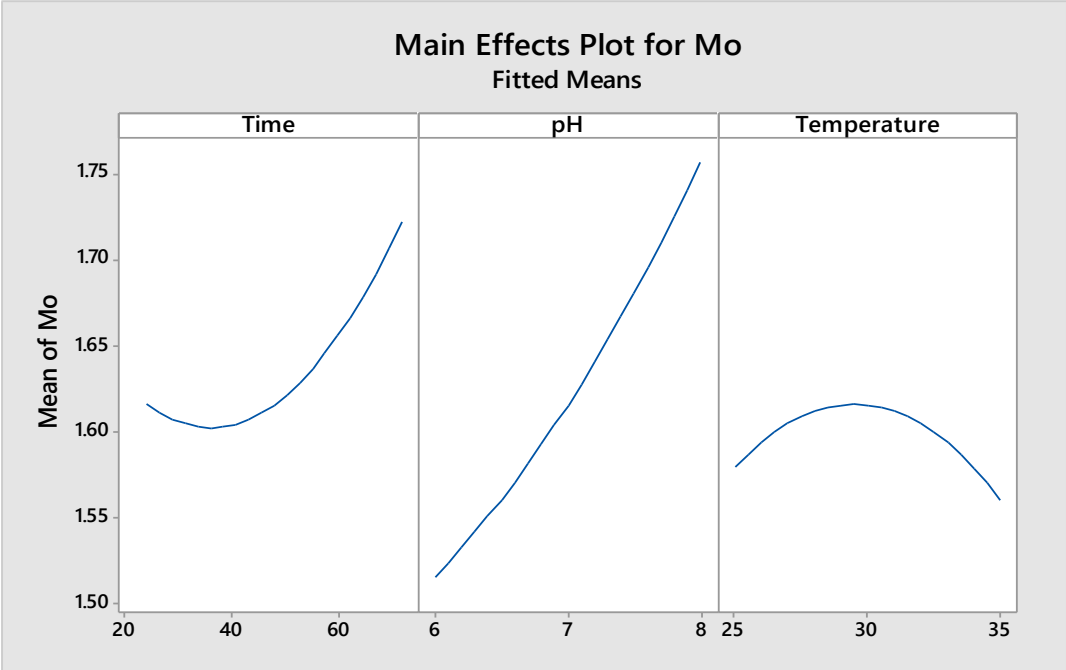

Figure 4.7: Main Effect Plots for Moriga Nanoparticle Production

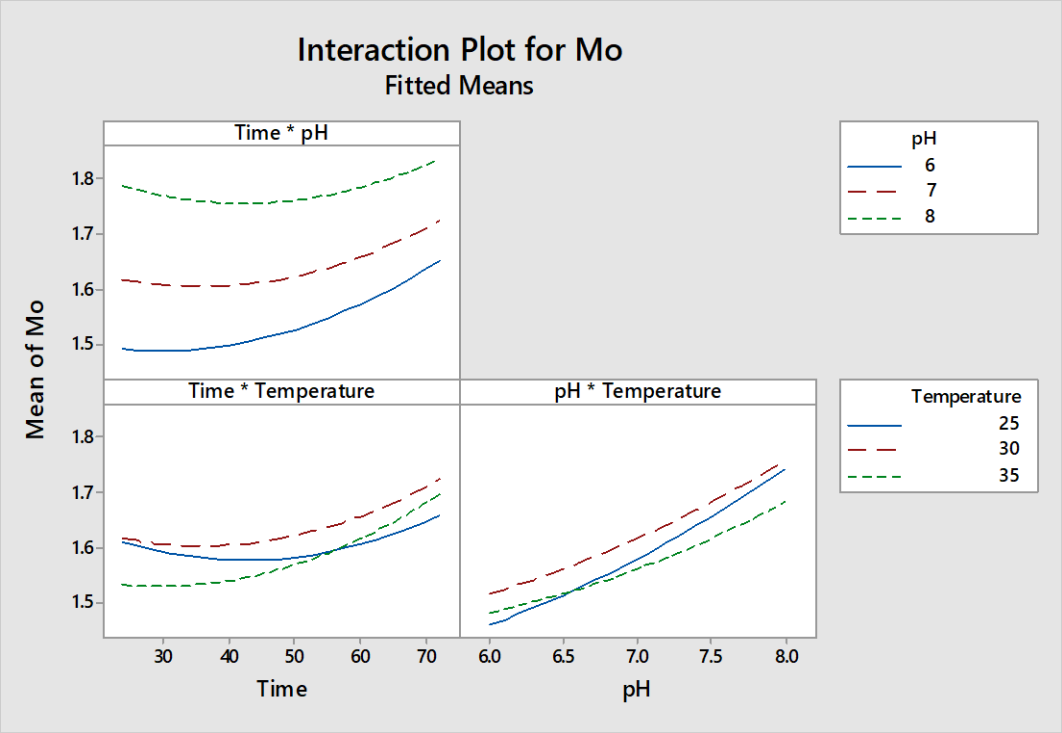

Figure 4.8: Interaction Plots for Moriga Nanoparticle Production (Temperature in Degrees Celsius)

4.5 Response Surface Plots for the Production Morringa Nanoparticles (MoNP)

Figure 4.9 shows the response surface plot of the production of MoNP at constant holding temperature. The observation displayed shows that there was a considerable increase in the production of MoNP as the time increased. Also, increase in the pH significantly increased the production of the MoNP as pH approached pH 8.

Figure 4.10 shows the response surface plot for the production of MoNP at constant holding pH. Findings displayed that there was also a considerable increase in production of the MoNP as time increases but a small negative slope was recorded for the production of MoNP as Temperature increased.

Figure 4.11 shows the response surface plot for the production of MoNP at holding time value. Findings showed that there was no increase in the production of MoNP with increased pH as the pH approached pH 8. Also, temperature had a later decline in MoNP production as the temperature approached 35 degrees after an initial increase in MoNP production at temperature 30 ^{0}C.

The findings of the response surface regression shows that time an overall significant single effect while time - time and pH - pH had significant interactive effect on the production of the MoNP at $P<0.05$ as shown in the appendix A. the regression had an R^2 value of 89.96% indicating that about 6% of the findings occurred by chance.

The Regression Equation in Units is given by

$$Mo - Response = -0.62 - 0.0058\,Time(hrs) + 0.013\,pH + 0.1254\,Temperature + 0.000092\,Time(hrs) * Time(hrs) + 0.0205\,pH * pH - 0.00183\,Temperature * Temperature + 0.00283\,Time(hrs) * pH - 0.000894\,Time(hrs) * Temperature - 0.00415\,pH * Temperature$$

4.6 Optimization of the production of Moringia Nanoparticle

Figure 4.12 shows the optimization plots for the production of MoNP. The result had it that the optimum conditions for the production of MoNP are pH 8.0, temperature 29.9^{0}C and time of 72 hours. At these conditions, the Moringa leaf extract would have a yield of 1.8356.

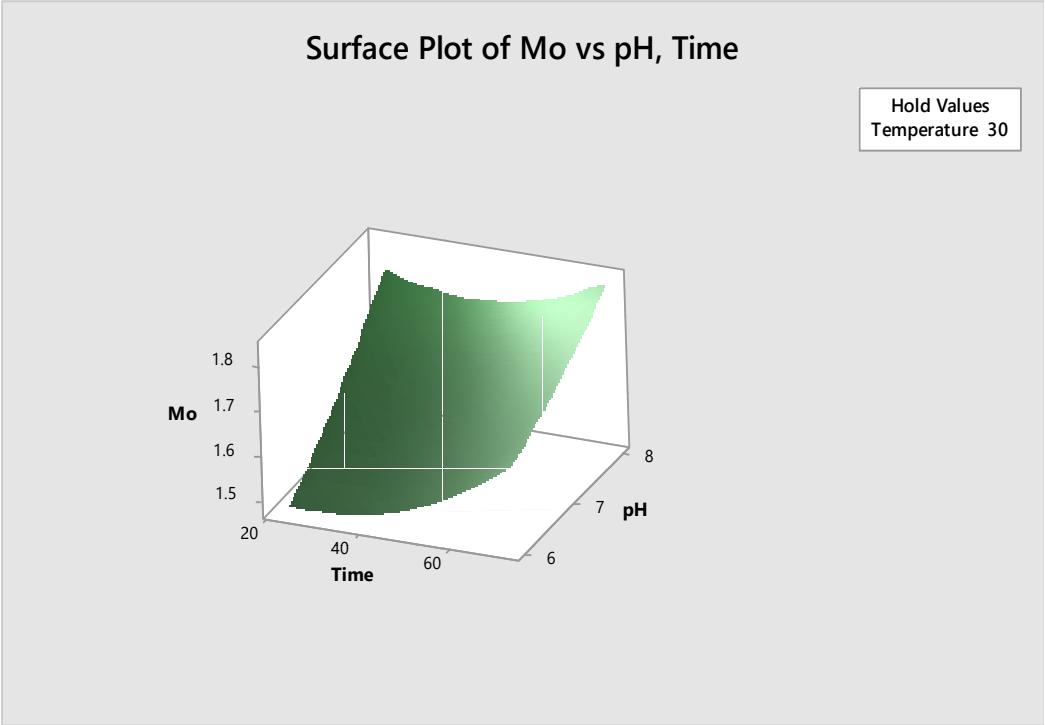

Figure 4.9: Surface Plot of Mo-Response vs pH, Time (hrs)

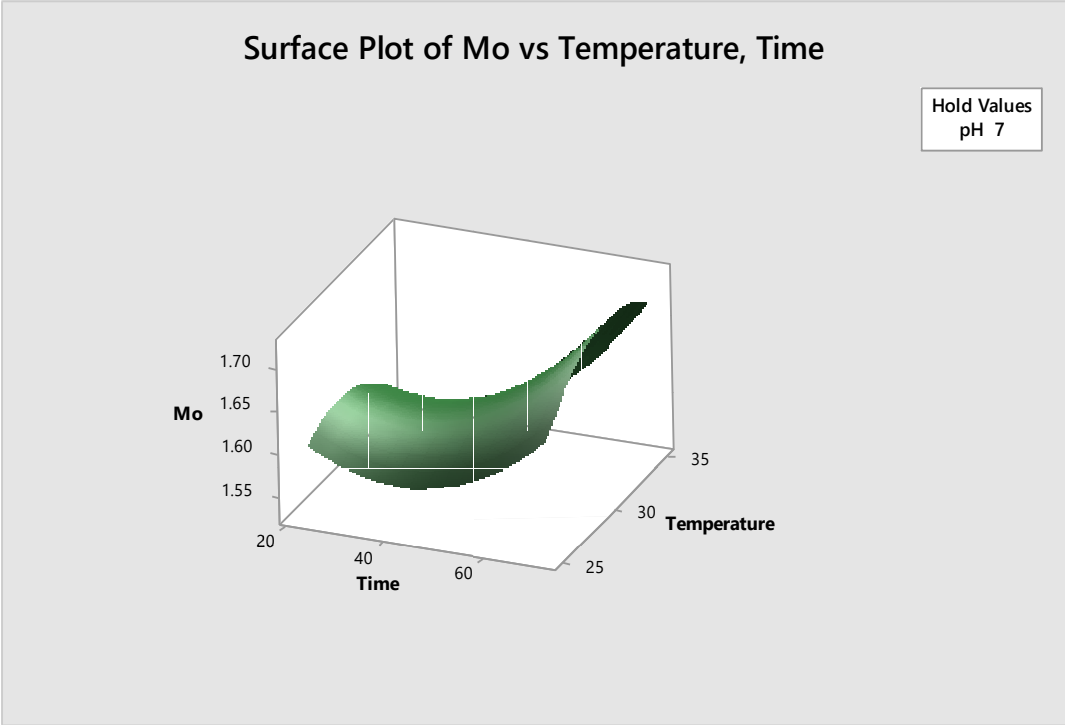

Figure 4.10: Surface Plot of Mo-Response vs Temperature, Time (hrs)

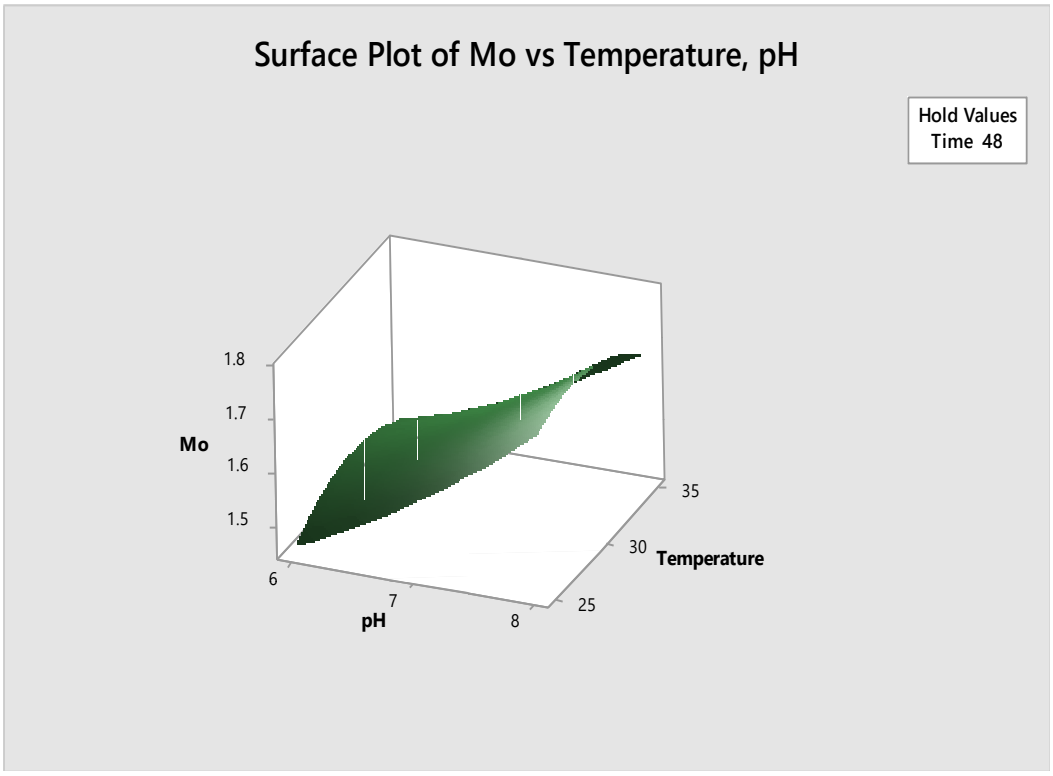

Figure 4.11: Surface Plot of Mo-Response vs Temperature, pH (hrs)

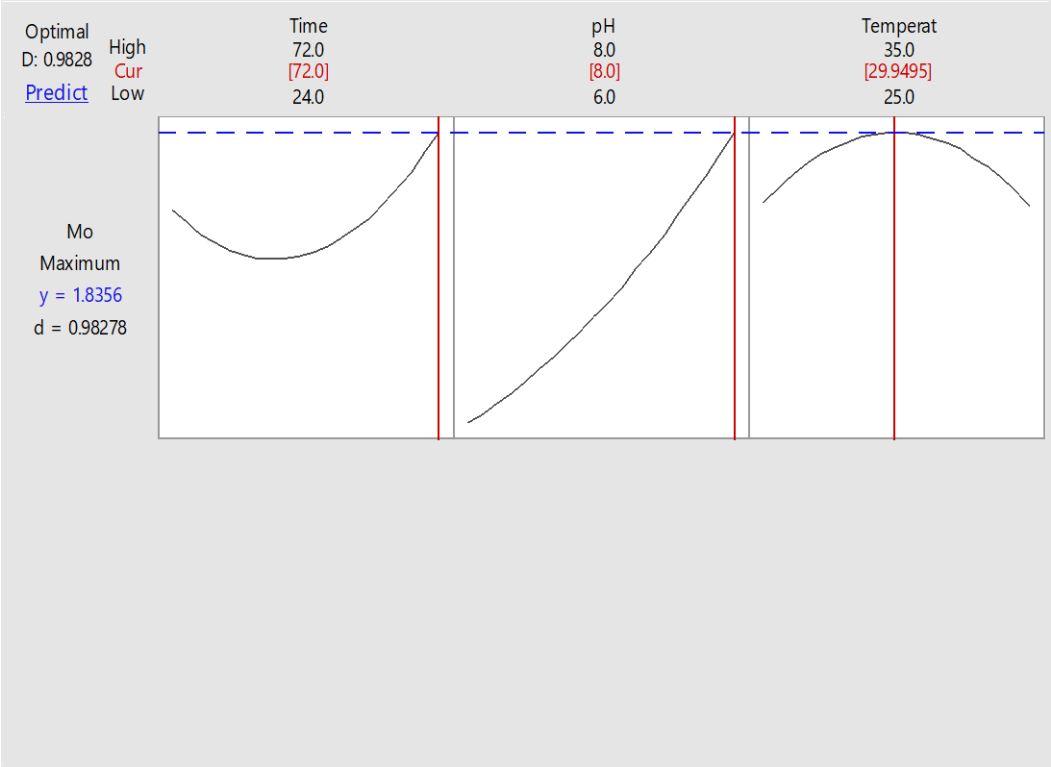

Figure 4.12: Optimization Plot for Moringia Nanoparticle production

4.7 Main Effect and Interaction Plots for the Production of Ugu Leaf Synthesized Silver Nanoparticle (UgNP)

Figure 4.13 shows the main effects plots for the production of Ugu leaf synthesized silver nanoparticle (UgNP). The findings from the plotshowed that there was a considerable increase in the production of UgNP with increase in time following an initial lag in production. This signifies that time is an essential component in the production of the nanoparticle, On the other hand, an increase in pH resulted in an initial increase in production of UgNP as the pH approached pH 7. However, the production decreased as the pH approached pH 8. Increase in temperature resulted in a sharp initial decrease in production of UgNP and subsequent increase in production as temperature increased.

The observation of the interaction plots of the production of UgNP (Figure 4.14) shows that at constant time, time - pH, there was a continuous interaction between the pH 6 and 8. On the other hand, time - temperature recorded interaction at all three measured temperatures. The obervation of this interactions resulted in a considerable increase in the production of UgNP at temperatures of 30 and 35 degrees Celsius but, decreased production was observed at 25^{o}C with a slight increased production at 70 (hours). pH - temperature showed perpetual interaction from pH 6.0 – 8.0 which resulted in an initial slight increase in the production of UgNP and a considerable decrease in the production of UgNP as the increase in pH approached 8.0.

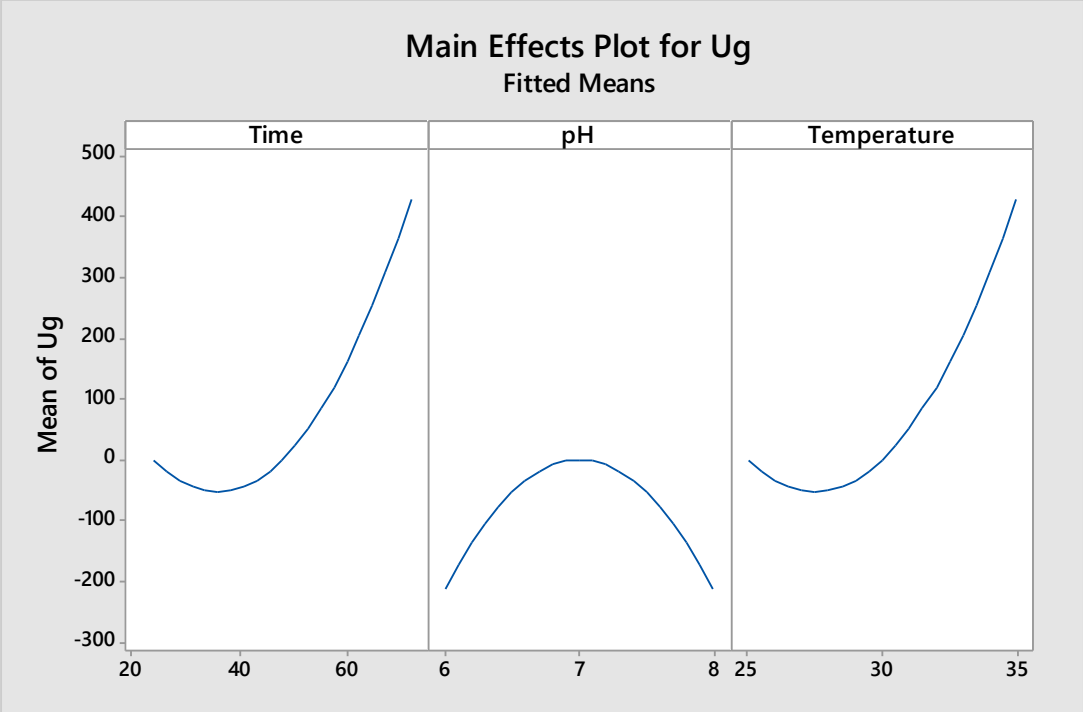

Figure 4.13: Main Effect Plots for Ugwu Nanoparticle Production

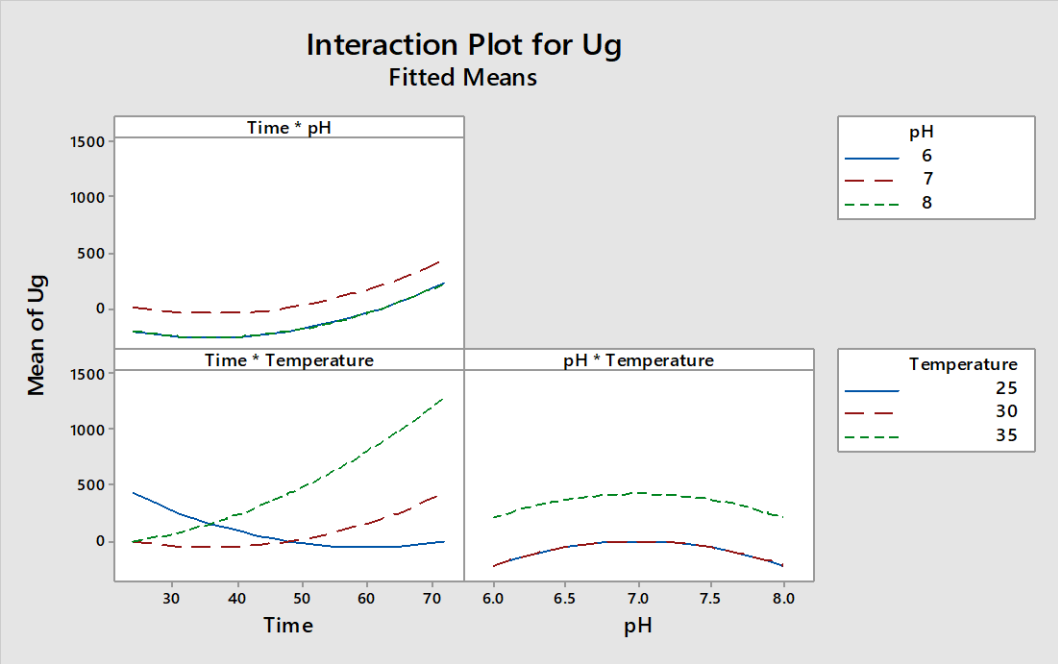

Figure 4.14: Interaction Plots for Nanoparticle Production

4.8 Response Surface Plots for the Production Nanoparticle

Figure 4.15 shows the response surface plot of the production of UgNP at constant holding temperature, holding pH, and holding time value. The findings from the plot showed that there was a considerable initial increase in the production of UgNP as the time increased with a later decrease as the time was increased to 60 (hrs). On the other hand, the pH initially increased the production of the UgNP followed by a decrease in production as pH approached pH 8.

The response surface plot for the production of UgNP at holding time value showed that the production of the UgNP increased initially with increased temperature but, continued to decrease as the pH approached pH 8 and temperature approached 35 degrees as shown in figure 4.16.

Figure 4.17 shows the response surface plot for the production of UgNP at constant holding pH. It showed an increase in production of the UgNP as temperature increased. As pH approached pH 8, the plot recorded a continuous increased production of UgNP as pH.

Findings of the response surface regression shows that time had no overall significant single effect, while time - time and pH - pH had no significant interactive effect on the production of the UgNP at $P<0.05$ as shown in the appendix A. The regression had an R^2 value of 73.21% indicating that about 6% of the results occurred by chance.

The Regression Equation in Units is given as:

$$
\begin{aligned}
Ug - Response \\
&= 1492 - 133.7\,Time(hrs) + 2996\,pH \\
&- 642\,Temperature + 0.371\,Time(hrs) * Time(hrs) \\
&- 214\,pH * pH + 8.56\,Temperature * Temperature \\
&+ 0.00\,Time(hrs) * pH + 3.57\,Time(hrs) * Temperature \\
&- 0.0\,pH * Temperature
\end{aligned}
$$

4.9 Optimization of the Production of Ugwu Nanoparticle

Figure 4.18 shows the optimization plots for the production of UgNP. The findings show that the optimum conditions for the production of UgNP are pH 8.0, Temperature of 35 degrees Celsius and a time of 72 hours. At this conditions the maximum yield that will be achieved will have a response of 1285.13.

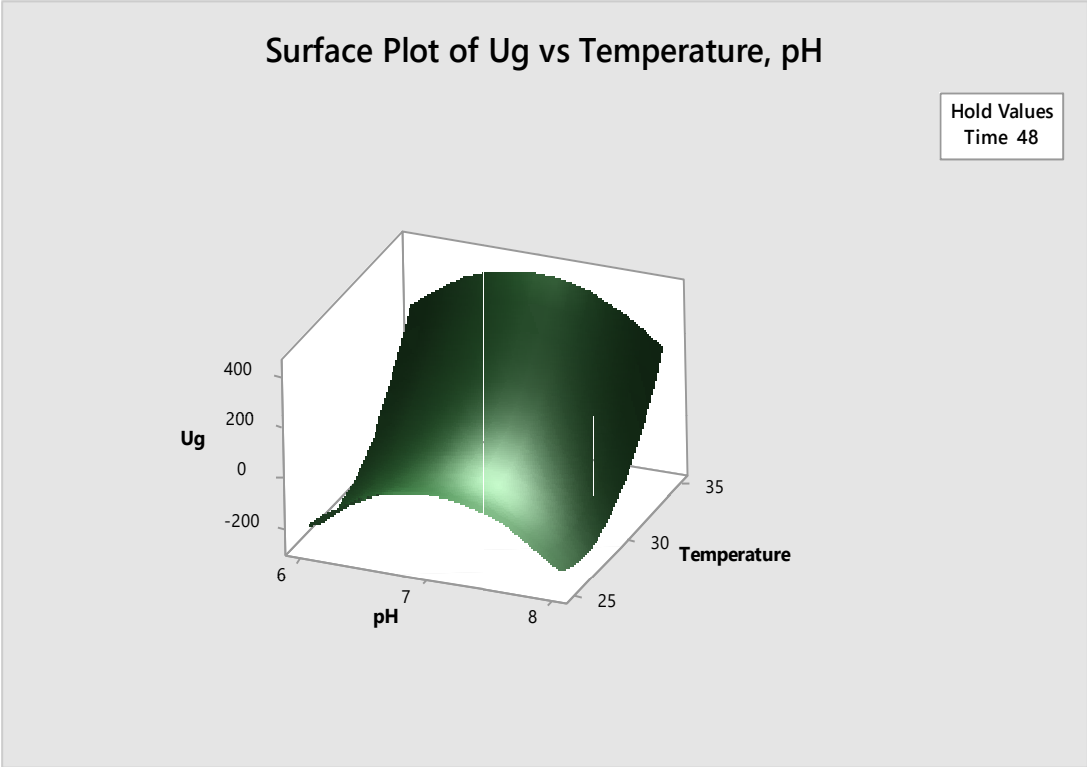

Figure 4.15: Surface Plot of Ug-Response vs Temperature, pH (hrs).

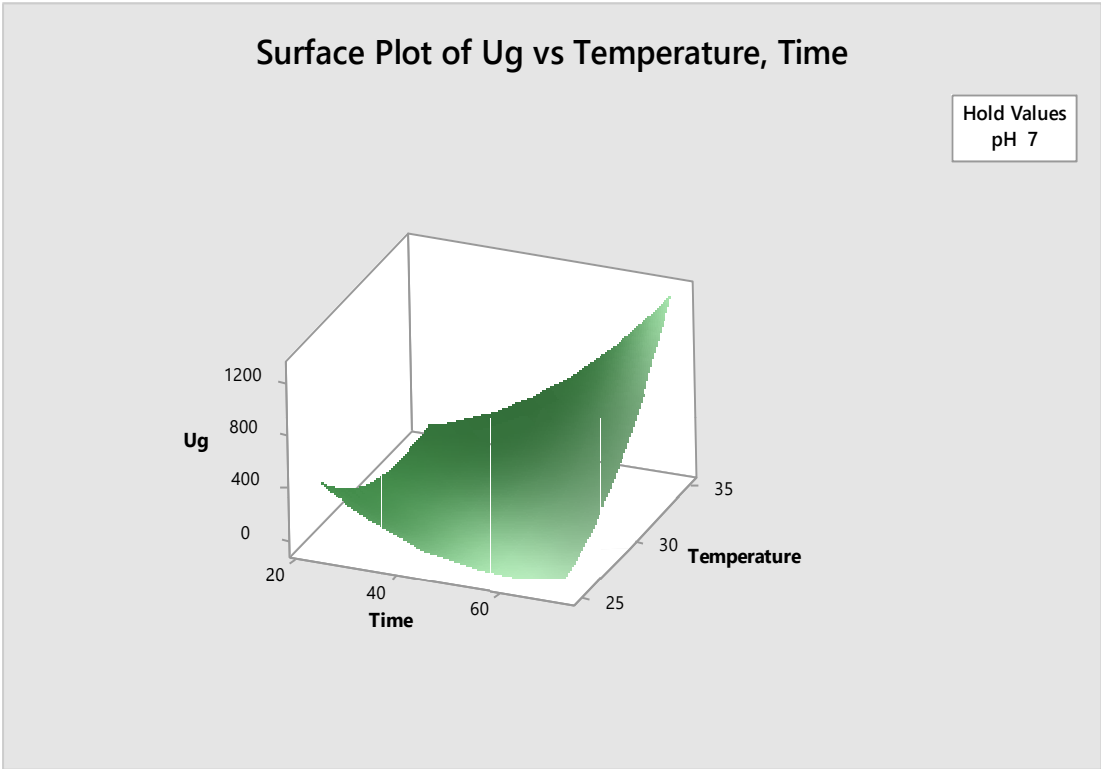

Figure 4.16: Surface Plot of Ug-Response vs Temperature, Time (hrs)

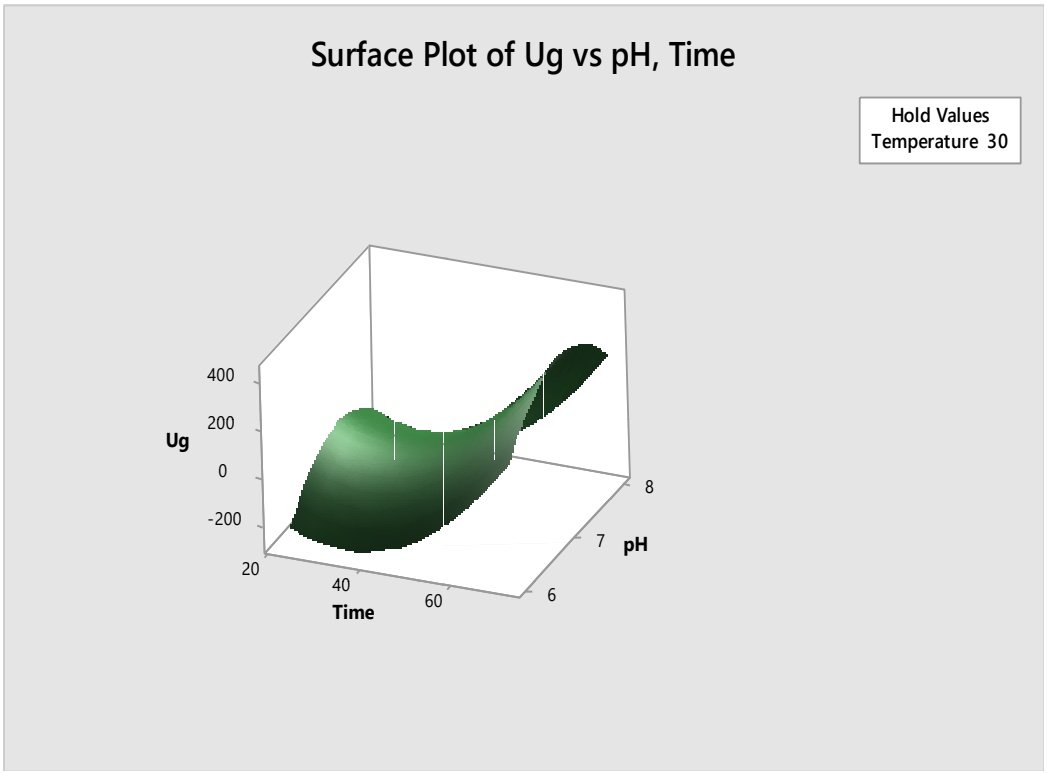

Figure 4.17: Surface Plot of Ug-Response vs pH, Time (hrs)

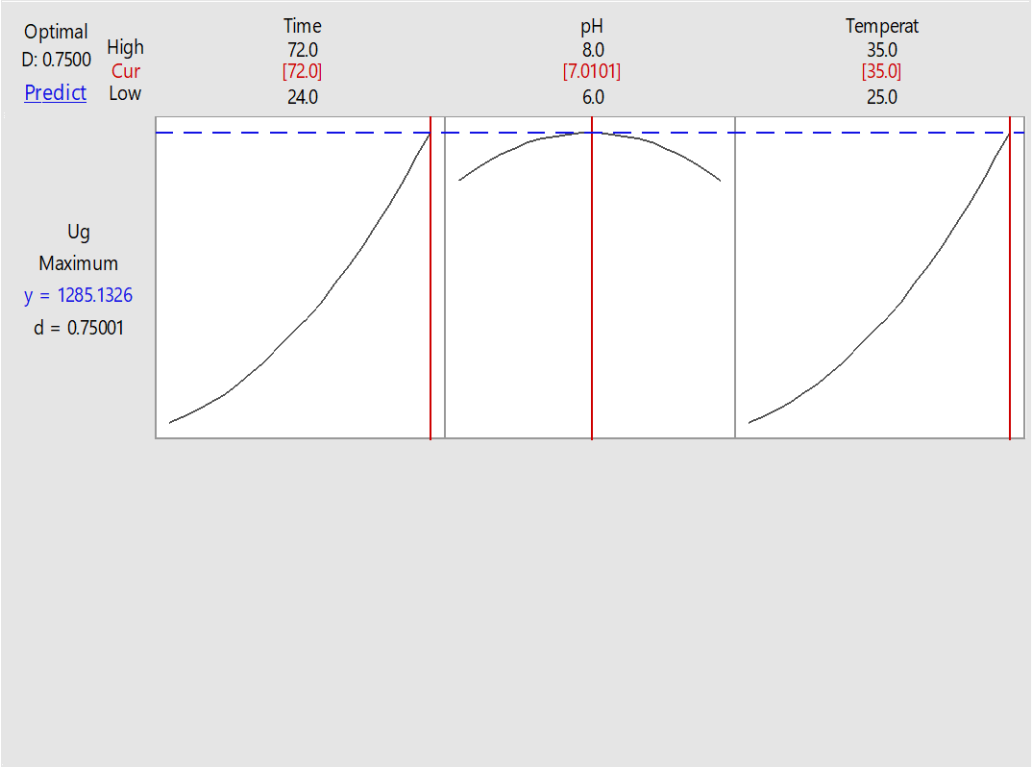

Figure 4.18: Optimization plot for UgNP production

4.10 Main Effect and Interaction Plots for the Production of Cassava Leaf Synthesized Silver Nanoparticle (CaNP)

The main effects plots for the production of Cassava leaf synthesized Silver nanoparticles (CaNP) (Figure 4.19). The finding from the plot showed that there was a slight increase in the production of CaNP with increase in time following an initial lag in production. This signifies that time is an essential component in the production of this nanoparticle, on the other hand, an increase in pH resulted in a continuous increase in the production of CaNP as the pH approached pH 8. Increase in temperature resulted in a slow and steady increase in production of CaNP.

The observation of the interaction plots of the production of CaNP (Figure 4.20) shows that at constant time, time - pH, there was no interaction. On the other hand, time - temperature recorded interaction at all three measured temperatures as the time approached 70 (hrs). The findings of this interactions resulted in no considerable increase in the production of CaNP at any temperature range. pH - temperature showed perpetual interaction from pH 6.0 – 6.5 which resulted in a continuous increase in the production of CaNP as the increase in pH approached 8.0.

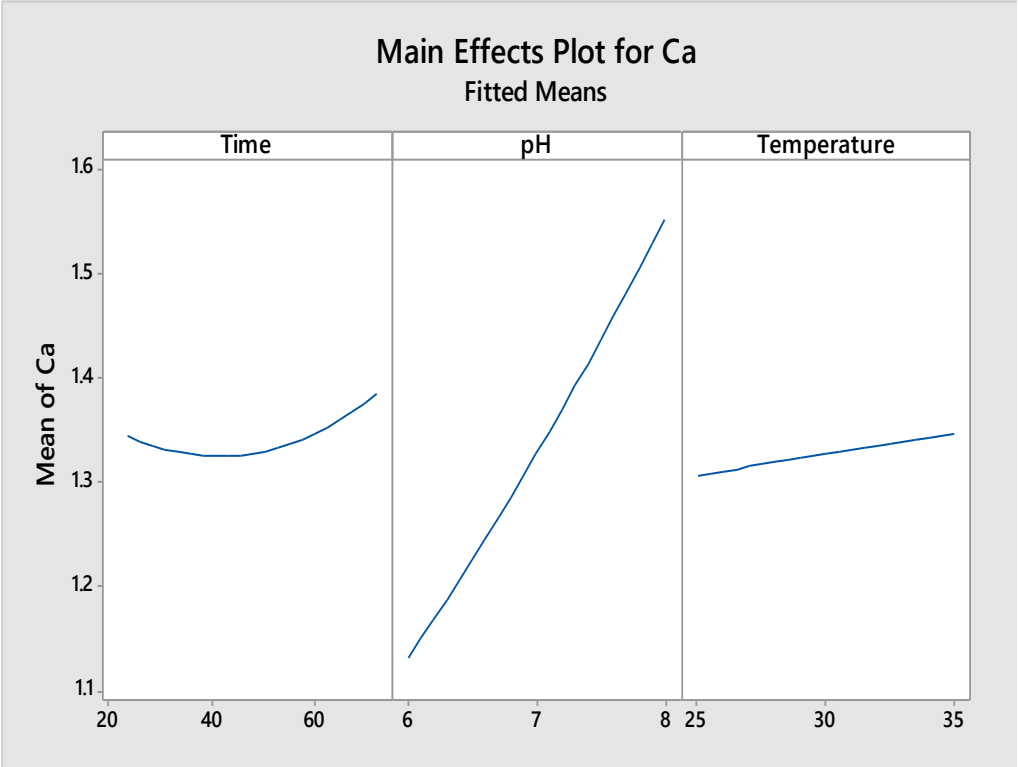

Figure 4.19: Main Effect Plots for Cassava Nanoparticle production

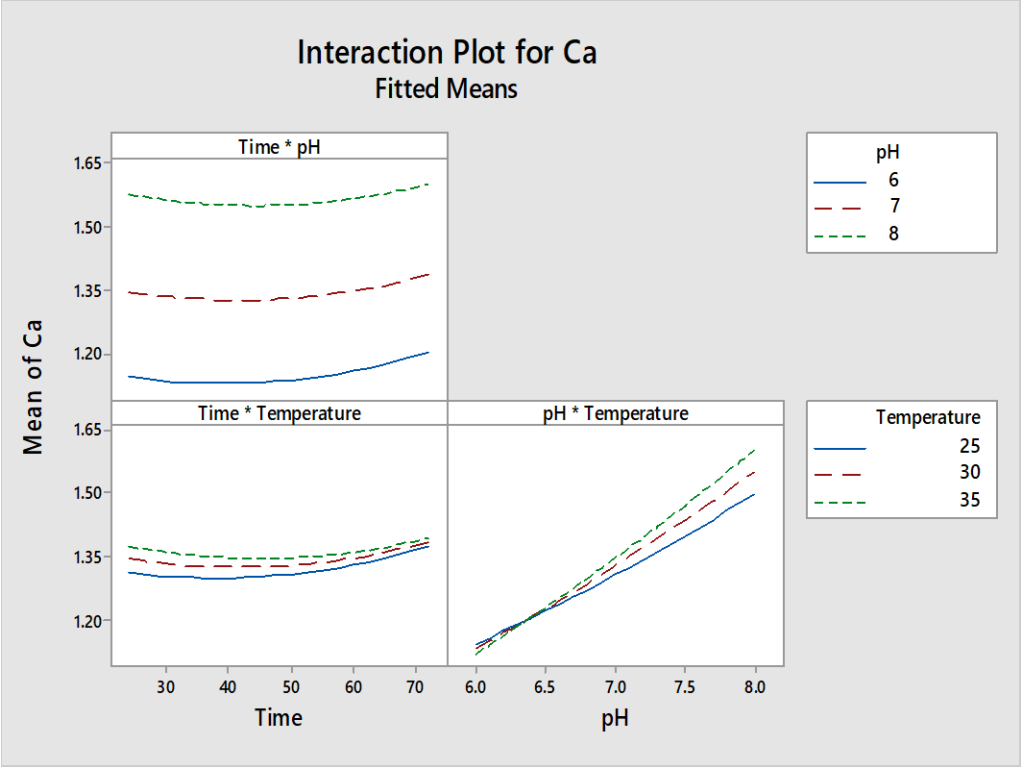

Figure 4.20: Interaction Plots for Cassava Nanoparticle production

4.11 Response Surface Plots for the Production Cassava Nanoparticles

The response surface plot results for the production of CaNP at constant holding Time value (Figure 4.21), showed that there was a steady increase in the production of CaNP as the temperature and pH was increased.

Also, the response surface plot for the production of CaNP at constant holding pH (figure 4.22) showed marked increase in production of the CaNP as temperature and time increased and approached 35^0C and 60 hours respectively.

The response surface plot for the production of CaNP at holding temperature value findings showed increased production of the CaNP with increased pH and no increased production with increased time as time and pH approached 70 (hours) and pH 8 respectively (figure 4.23).

Findings of the response surface regression shows that pH had an overall significant single effect while time - time and pH - temperature had significant interactive effect on the production of the CaNP at $P<0.05$ as shown in appendix A. the regression had an R^2 value of 99.14% indicating that about 9% of the observaton occurred by chance.

The Regression Equation in Uncoded Units is given as:

$$
\begin{aligned}
Ca - Response \\
&= 1.63 - 0.00032\,Time(hrs) - 0.169\,pH \\
&- 0.0343\,Temperature + 0.000065\,Time(hrs) * Time(hrs) \\
&+ 0.0146\,pH * pH - 0.000037\,Temperature * Temperature \\
&- 0.000354\,Time(hrs) * pH - 0.000087\,Time(hrs) \\
&* Temperature + 0.00640\,pH * Temperature
\end{aligned}
$$

4.12 Optimization of the Production of Camolina Nanoparticles

Figure 4.24 shows the optimization plots for the production of CaNP. The plot indicated that the optimum conditions for the production of CaNP were pH 8.0, temperature of 35 degrees Celsius and a time of 72 hours. At this conditions the maximum yield that would be achieved would have a response of 1.6418.

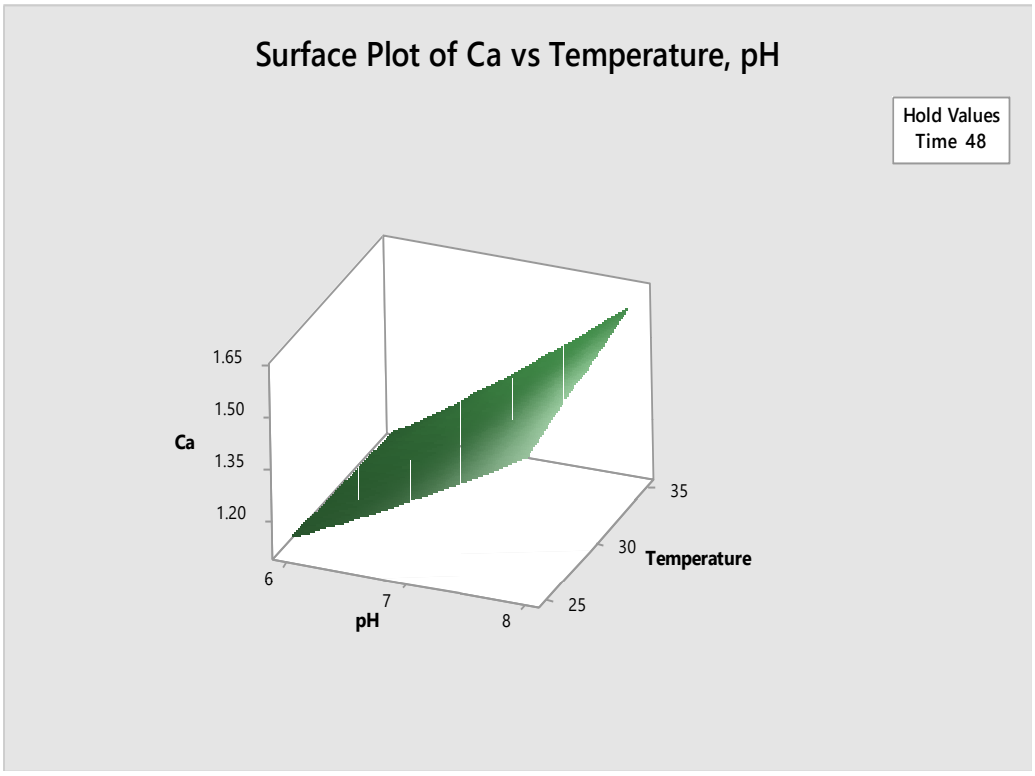

Figure 4.21: Surface Plot of Ca-Response vs Temperature, pH (hrs)

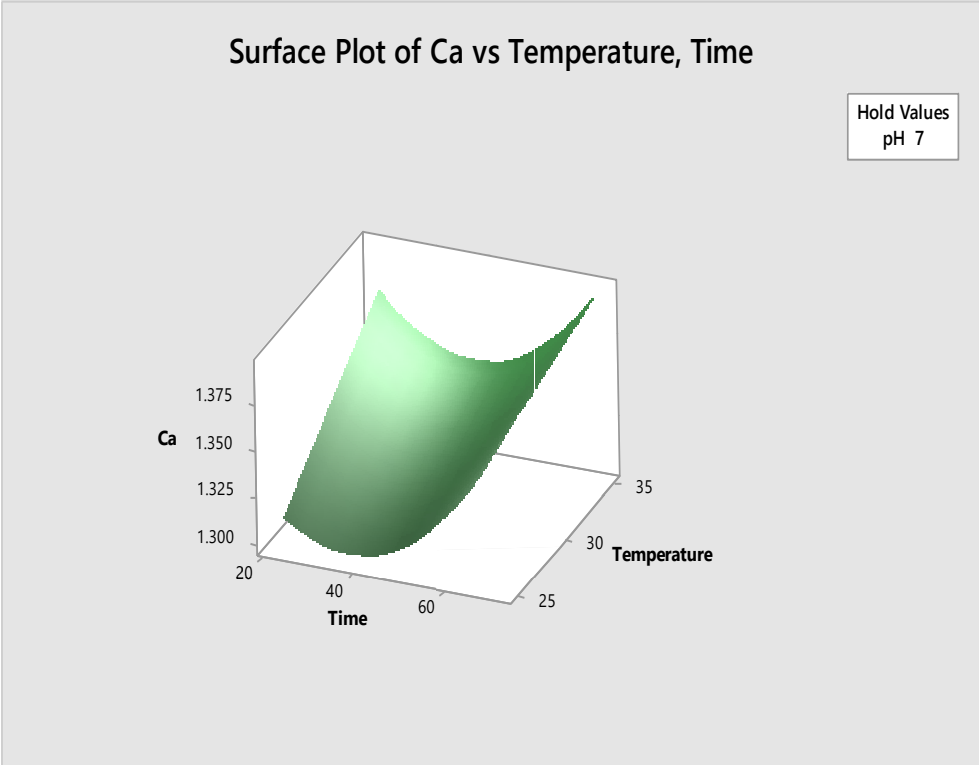

Figure 4.22: Surface Plot of Ca-Response vs Temperature, Time (hrs)

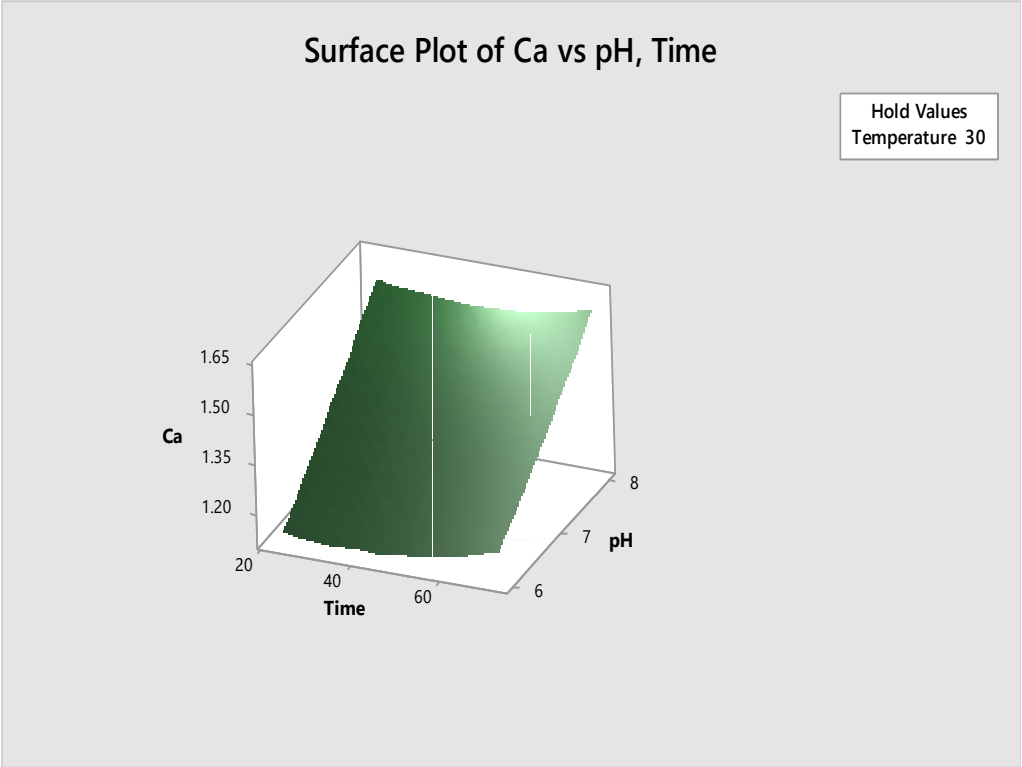

Figure 4.23: Surface Plot of Ca-Response vs pH, Time (hrs)

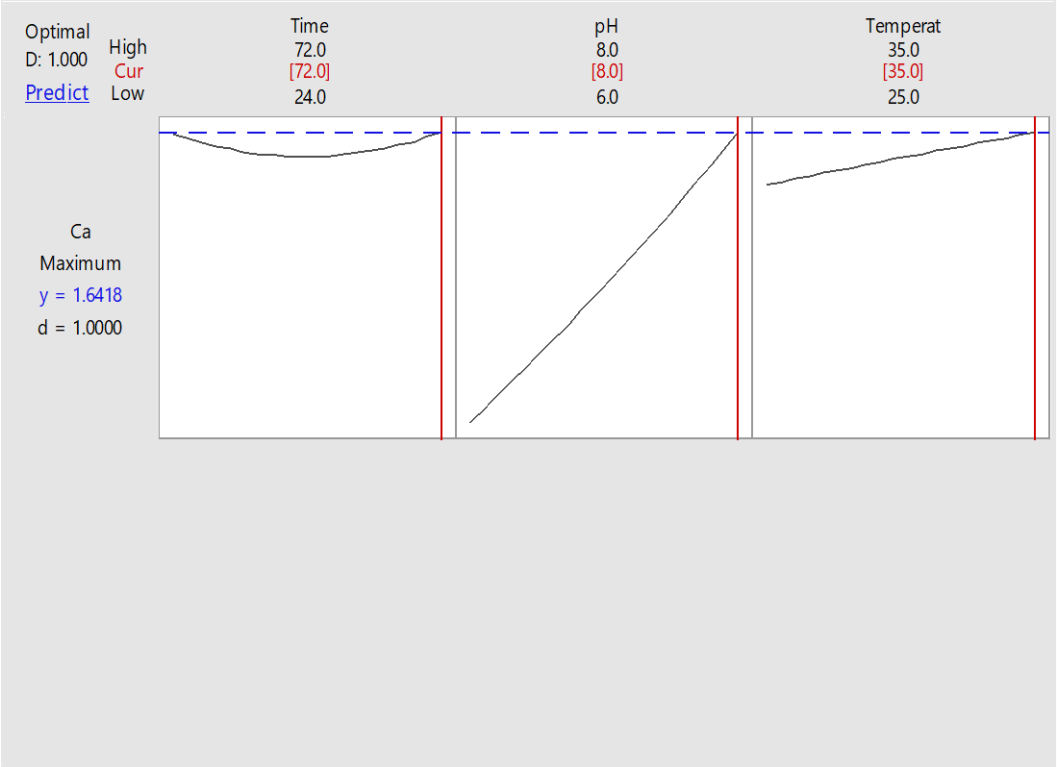

Figure 4.24: Optimization plot for CaNP production

4.13 Main Effect and Interaction Plots for the Production of Comelina Leaf Synthesized Silver Nanoparticle (CoNP)

The findings of main effects plot for the production of Comelina leaf synthesized Silver nanoparticles (CoNP) (Figure 4.25) showed that there was a slight increase in the production of CoNP with increase in time followed by a perpetual decrease in production after the 40 (hour) mark.. This signifies that time is an essential component in the production of this nanoparticle, increase in pH resulted in a continuous increase in the production of CoNP as the pH approached pH 8, while increase in temperature resulted in a steady increase in production of CoNP as temperature approached 35^0C.

The observations of the interaction plots of the production of CoNP (Figure 4.26) shows that at constant time, time - pH, there was no interaction. time - temperature recorded no interaction at all three measured temperatures as the time approached 70 (hrs). The result of this interactions resulted in noticeable decrease in the production of CoNP at time - pH and time - temperature plots. pH - temperature showed no interaction but showed a continuous increase in the production of CoNP as the increase in pH approached 8.0.

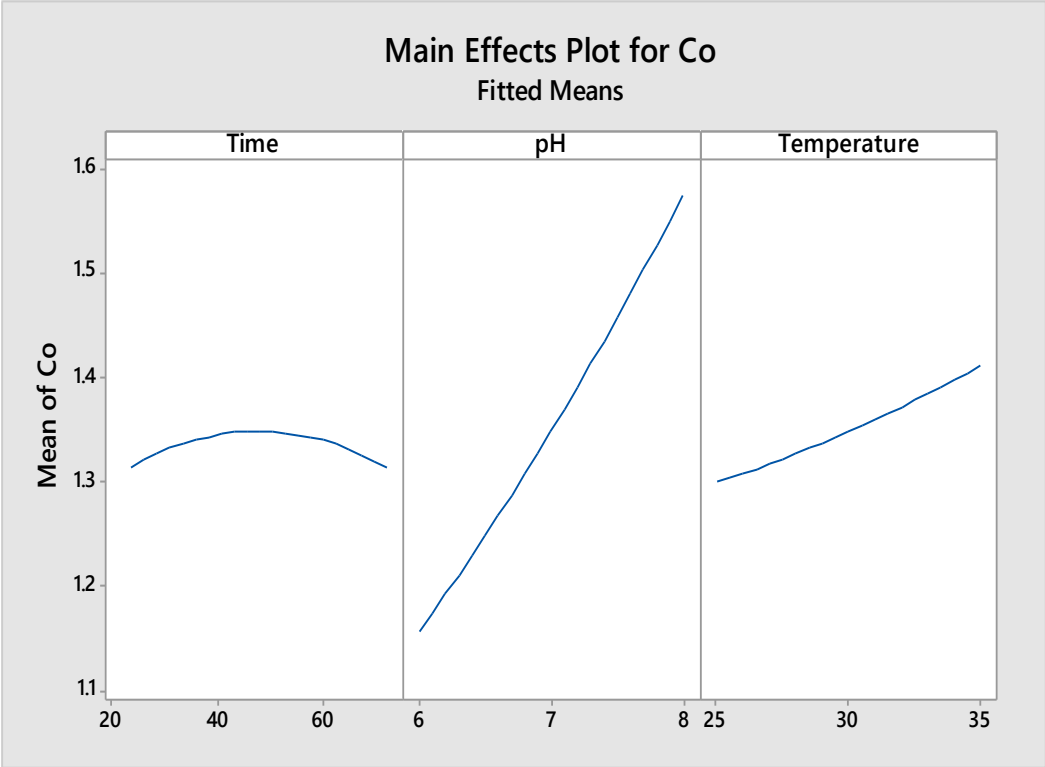

Figure 4.25: Main Effect Plots for Comelina Nanoparticle production

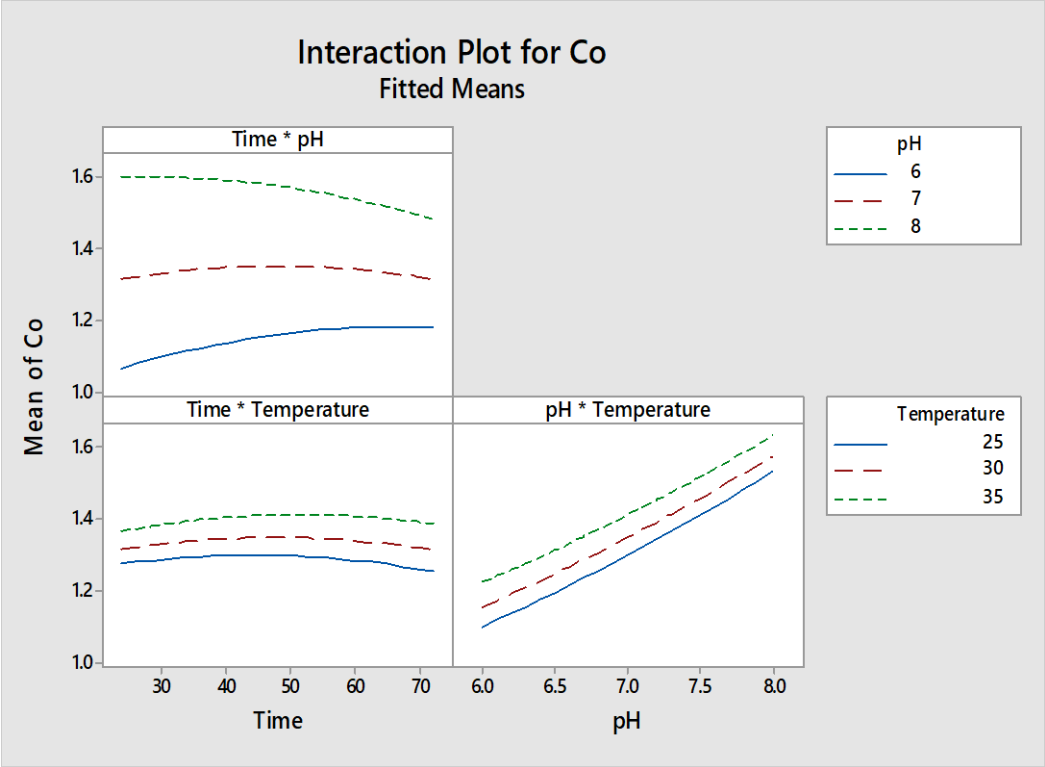

Figure 4.26: Interaction Plots for Comelina Nanoparticle production

4.14 Response Surface Plots for the Production Comelina Nanoparticle

The response surface plot for the production of CoNP at holding time value observations showed no increase in production of the CoNP with increased temperature and pH as temperature and pH approached 35 degrees and 8 respectively (Figure 4.27).

Also, the response surface plot for the production of CoNP at constant holding pH showed steady increase in production of the CoNP as temperature and time were increased and approached 35^{o}C and 70 (hours) respectively (Figure 4.28).

The response surface plot observations for the production of CoNP at constant holding Temperature value (Figure 4.29), showed that there was a steady increase in the production of CoNP as the time and pH was increased.

Findings of the response surface regression shows that pH had an overall significant single effect while time - time and pH - temperature had no significant interactive effect on the production of the CoNP at $P<0.05$ as shown in appendix A. the regression had an R^2 value of 87.90% indicating that little percentage of the finding occurred by chance.

The Regression Equation in Uncoded Units is given as:

$$\begin{aligned} Co - Response \\ &= 0.46 + 0.0203\, Time(hrs) + 0.126\, pH \\ &- 0.001\, Temperature - 0.000060\, Time(hrs) * Time(hrs) \\ &+ 0.0168\, pH * pH + 0.000027\, Temperature * Temperature \\ &- 0.000245\, Time(hrs) * pH + 0.000085\, Time(hrs) \\ &* Temperature - 0.0011\, pH * Temperature \end{aligned}$$

4.15 Optimization of the production of Comelina Nanoparticle

Figure 4.30 shows the optimization plots for the production of CoNP. The plot indicated that the optimum conditions for the production of CoNP are pH 8.0, temperature of 35 degrees Celsius and a time of 72 hours. At this conditions the maximum yield that would be achieved would have a response of 1.6485.

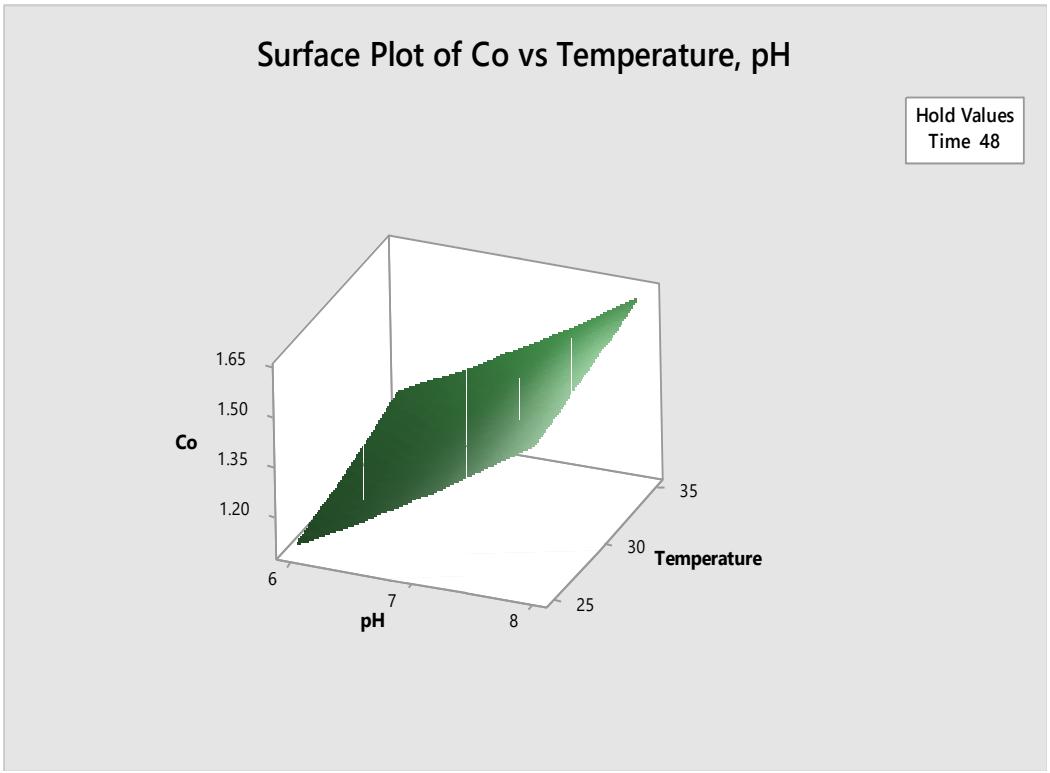

Figure 4.27: Surface Plot of Co-Response vs Temperature, pH (hrs)

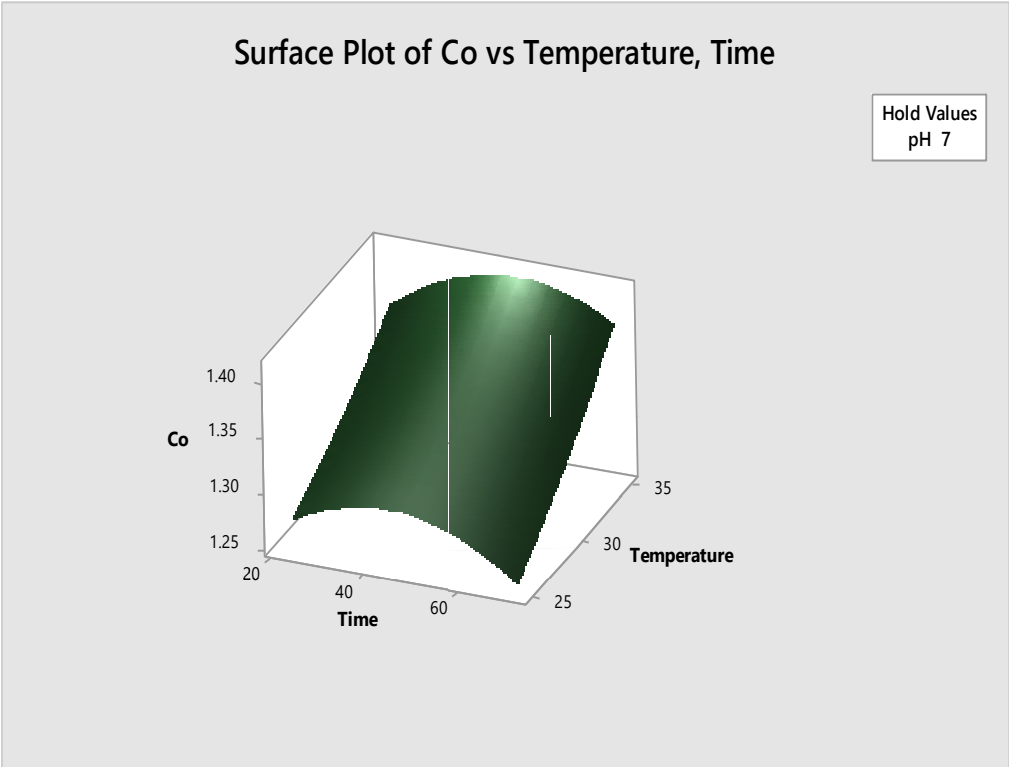

Figure 4.28: Surface Plot of Co-Response vs Temperature, Time (hrs)

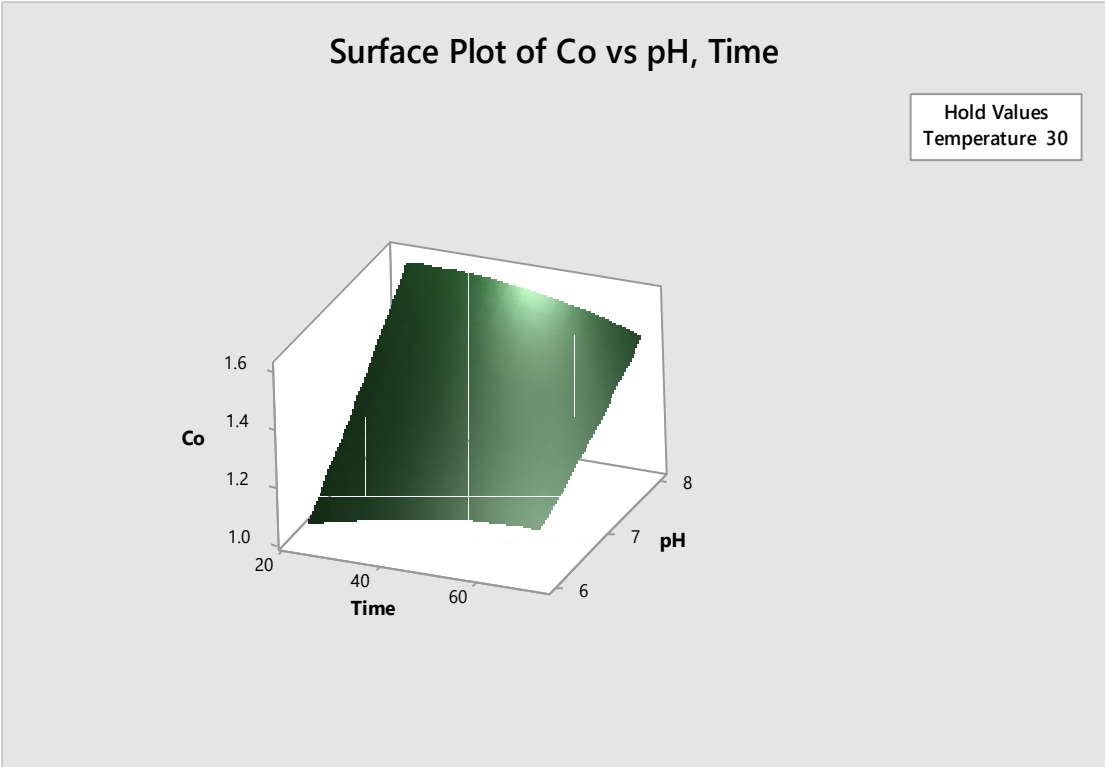

Figure 4.29: Surface Plot of Co-Response vs pH, Time (hrs)

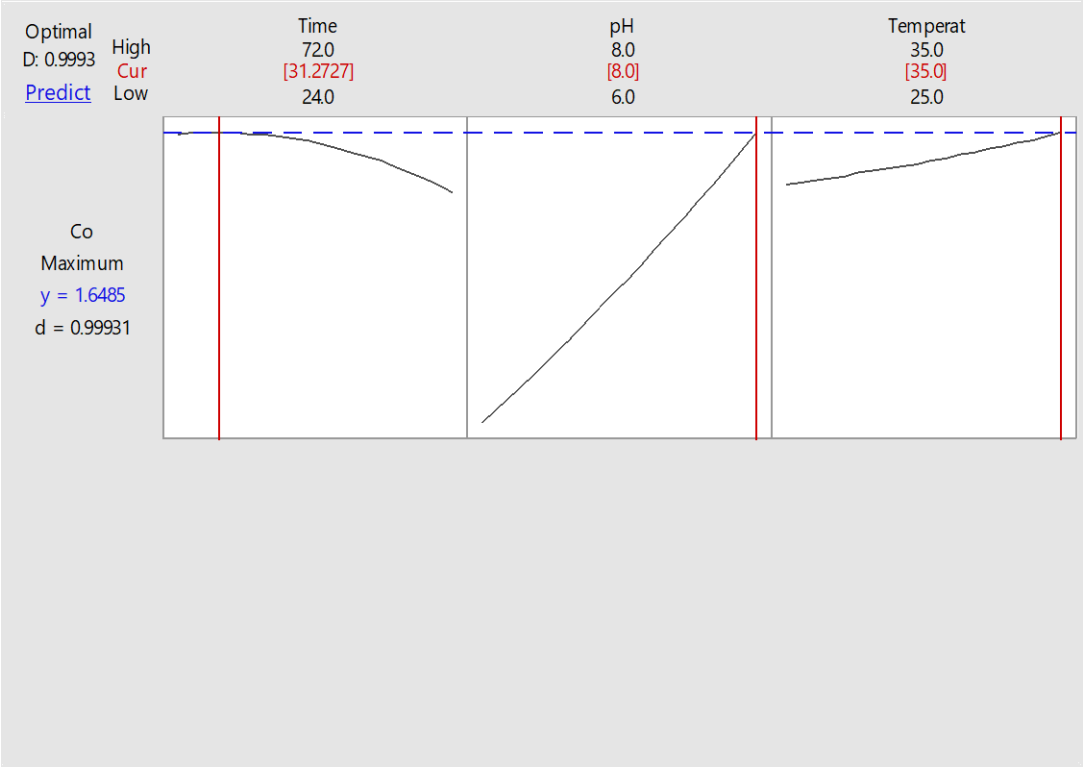

Figure 4.30: Optimization Plot for Comelina Nanoparticle production

4.16 Main Effect and Interaction Plots for the Production of Sweet Potato Leaf Synthesized Silver Nanoparticle (PoNP)

The findings of main effects plot for the production of sweet potato leaf synthesized silver nanoparticles (PoNP) (Figure 4.31) showed that there was continuous increase in the production of PoNP with increase in time after an initial slow production rate just before the 40 (hour) mark. This signifies that time is an essential component in the production of this Nanoparticle, Increase in pH resulted in a continuous increase in the production of PoNP as the pH approached pH 8, while increase in temperature resulted in a slow increase in production of PoNP as temperature approached 35^{o}C.

The findings of the interaction plots for the production of PoNP (Figure 4.32) shows that at constant time, time - pH, there was no interaction. Time - temperature recorded an interaction by the three measured temperatures as the time approached 20(hrs) mark. The observations of this interactions resulted in noticeable increase in the production of PoNP as time - temperature plot approached the 70 (hour) mark. pH - temperature showed no interaction but showed slow increase in the production of PoNP as the increase in pH approached 8.0.

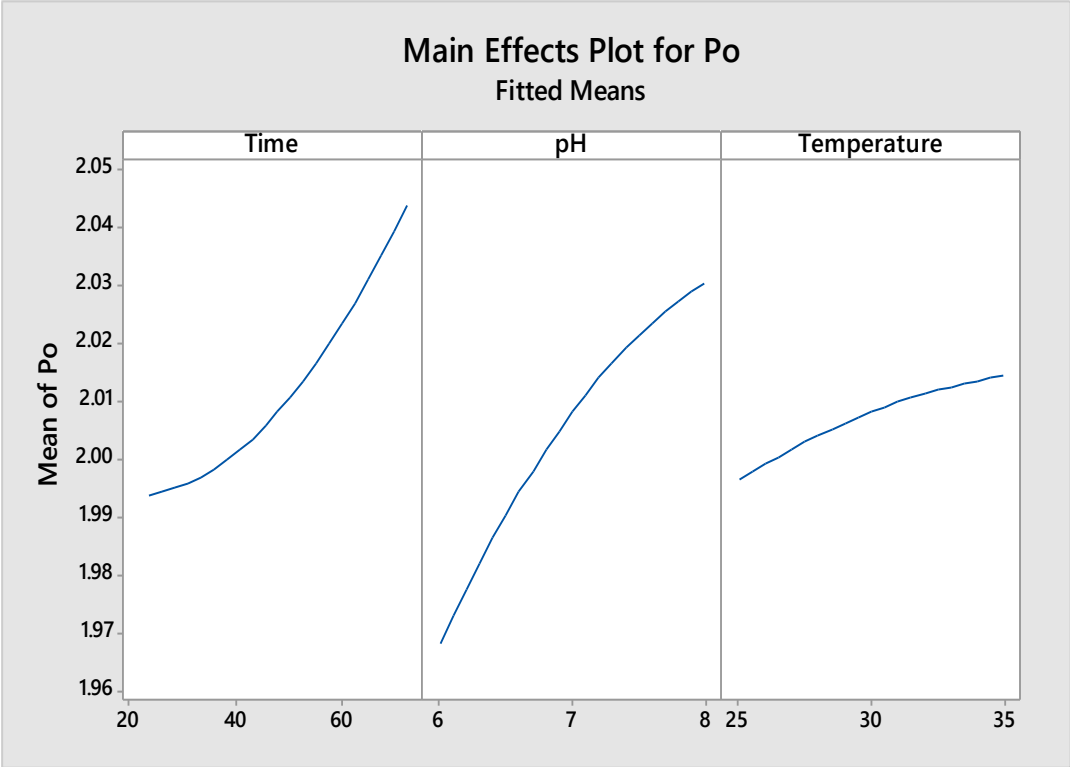

Figure 4.31: Main effect plots for Potato leaf Nanoparticle production

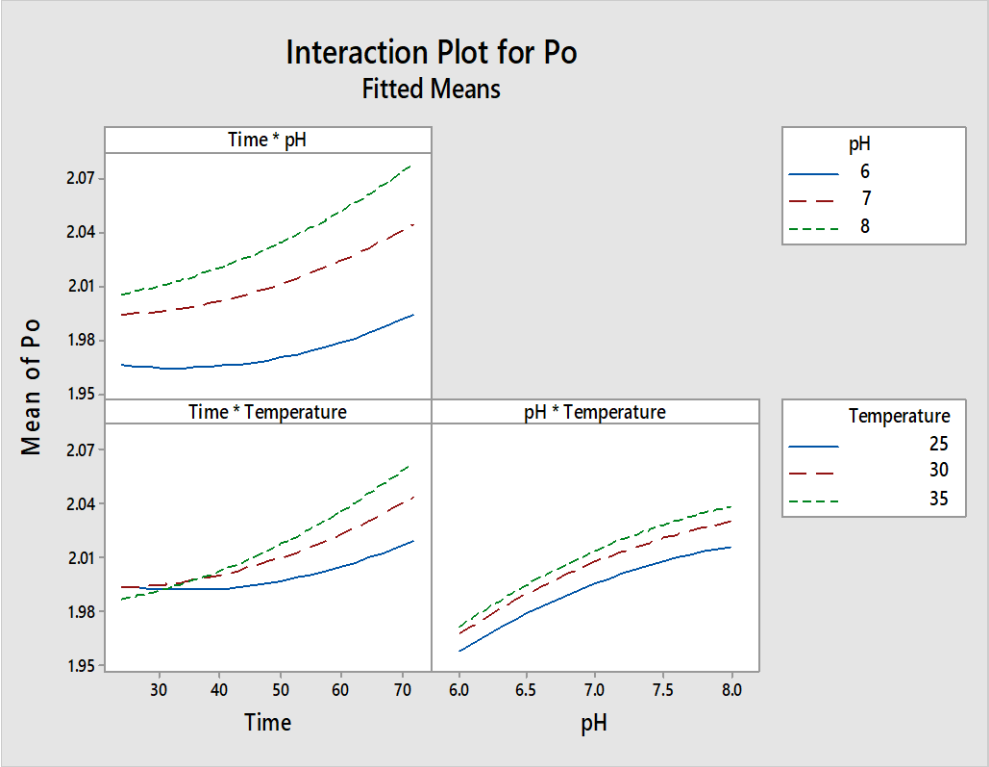

Figure 4.32: Interaction plots for Potato leaf Nanoparticle production

4.17 Response Surface Plots for the Production Potato leaf Nanoparticle

The response surface plot for the production of PoNP at holding time values showed slight increase production of the PoNP with increased Temperature and pH as temperature and pH approached 35 degrees and 8 respectively (Fig. 4.33).

Also, the response surface plot for the production of PoNP at constant holding pH showed no increase in production of the PoNP as temperature and pH increased and approached 35^{o}C and pH 8 respectively (Fig. 4.34).

The response surface plot results for the production of PoNP at constant holding temperature value (Figure 4.35), showed that there was a steady increase in the production of PoNP as the Time and pH was increased.

Observation of the response surface regression showed that pH and Time both had overall significant single effect, while the combinations of time - time, pH - pH, temperature - temperature, time - pH, time - temperature, and pH - temperature had no significant interactive effect on the production of the PoNP at $P<0.05$ as shown in the appendix A. the regression had an R^2 value of 96.83% indicating that about 11% of the results occurred by chance.

The Regression Equation in Uncoded Units is given as:

$$
\begin{aligned}
Po - Response \\
&= 1.590 - 0.00708\, Time(hrs) + 0.1195\, pH \\
&+ 0.0006\, Temperature + 0.000019\, Time(hrs) * Time(hrs) \\
&- 0.00875\, pH * pH - 0.000110\, Temperature * Temperature \\
&+ 0.000458\, Time(hrs) * pH + 0.000104\, Time(hrs) \\
&* Temperature + 0.00040\, pH * Temperature
\end{aligned}
$$

4.18 Optimization of the Production of Potato leaf Nanoparticle

Figure 4.36 shows the optimization plots for the production of PoNP, which indicated that the optimum conditions for the production of PoNP are pH 8.0, temperature of 35 degrees Celsius and a time of 72 hours. At this conditions the maximum yield that would be achieved would have a response of 2.0977.

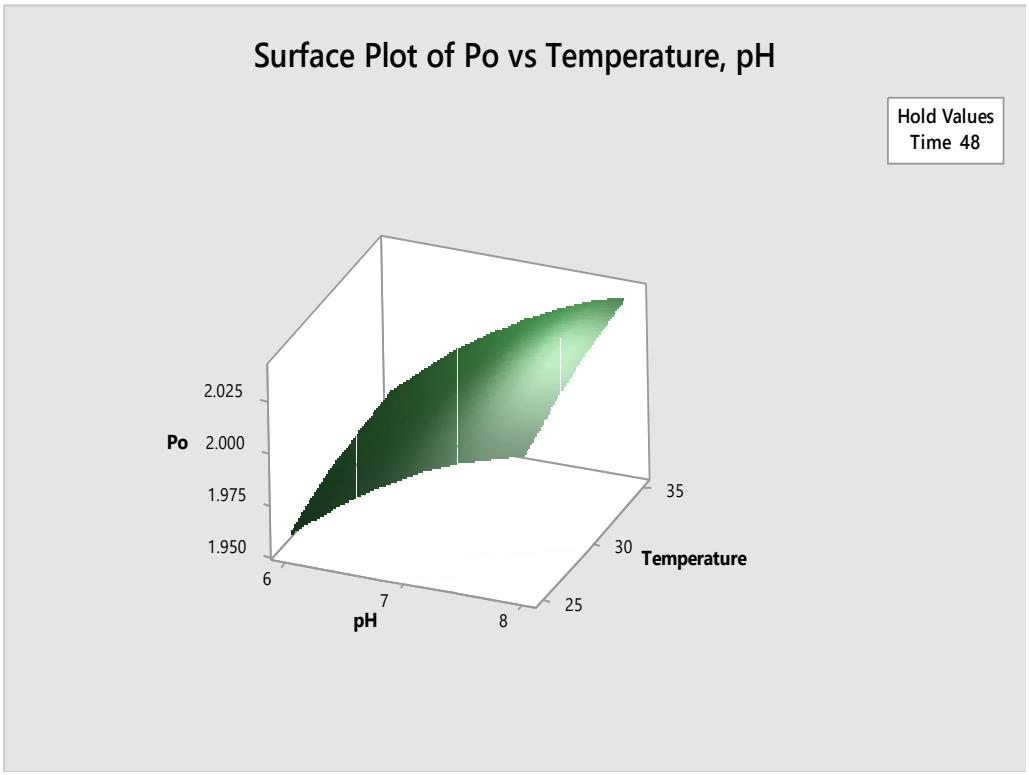

Figure 4.33: Surface Plot of Po-Response vs Temperature, pH (hrs)

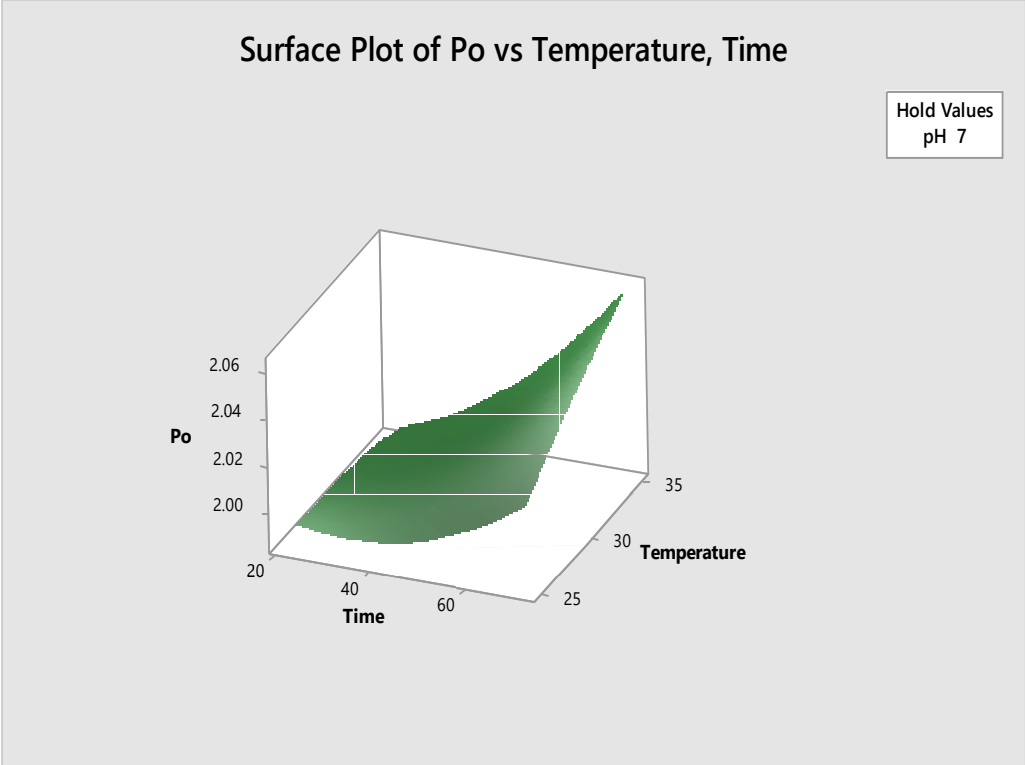

Figure 4.34: Surface Plot of Po-Response vs Temperature, Time (hrs)

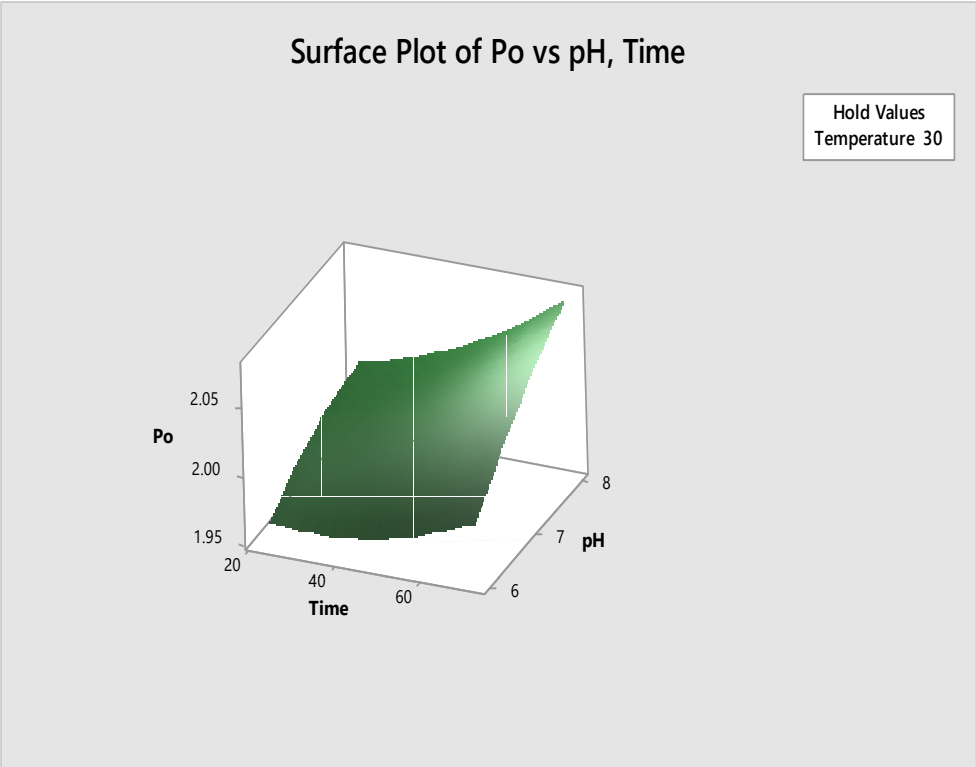

Figure 4.35: Surface Plot of Po-Response vs pH, Time (hrs),

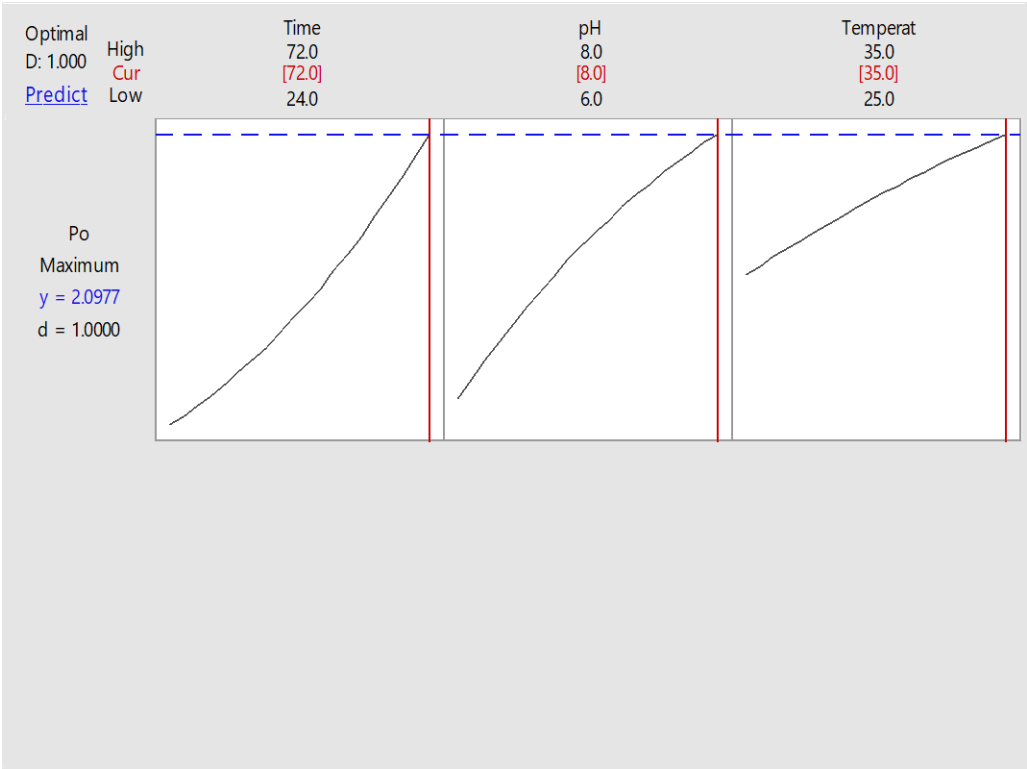

Figure 4.36: Optimization Plot for Potato leaf Nanoparticle production

4.19 Main Effect and Interaction Plots for the Production of Uziza Leaf Synthesized Silver Nanoparticle (UzNP)

The findings of main effects plot for the production of Uziza leaf synthesized silver nanoparticles (UzNP) (Figure 4.37) showed that there was little increase in the production of UzNP at 70 (hours) after a very long lag phase just after the 60 (hour) mark. This signifies that time was not really an essential component in the production of this nanoparticle. Increase in pH resulted in a continuous increase in the production of UzNP as the pH approached pH 8, while increase in temperature resulted in a sharp decrease in production of UzNP, but production of UzNP increased as temperature approached 35^0C.

The findings of the interaction plots for the production of UzNP (Figure 4.38) shows that at constant time, time - pH, there was no interaction. time - temperature recorded an interaction between the 30 and 40 (hrs) mark which influenced the production of UzNP at a temperature of 25^0C at the time approached the 70 (hour) mark. pH - temperature showed an interaction in between pH 5 and 70. The finding of this interactions resulted in noticeable increase in the production of UzNP as pH approached 8.0.

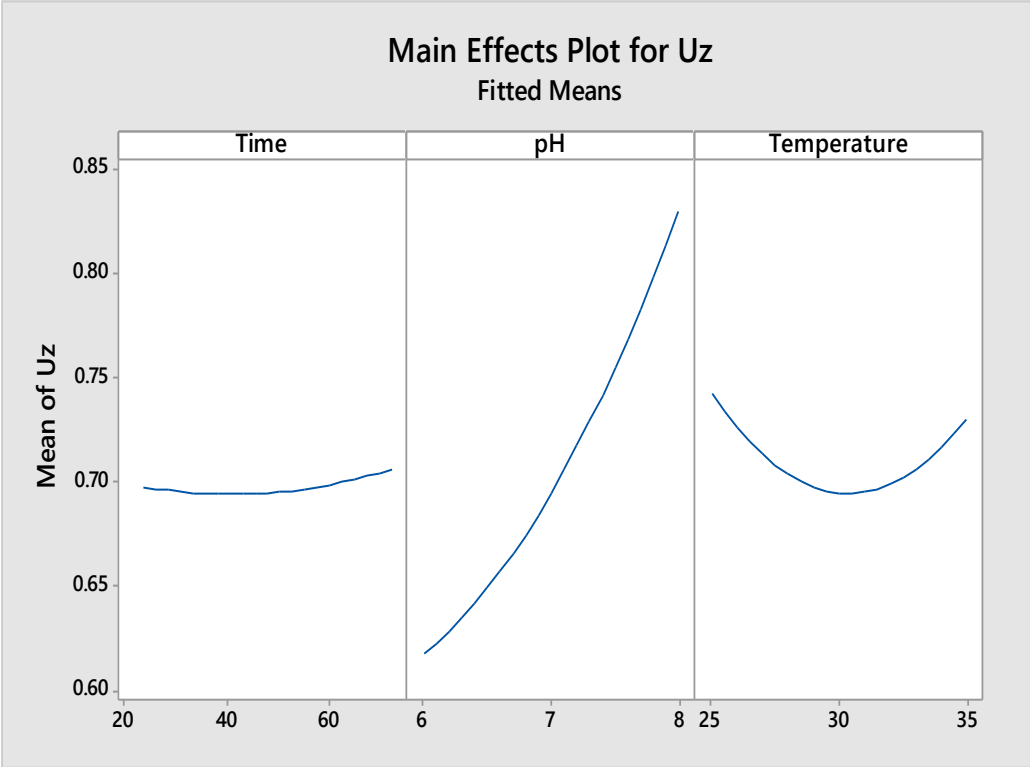

Figure 4.37: Main Effect Plots for Uziza Nanoparticle production

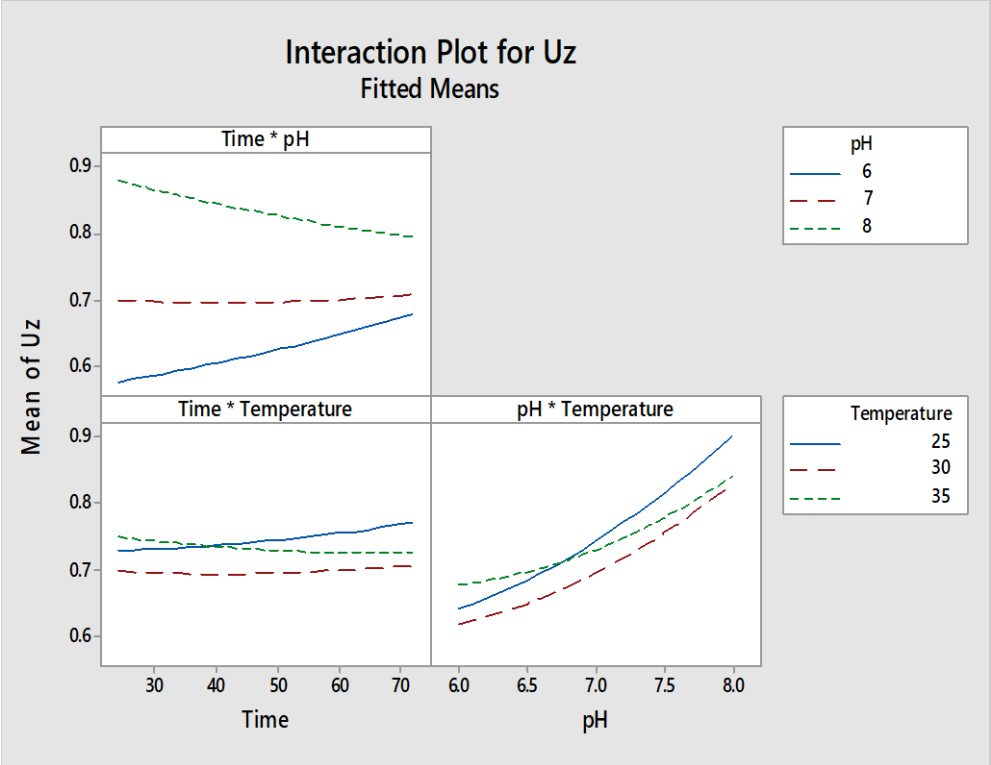

Figure 4.38: Interaction Plots for Uziza Nanoparticle production

4.20 Response Surface Plots for the Production Uziza Nanoparticle

The response surface plot for the production of UzNP at constant holding Time (Figure 4.39), showed slight increase in production of the UzNP as temperature and pH increased and approached 35^{o}C and pH 8 respectively.

The response surface plot observation for the production of UzNP at holding pH value (Figure 4.40), showed an initial decrease in the production of UzNP with increased Temperature and Time. But as Temperature and Time approached 35 degrees and 70 (hours) respectively, there was a sharp increase in the production of UzNP.

The response surface plot results for the production of UzNP at constant holding Temperature value (Figure 4.41), showed that there was a steady increase in the production of UzNP as the Time and pH was increased.

Findings of the response surface regression showed that pH had an overall significant single effect, while the combinations of time - time, pH - pH, temperature - temperature, time - pH, time - temperature, and pH - Temperature had significant interactive effects on the production of the UzNP at $P < 0.05$ as shown in the appendix A. the regression had an R^2 value of 96.43% indicating that about 9% of the findings occurred by chance.

The Regression Equation in Uncoded Units is given as:

$$
\begin{aligned}
Uz - Response \\
&= 1.060 + 0.01666\, Time(hrs) - 0.058\, pH \\
&- 0.0611\, Temperature + 0.000013\, Time(hrs) * Time(hrs) \\
&+ 0.02879\, pH * pH + 0.001672\, Temperature * Temperature \\
&- 0.001948\, Time(hrs) * pH - 0.000135\, Time(hrs) \\
&* Temperature - 0.00485\, pH * Temperature
\end{aligned}
$$

4.21 Optimization of the Production of Uziza Nanoparticle

Figure 4.42 shows the optimization plots for the production of UzNP, which indicated that the optimum conditions for the production of UzNP are pH 8.0, Temperature of 35 degrees Celsius and a time of 72 hours. At this conditions the maximum yield that would be achieved would have a response of 0.9350.

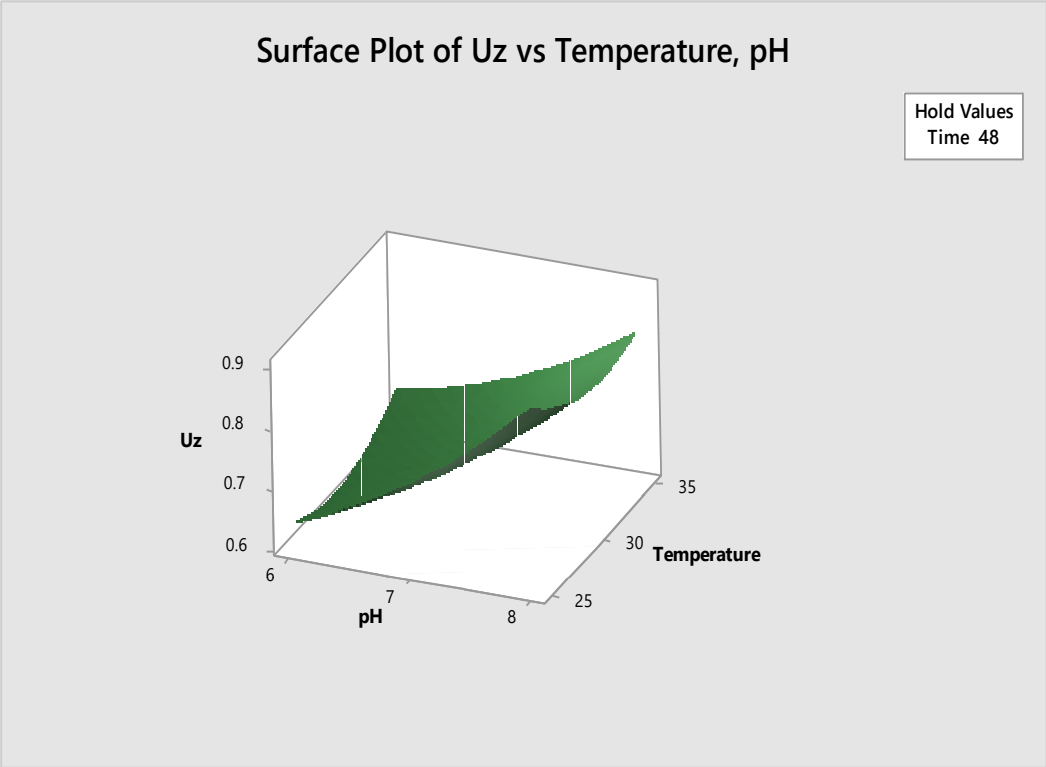

Figure 4.39: Surface Plot of Uz-Response vs Temperature, pH (hrs)

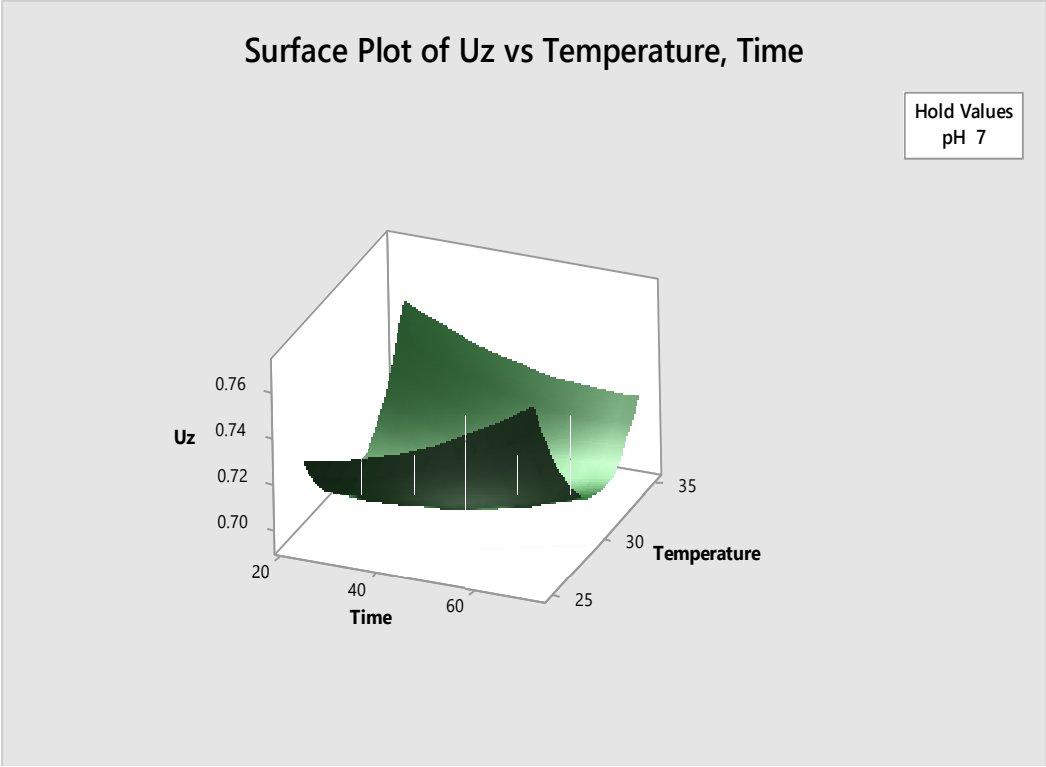

Figure 4.40: Surface Plot of Uz-Response vs Temperature, Time (hrs)

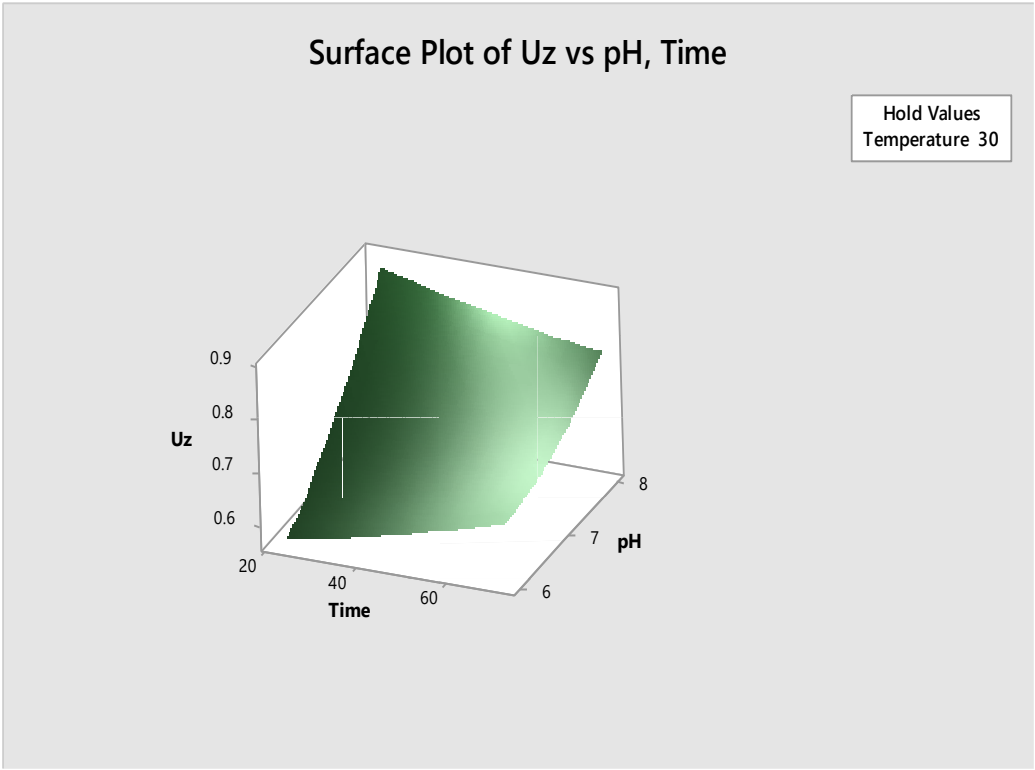

Figure 4.41: Surface Plot of Uziza -Response vs pH, Time (hrs),

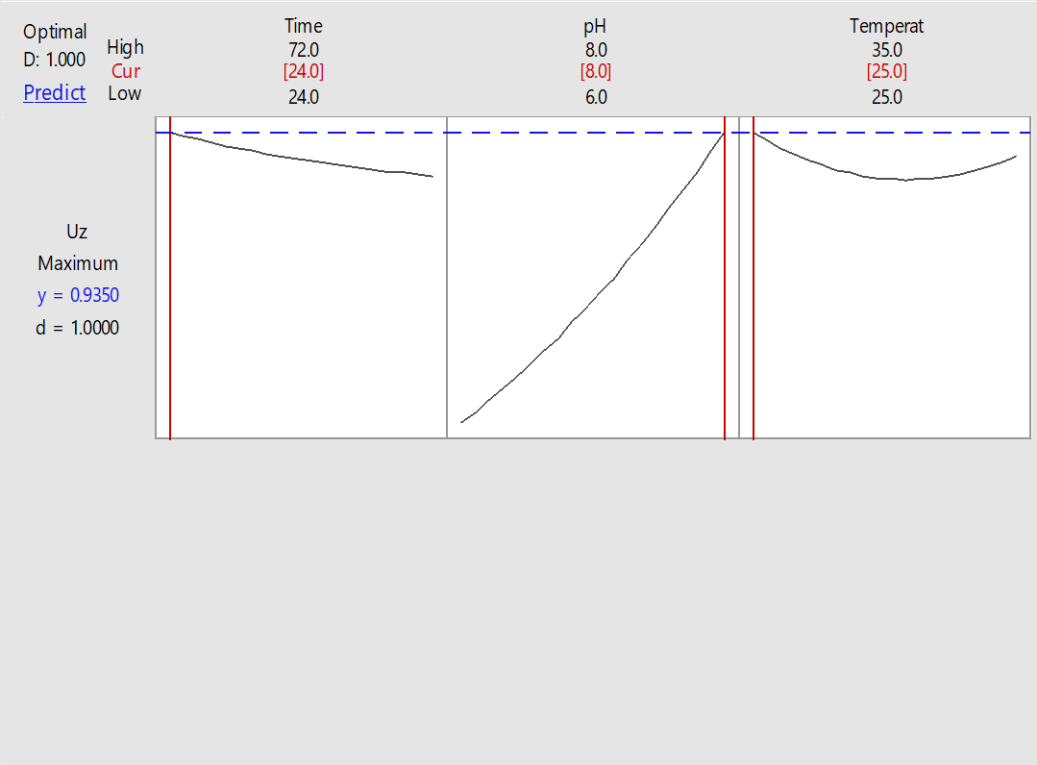

Figure 4.42: Optimization plot for Uziza Nanoparticle production

4.22 Main Effect and Interaction Plots for the Production of Neem Leaf Synthesized Silver Nanoparticle (NeNP)

The finding of main effects plot for the production of Neem leaf synthesized Silver nanoparticles (NeNP) (Figure 4.43) showed that there was an initial increase in the production of NeNP, followed by decline in production just after the 60 (hour) mark. This signifies that time was not really an essential component in the production of this nanoparticle, increased in pH resulted in a steady increase in the production of NeNP as the pH approached pH 8, while increase in temperature resulted in a slow increase in the production of NeNP as temperature approached 35^0C.

The findings of the interaction plots for the production of NeNP (Figure 4.44) shows that at constant time, time - pH, there was no interaction. Time - temperature recorded no interaction. pH - temperature showed no interaction. The findings of these non-interactions did not affect the production of NeNP.

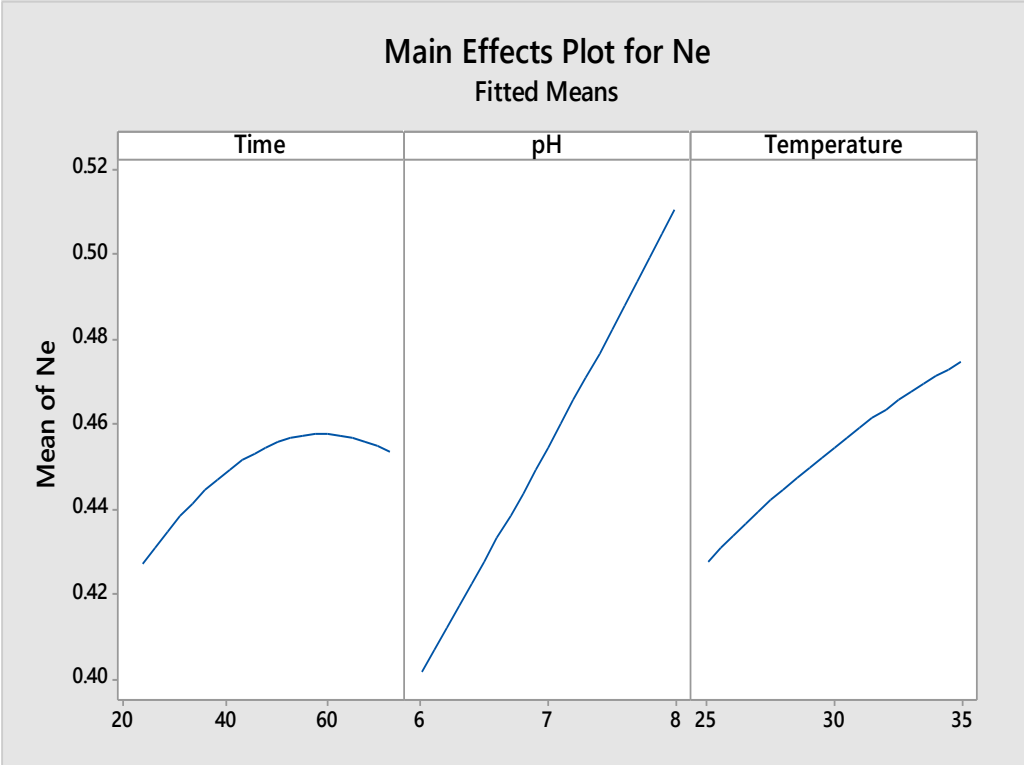

Figure 4.43: Main Effect Plots for Neem Nanoparticle production

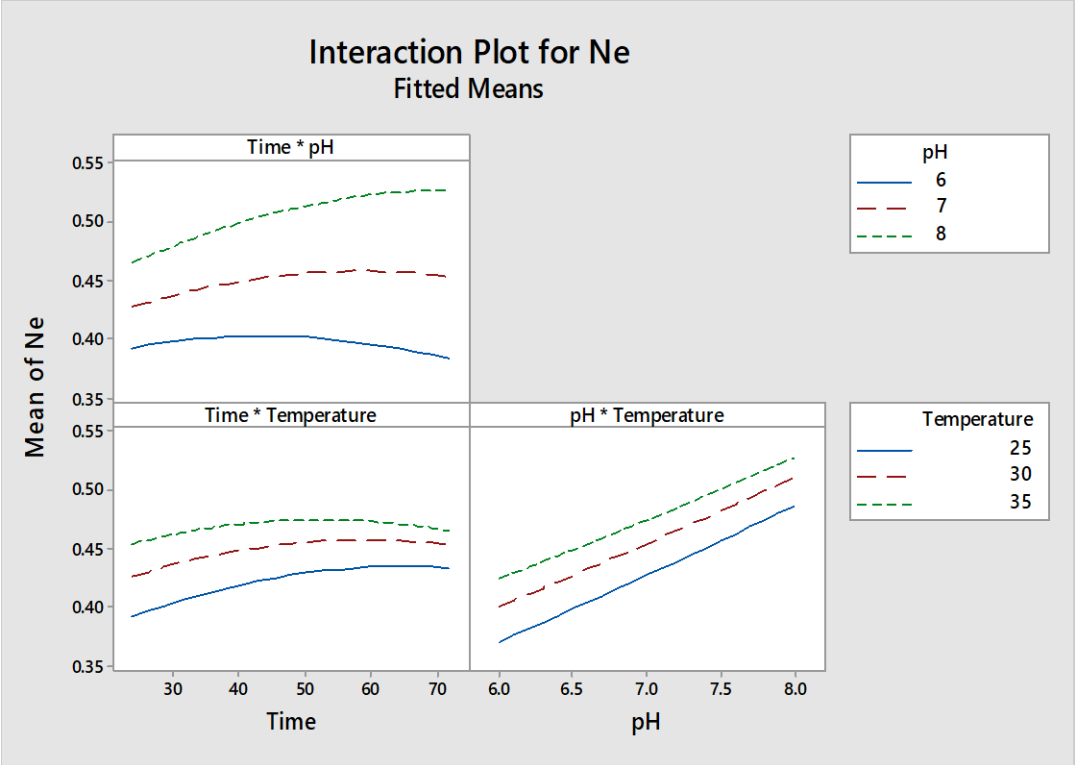

Figure 4.44: Interaction plots for Neem Nanoparticle production

4.23 Response Surface Plots for the Production Neem Nanoparticle

The response surface plot for the production of NeNP at holding time value (4.45) showed no increase in the production of NeNP with increased pH, but as temperature approached 35^0C, there was a marked increase in the production of NeNP.

Also, the response surface plot for the production of NeNP at constant holding pH (4.46), showed sharp decrease in production of NeNP as time increased and approached 70 (hour) mark after an initial increase in production of NeNP up to the 60 (hour) mark.

The response surface plot observations for the production of NeNP at constant holding temperature value (Figure 4.47), showed that there was increase in the production of NeNP as the time and pH was increased but a sharp decrease in production was observed as the time approached the 70 (hour) mark.

Findings of the response surface regression showed that pH and temperature had an overall significant single effect, while the combinations of time - time, pH - pH, temperature - temperature, time - pH, time - temperature, and pH - temperature had no significant interactive effects on the production of the NeNP at $P<0.05$ as shown in the appendix A. The regression had an R^2 value of 95.04% indicating that about 11% of the results occurred by chance.

The Regression Equation in Uncoded Units is given as:

$$
\begin{aligned}
Uz - Response \\
&= 1.175 - 0.00042\,Time(hrs) + 0.016\,pH \\
&+ 0.0207\,Temperature - 0.000025\,Time(hrs) * Time(hrs) \\
&+ 0.00154\,pH * pH - 0.000138\,Temperature * Temperature \\
&+ 0.000760\,Time(hrs) * pH - 0.000065\,Time(hrs) \\
&* Temperature - 0.00065\,pH * Temperature
\end{aligned}
$$

4.24 Optimization of the production of Neem Nanoparticle

Figure 4.48 shows the optimization plots for the production of NeNP, which indicated that the optimum conditions for the production of NeNP are pH 8.0, Temperature of 35 degrees Celsius and a time of 72 hours. At this conditions the maximum yield that would be achieved would have a response of 0.5373.

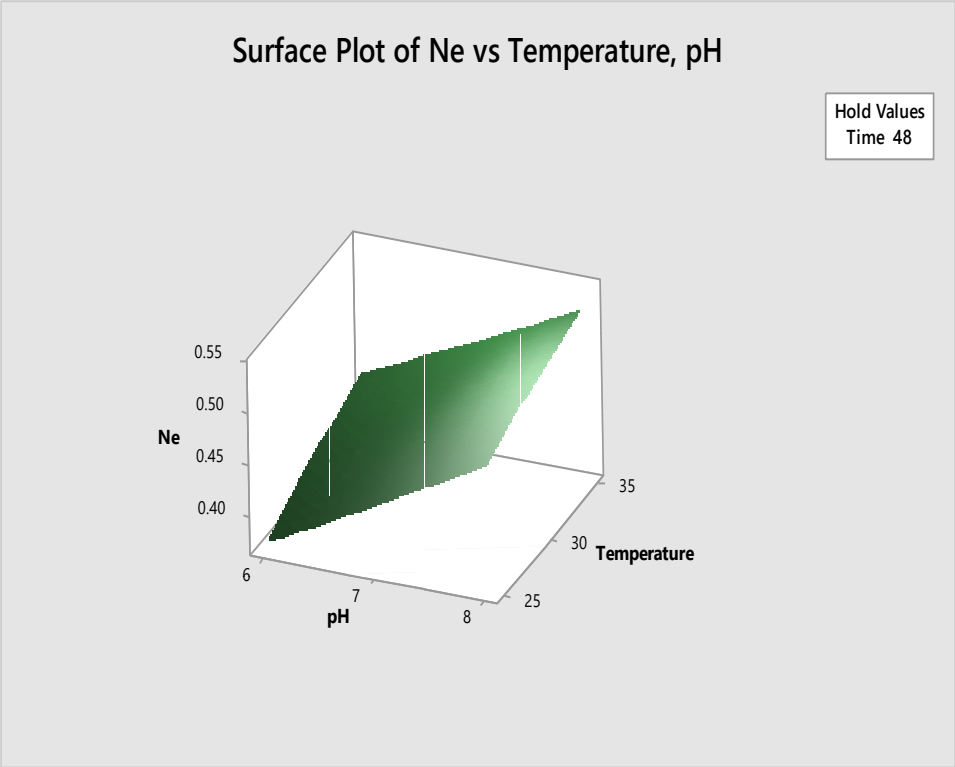

Figure 4.45: Surface Plot of Neem-Response vs Temperature, pH (hrs)

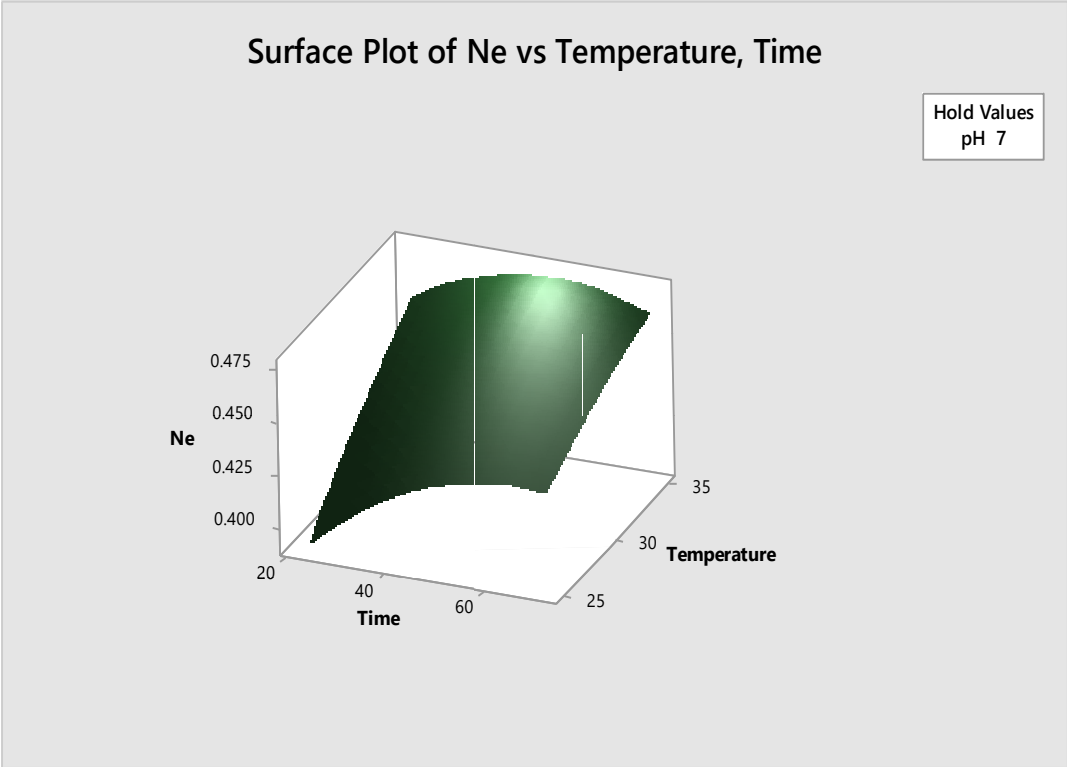

Figure 4.46: Surface Plot of Neem-Response vs Temperature, Time (hrs)

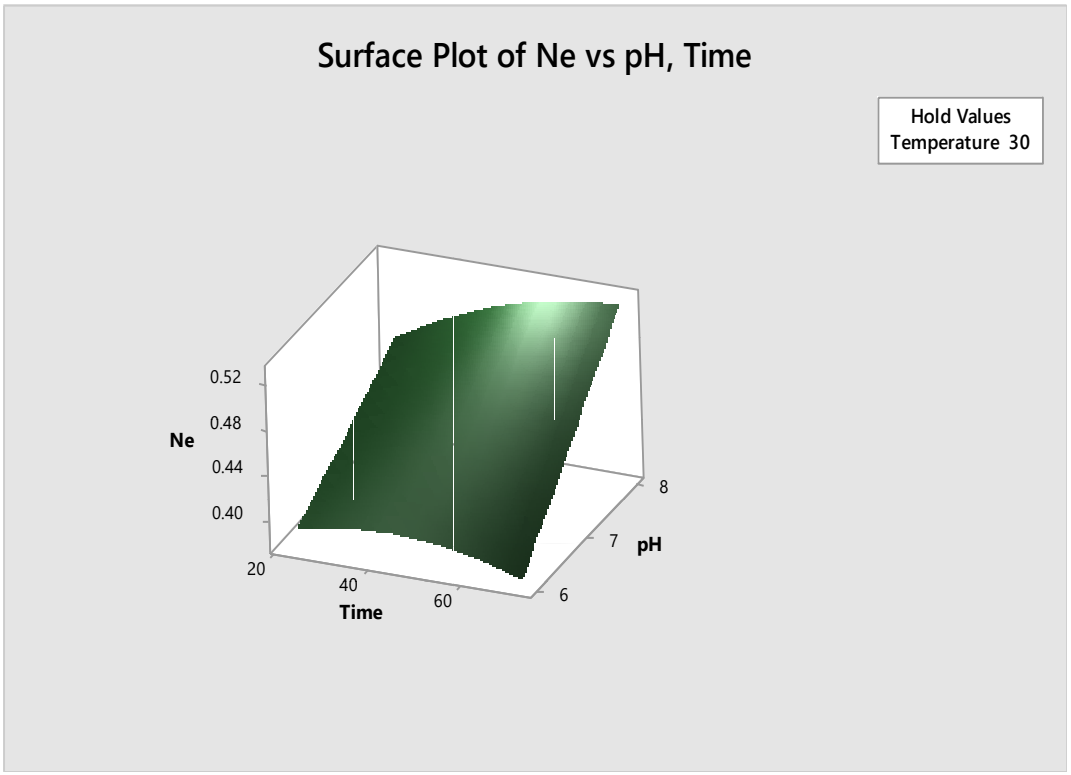

Figure 4.47: Surface Plot of Neem-Response vs pH, Time (hrs)

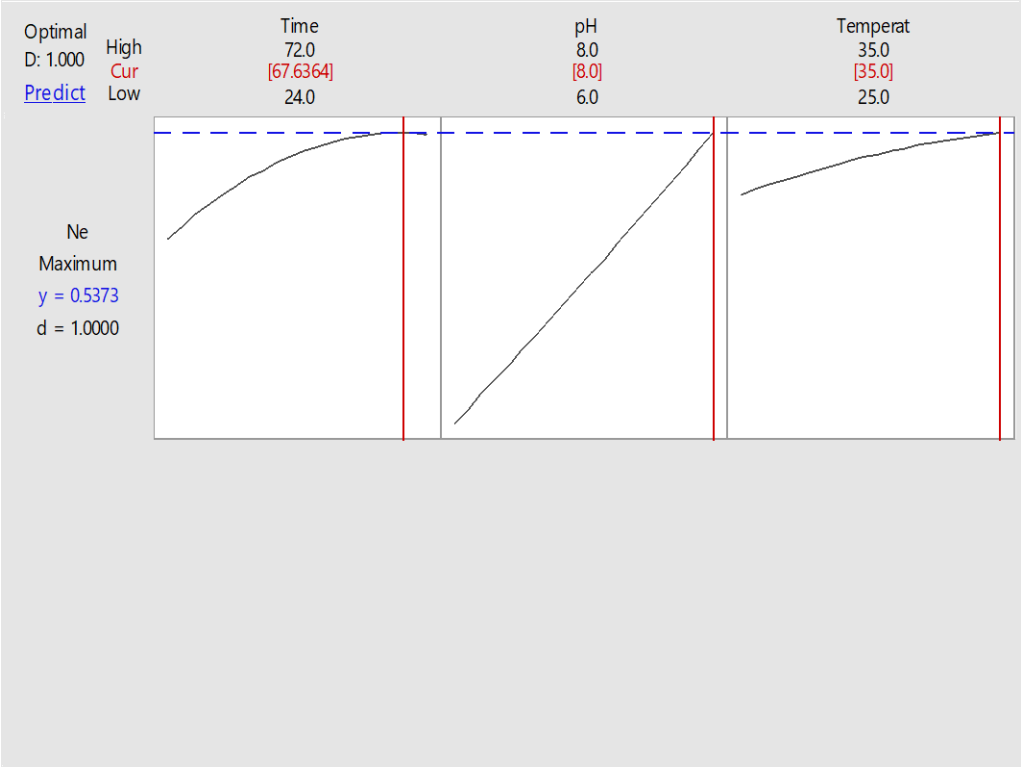

Figure 4.48: Optimization plot for Neem Nanoparticle production

4.25 Main Effect and Interaction Plots for the Production of Bitter Leaf Synthesized Silver Nanoparticle (BLNP)

The findings of main effects plot for the production of Bitter leaf synthesized Silver Nanoparticles (BLNP) (Figure 4.49) showed that there was an initial decrease in the production of BLNP, followed by an increase in the production of BLNP just after the 40 (hour) mark. This signifies that time was an essential component in the production of this nanoparticle, increased in pH resulted in a very high increase in the production of BLNP as the pH approached pH 8 after an initial lag phase at pH 6. Increase in temperature resulted in an initial increase in the production of BLNP as temperature approached 30^0C, which was subsequently followed by a sharp decrease in production as temperature approached 35^0C.

The findings of the interaction plots for the production of BLNP (Figure 4.50) shows that at constant time, time - pH had an interaction at the 30 (hour) mark, this interaction did not however, influence the increased production of BLNP. time - temperature recorded interactions at all temperatures at the 40 and 70 (hours) mark. pH - temperature showed no interaction. The findings of these non-interactions did not affect the positively, the increased production of BLNP.

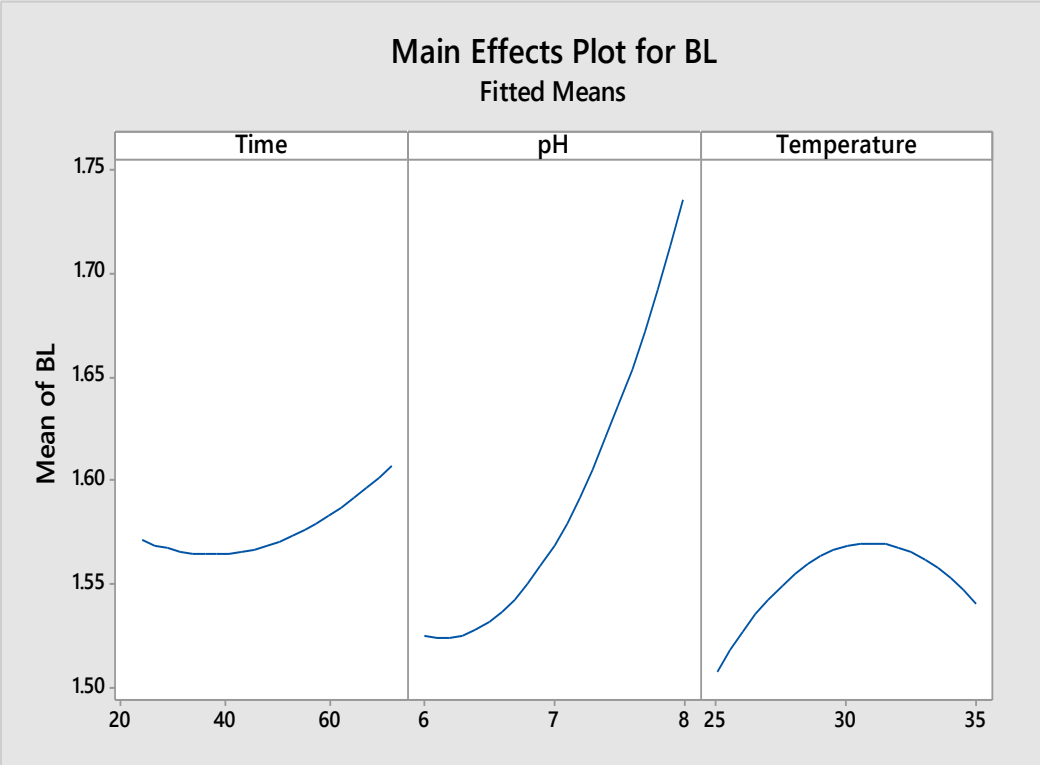

Figure 4.49: Main effect plots for Bitter Leaf Nanoparticle production

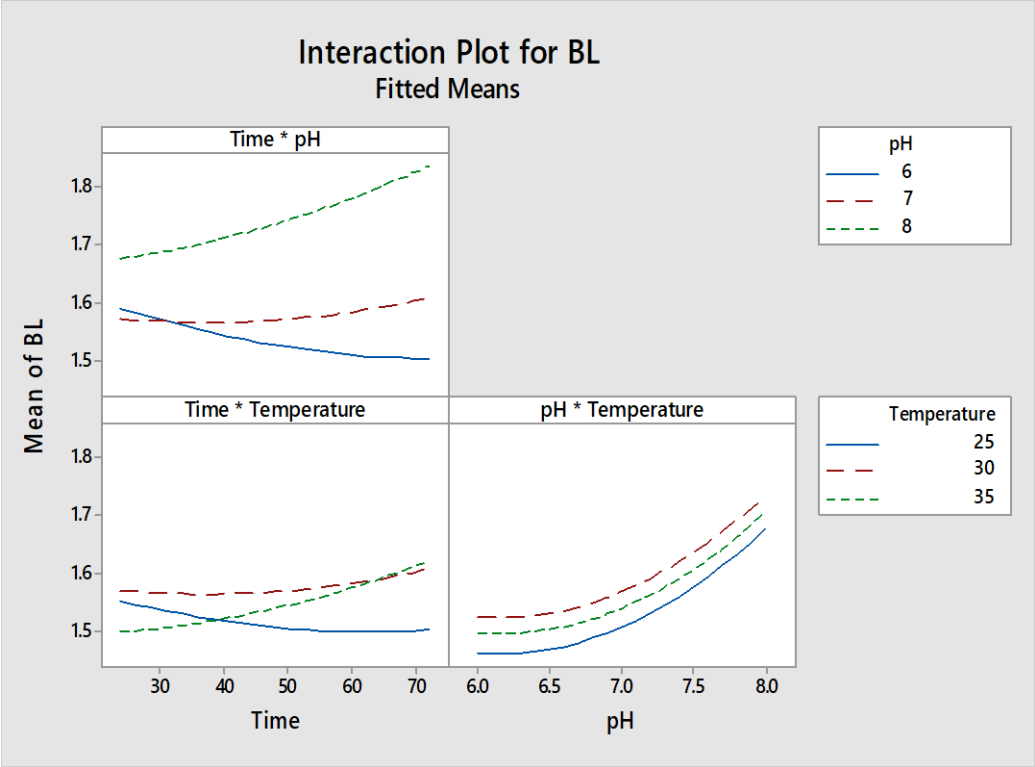

Figure 4.50: Interaction plots for Bitter Leaf Nanoparticle production

4.26 Response Surface Plots for the Production Bitter Leaf Nanoparticle

The response surface plot for the production of BLNP at holding time value (Figure 4.51), showed that there was no increase in the production of BLNP as the time was increased but an increase in production was observed as the pH approached pH8.

Also, the response surface plot for the production of BLNP at constant holding pH (Figure 4.52), showed an initial increase in the production of BLNP with increased Temperature and Time. But as time approached 50(hours) and Temperature 35^0 C, there was sharp decrease in the production of BLNP.

The response surface plot findings for the production of BLNP at constant holding Temperature value (Figure 4.53), showed that there was an initial increase in the production of BLNP as the time and was increased, this was followed by a continuous decrease in production after the 40(hour) mark. Also an initial increase was observed with increase in pH, this also was followed by a sharp decrease, and then subsequent continuous increase in the production of BLNP as the pH approached pH8.

Findings of the response surface regression showed that pH had an overall significant single effect, while the combinations of time - time, pH - pH, temperature - temperature, time - pH, time - temperature, and pH - temperature had no significant interactive effects on the production of the BLNP at $P<0.05$ as shown in the appendix A. The regression had an R^2 value of 92.29% indicating that about 9% of the findings occurred by chance.

The Regression Equation in Uncoded Units is given as:

$$BL - Response = 3.49 - 0.0315\,Time(hrs) - 0.0867\,pH + 0.0959\,Temperature + 0.000036\,Time(hrs) * Time(hrs) + 0.00615\,pH * pH - 0.00178\,Temperature * Temperature + 0.00258\,Time(hrs) * pH + 0.000358\,Time(hrs) * Temperature - 0.00045\,pH * Temperature$$

4.27 Optimization of the production of Bitter Leaf Nanoparticle

Figure 4.54 shows the optimization plots for the production of BLNP, which indicates that the optimum conditions for the production of BLNP are pH 8.0, temperature of 35 degrees celsius and a time of 72 hours. At this conditions the maximum yield that would be achieved would have a response of 1.8543.

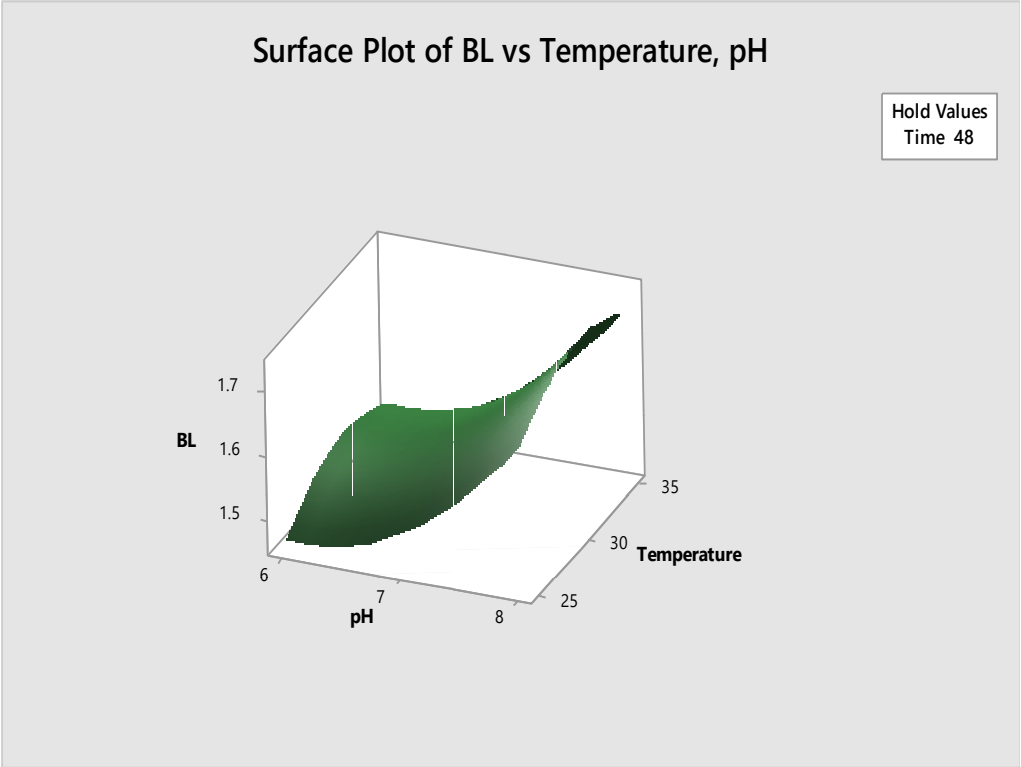

Figure 4.51: Surface Plot of BL-Response vs Temperature, PH

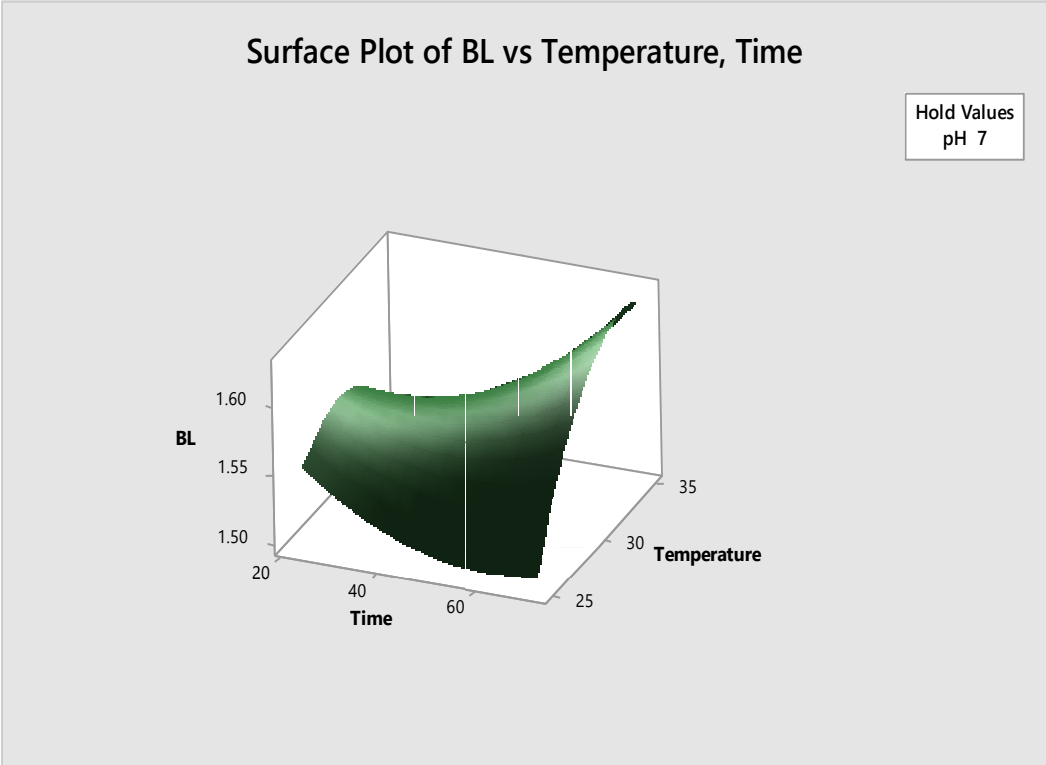

Figure 4.52: Surface Plot of BL-Response vs Temperature, Time (hrs)

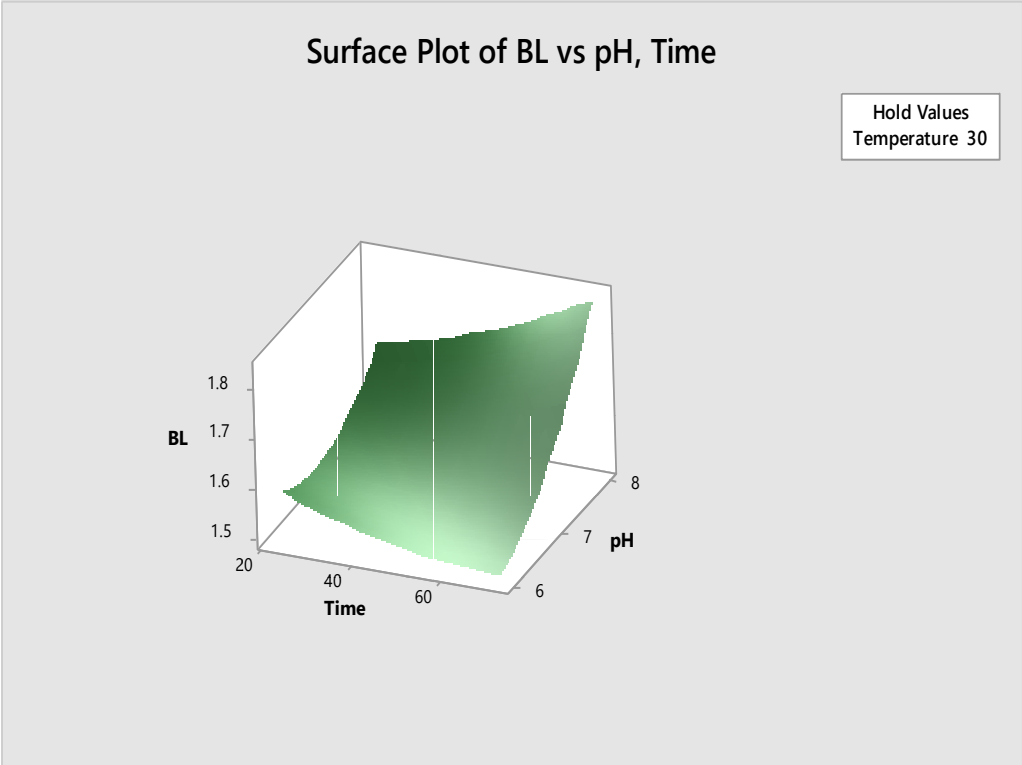

Figure 4.53: Surface Plot of BL-Response vs pH, Time (hrs)

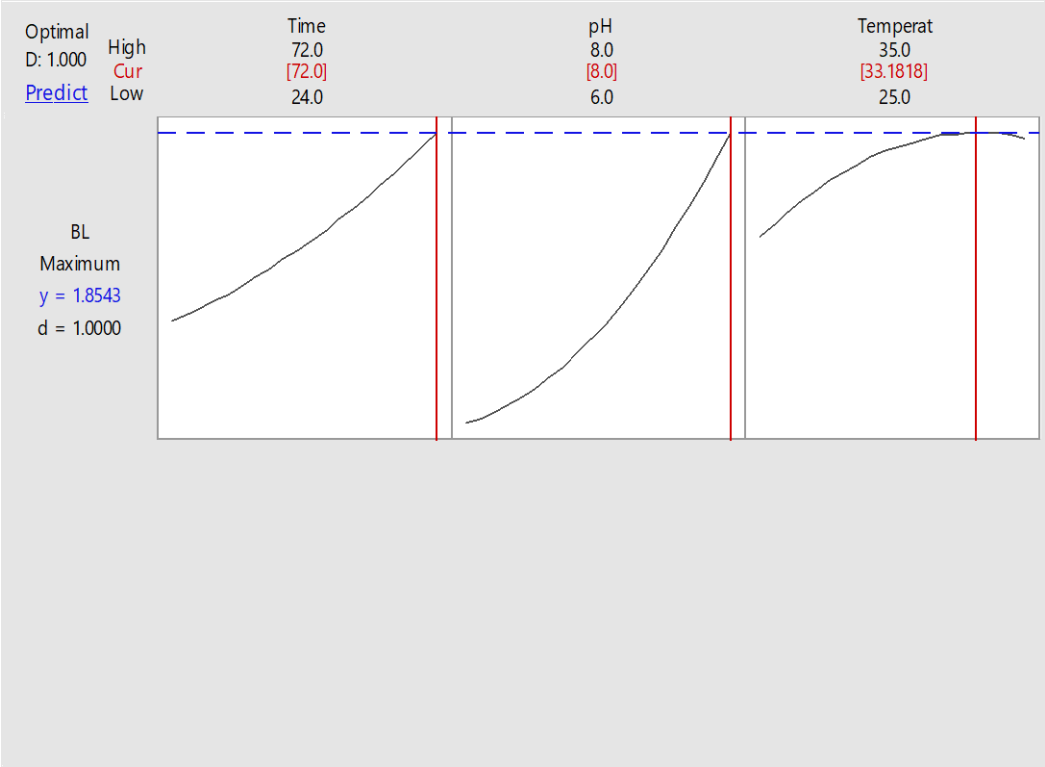

Figure 4.54: Optimization plot for Bitter Leaf Nanoparticle production

4.28 Main Effect and Interaction Plots for the Production of Independence leaf (*Chromolaena odorata*) Synthesized Silver Nanoparticle (XXYNP)

The findings of main effects plot for the production of Independence leaf (*Chromolaena Odorata*) synthesized silver nanoparticles (XXYNP) (Figure 4.55) showed an increase in in the production of XXYNP, after an lag phase just before the 40 (hour) mark. This signifies that time was an essential component in the production of this Nanoparticle, Increase in pH resulted in a very high increase in the production of XXYNP as the pH approached pH 8. Increase in temperature resulted in continuous decrease as temperature in the production of XXYNP as temperature approached 35^{o}C.

The findings of the interaction plots for the production of XXYNP (Figure 4.56) show that at constant time, time - pH had no interaction. time - temperature recorded interactions between all measured temperatures just before the 40 (hour) mark. pH - temperature showed interactions at the three measured pH. The findings of these interactions increased the production of XXYNP.

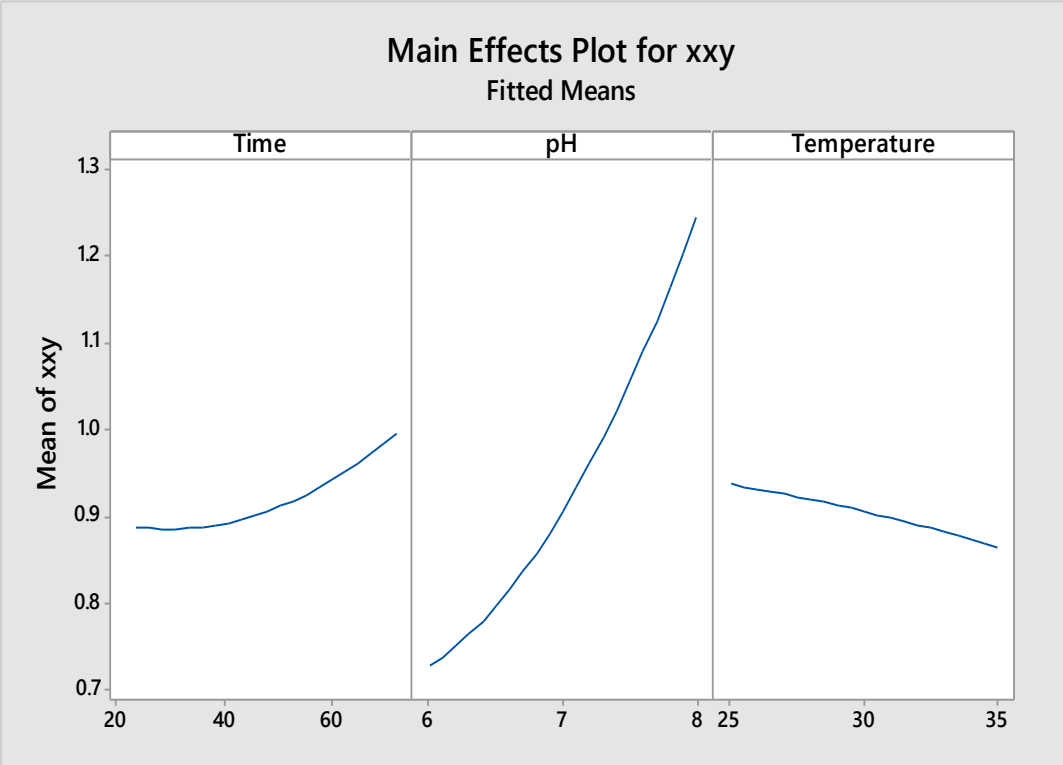

Figure 4.55: Main Effect plots for *Chromolaena odorata* Nanoparticle Production

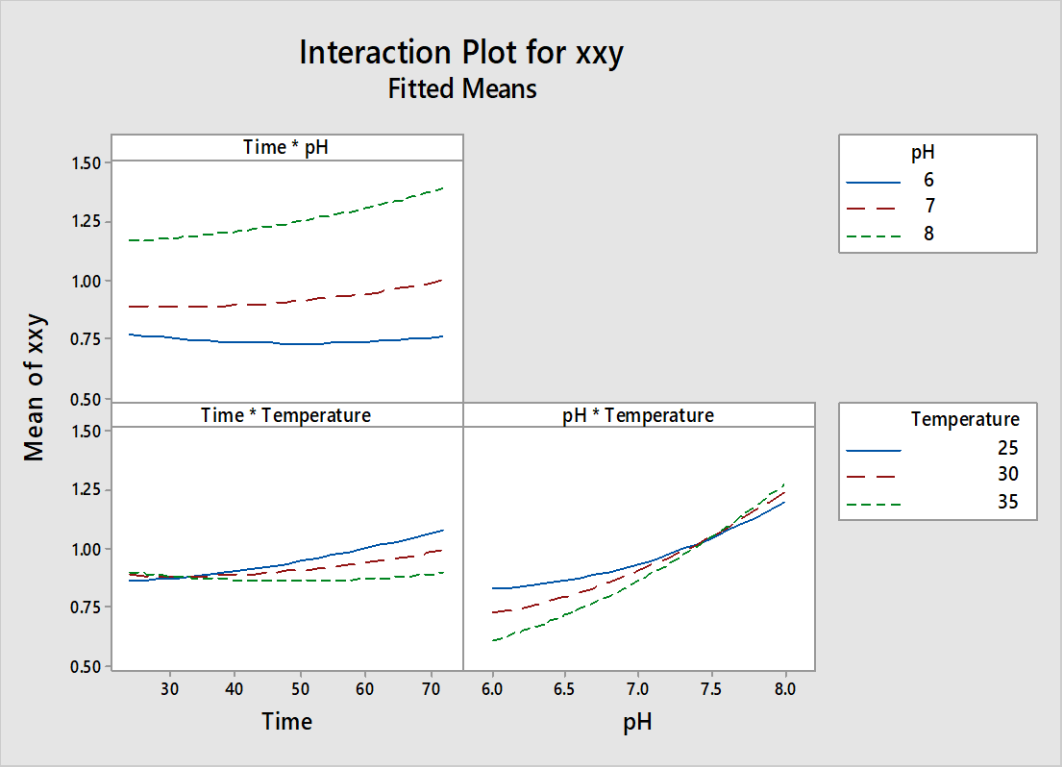

Figure 4.56: Interaction plots for *Chromolaena odorata* Nanoparticle Production

4.29 Response Surface Plots for the Production XXYNP

The response surface plot for the production of XXYNP at holding time value (Figure 4.57), showed slight increase in production of XXYNP as temperature and pH increased and approached 35^0C and pH 8 respectively. However, the increase observed with increase in temperature was lesser than that observed with increase in pH.

Also, the response surface plot for the production of XXYNP at constant holding pH (Figure 4.58), showed increase in the production of XXYNP with increased temperature and time.

The response surface plot results for the production of XXYNP at constant holding temperature value (Figure 4.59), showed that there was no increase in the production of XXYNP as the time was increased but an increase in production was observed as the pH approached pH 8.

Findings of the response surface regression showed that pH had an overall significant single effect, while the combinations of time - time, pH - pH, temperature - temperature, time - pH, time - temperature, and pH - temperature had no significant interactive effects on the production of the XXYNP at $P<0.05$ as shown in the appendix A. the regression had an R^2 value of 92.59% indicating that about 9% of the results occurred by chance.

The Regression Equation in Uncoded Units is given as:

$$\begin{aligned} XXY - Response &= 6.33 - 0.0068\, Time(hrs) - 1.418\, pH \\ &- 0.076\, Temperature + 0.000063\, Time(hrs) * Time(hrs) \\ &+ 0.0795\, pH * pH - 0.00020\, Temperature * Temperature \\ &+ 0.00246\, Time(hrs) * pH - 0.000471\, Time(hrs) \\ &* Temperature + 0.0148\, pH * Temperature \end{aligned}$$

4:30 Optimization of the production of XXYNP

Figure 4.60 shows the optimization plots for the production of XXYNP, which indicated that the optimum conditions for the production of XXYNP were pH 8.0, temperature of 35 degrees Celsius and a time of 72 hours. At this conditions the maximum yield that would be achieved would have a response of 1.4053.

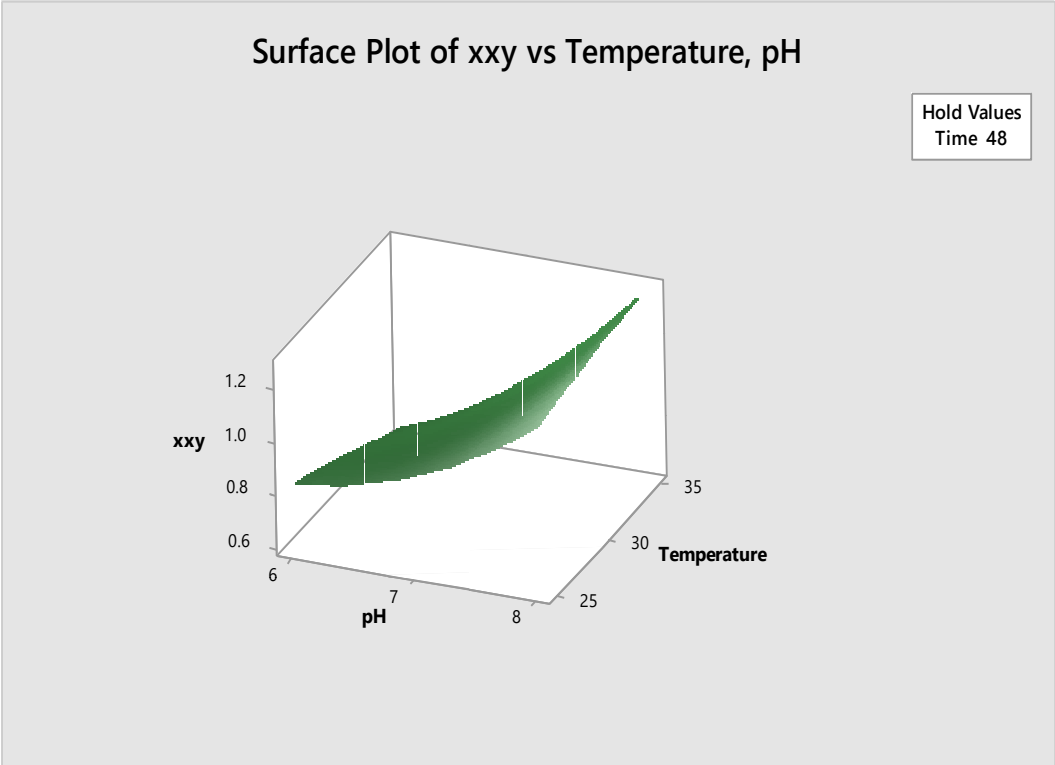

Figure 4.57: Surface Plot of *Chromolaena odorata* Response vs Temperature, pH (hrs)

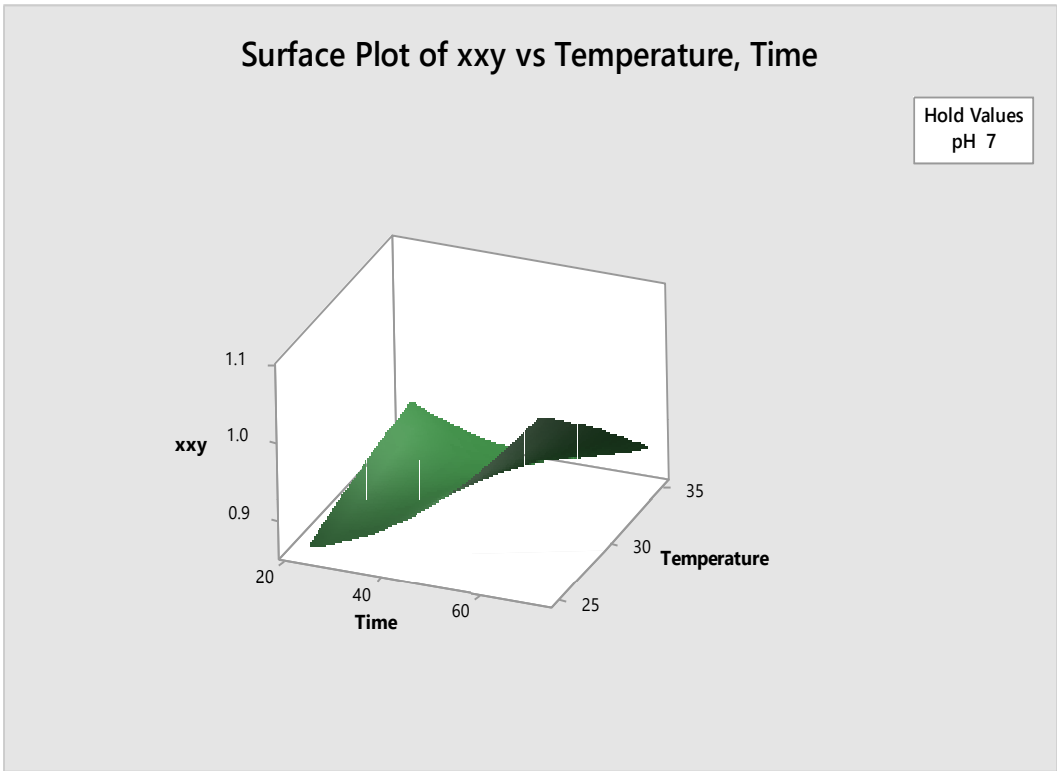

Figure 4.58: Surface Plot of *Chromolaena odorata* Response vs Temperature, Time (hrs)

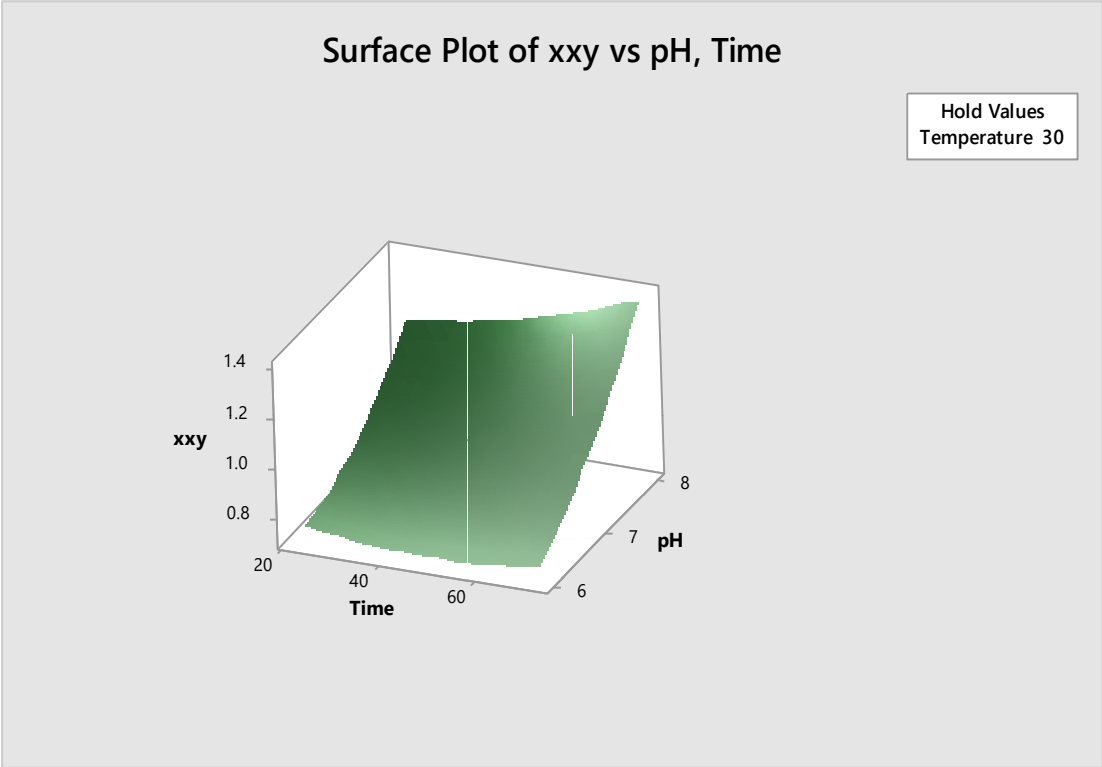

Figure 4.59: Surface Plot of *Chromolaena odorata* Response vs pH, Time

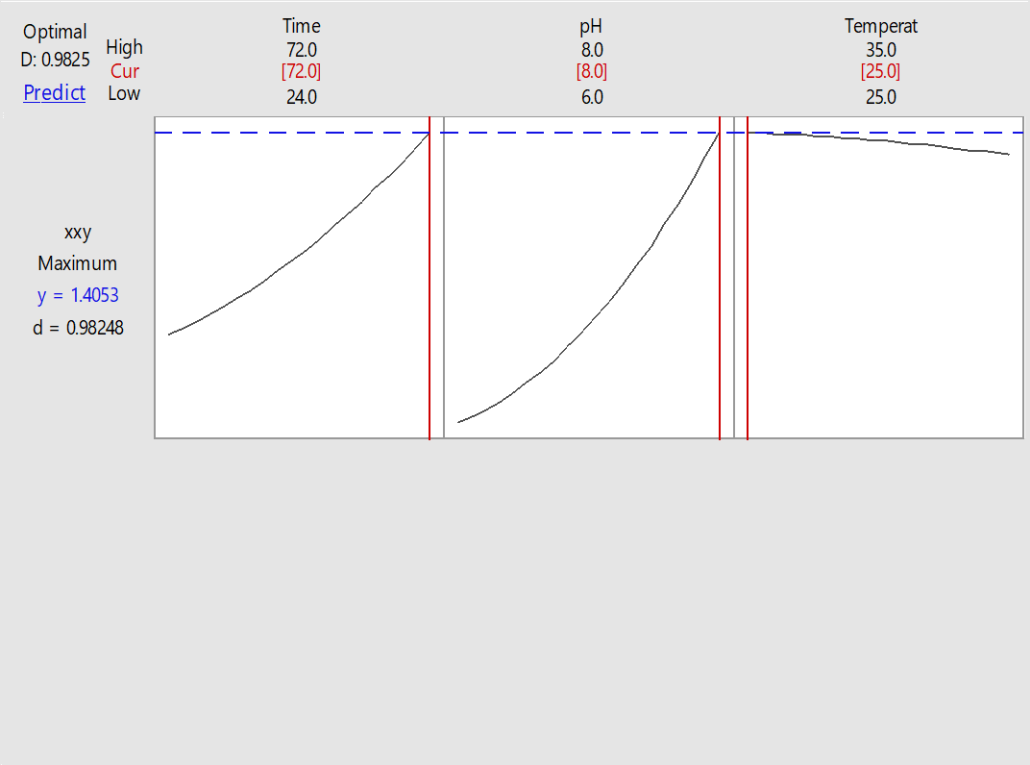

Figure 4.60: Optimization plot for XXYNP production

Table 4.1: PHYTOCHEMICAL COPONENTS OF THE SELECTED PLANT

Phytochemical	Selected Plants									
	GW	MO	UG	CA	CO	PO	UZ	NE	BL	XXY
Phlobutannins	-	-	+	-	+	-	+	-	-	+
Saponin	+	-	-	+++	++	-	++	++	+++	++
Alkaloids	++	++	++	+++	+	+	++	+++	+++	+++
Carbohydrates	+++	+	++	+	-	++	+++	-	-	++
Sterols	-	-	-	-	-	-	-	-	-	-
Triterpenoids	+	+++	+	-	-	+	-	-	-	+
Tannins	+++*	+++*	+++†	+++*	+++†	+++*	+++†	+++*	+++*	+++†
Proteins and amino acids	+++	+++	+++	++	+	+++	-	+++	-	-
Flavonoids	+++	+++	-	+++	+	++	-	+++	-	-
Fixed fats and oils	+	-	-	-	-	+++	++	-	++	+
Anthraquinone glycosides	+++	++	++	-	-	++	+++	+	+++	+++
Phenolic compounds	+++	+++	+++	+++	+++	+++	+++	-	+	+
Cardiac glycosides	-	+++	-	-	-	-	+	-	-	-

- = Absent; + = Slightly present; ++ = Moderately present; +++ = Highly present; † = Condensed tannins; * = Catecholic tannins

KEY: GW – Goatweed, UG = Ugu Leaf, CA- Cassava Leaf, CO – Comelina Leaf, PO – Potatoe Leaf, UZ – Uziza, NE – Neem Leaf, BL – Bitter Leaf, XXY – Independent Leaf

RESULTS OF UV-VIS CHARACTERIZATION

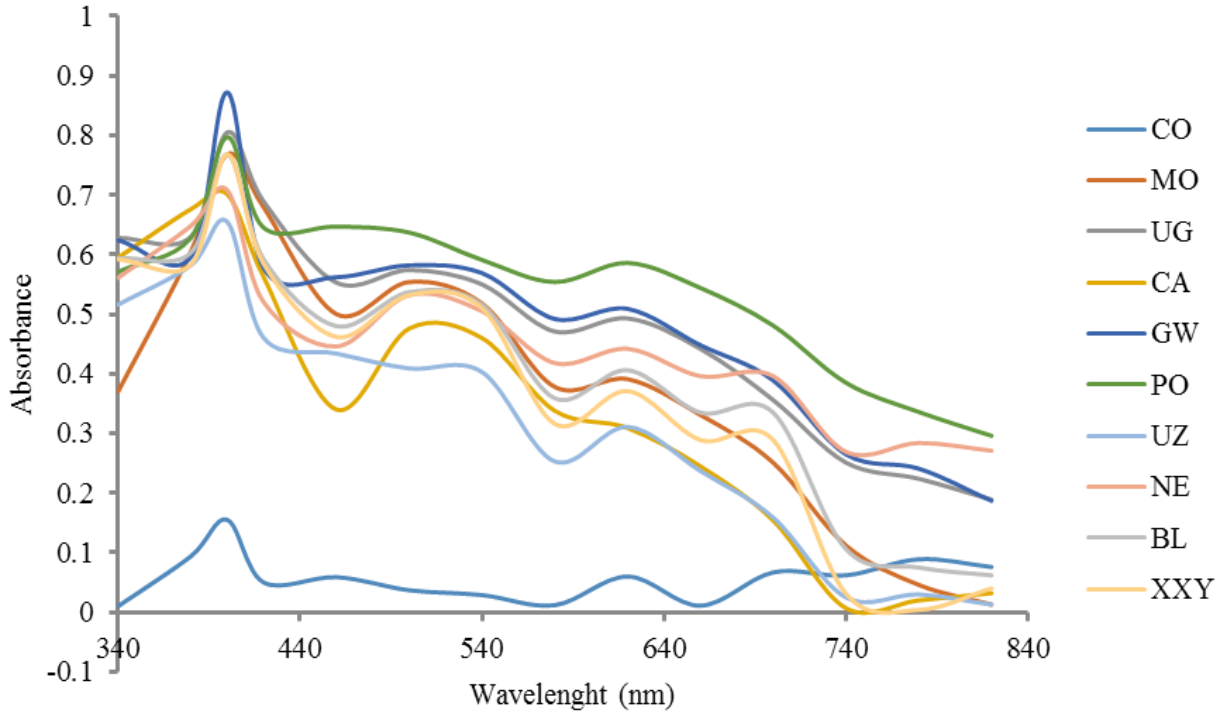

UV-Vis spectra for AgNPs from optimized synthesis

Table 4.2: Absorbance for Optimized synthesized $AgNO_3$ at different wavelenghts (nm)

Extracts	340	380	400	420	460	500	540	580	620	660	700	740	780	820
CO	0.01	0.094	0.155	0.05	0.059	0.037	0.029	0.012	0.06	0.011	0.067	0.062	0.089	0.076
MO	0.37	0.605	0.768	0.679	0.5	0.554	0.518	0.378	0.391	0.331	0.251	0.112	0.046	0.013
UG	0.628	0.63	0.805	0.689	0.553	0.574	0.55	0.471	0.493	0.442	0.356	0.251	0.224	0.189
CA	0.595	0.676	0.701	0.562	0.34	0.476	0.46	0.338	0.309	0.245	0.154	0.007	0.02	0.032
GW	0.624	0.596	0.872	0.577	0.562	0.582	0.569	0.492	0.509	0.448	0.389	0.265	0.241	0.187
PO	0.571	0.628	0.797	0.645	0.647	0.637	0.591	0.554	0.586	0.544	0.481	0.385	0.336	0.296
UZ	0.516	0.582	0.655	0.46	0.434	0.409	0.403	0.253	0.311	0.237	0.159	0.025	0.03	0.013
NE	0.561	0.648	0.708	0.52	0.446	0.532	0.505	0.418	0.442	0.396	0.396	0.269	0.284	0.271
BL	0.594	0.603	0.768	0.592	0.48	0.537	0.516	0.359	0.406	0.335	0.335	0.106	0.075	0.062
XXY	0.592	0.583	0.768	0.584	0.462	0.532	0.51	0.316	0.371	0.289	0.289	0.031	0.004	0.04

KEY: GW – Goatweed, UG = Ugu Leaf, CA- Cassava Leaf, CO – Comelina Leaf, PO – Potatoe Leaf, UZ – Uziza, NE – Neem Leaf, BL – Bitter Leaf, XXY – Independent Leaf

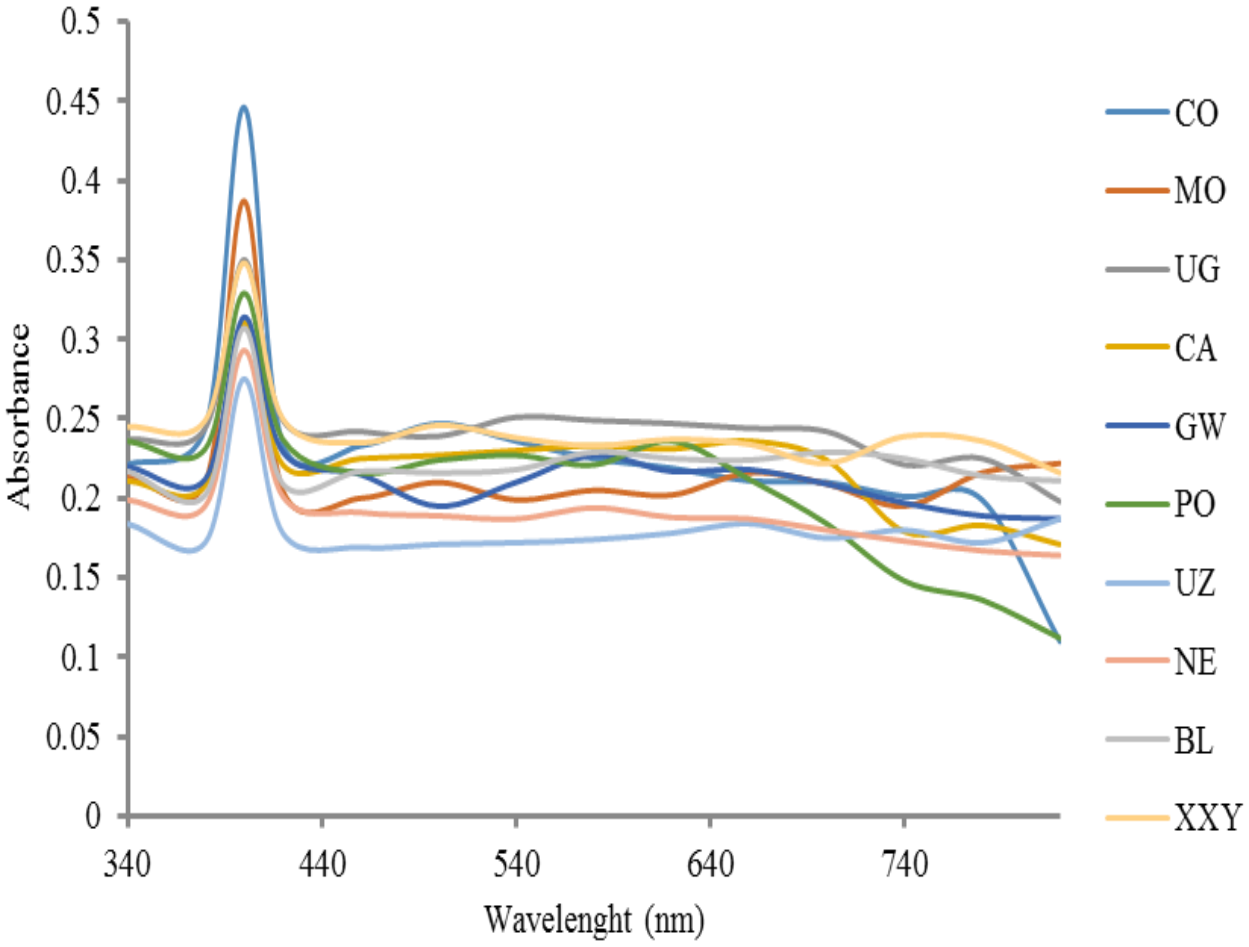

UV-Vis spectra for AgNPs from un-optimized synthesis

Table 4.3 Absorbance for un-optimized synthesized AgNO3 at different wavelenghts (nm)

Extracts	340	380	400	420	460	500	540	580	620	660	700	740	780	820
CO	0.221	0.244	0.446	0.234	0.233	0.247	0.236	0.225	0.219	0.211	0.21	0.201	0.199	0.11
MO	0.214	0.21	0.387	0.205	0.2	0.21	0.199	0.205	0.202	0.216	0.209	0.195	0.216	0.222
UG	0.237	0.244	0.35	0.249	0.242	0.239	0.251	0.249	0.247	0.244	0.242	0.221	0.225	0.198
CA	0.211	0.208	0.31	0.221	0.225	0.227	0.23	0.233	0.231	0.236	0.224	0.179	0.183	0.171
GW	0.22	0.212	0.314	0.229	0.215	0.195	0.21	0.227	0.217	0.218	0.209	0.197	0.189	0.187
PO	0.236	0.231	0.329	0.237	0.216	0.224	0.227	0.221	0.236	0.212	0.184	0.148	0.136	0.112
UZ	0.184	0.172	0.275	0.178	0.169	0.171	0.172	0.174	0.178	0.184	0.175	0.18	0.172	0.187
NE	0.199	0.195	0.293	0.201	0.191	0.189	0.187	0.194	0.188	0.187	0.18	0.173	0.167	0.164
BL	0.217	0.202	0.307	0.209	0.217	0.216	0.218	0.229	0.225	0.224	0.229	0.225	0.214	0.211
XXY	0.245	0.249	0.348	0.25	0.235	0.246	0.238	0.233	0.237	0.234	0.222	0.239	0.236	0.216

KEY: GW – Goatweed, UG = Ugu Leaf, CA- Cassava Leaf, CO – Comelina Leaf, PO – Potatoe Leaf, UZ – Uziza, NE – Neem Leaf, BL – Bitter Leaf, XXY – Independent Leaf

Table 4.4 Antibacterial Activity of the Sample Extracts

Extract	Sample	Zones of inhibition (mm)	
		P. aeruginosa	***E. coli***
CO	Raw extract (1)	0.0	0.0
	Un-optimized AgNPs (2)	10.0	11.0
	Optimized AgNPs (3)	12.0	13.0
	1mM $AgNO_3$ (4)	0.0	9.0
	Distilled water (5)	0.0	0.0
PO	Raw extract (1)	8.0	0.0
	Un-optimized AgNPs (2)	10.0	11.0
	Optimized AgNPs (3)	10.0	0.0
	1mM $AgNO_3$ (4)	0.0	0.0
	Distilled water (5)	0.0	0.0
GW	Raw extract (1)	0.0	0.0
	Un-optimized AgNPs (2)	11.0	13.0
	Optimized AgNPs (3)	12.0	12.0
	1mM $AgNO_3$ (4)	8.0	10.0
	Distilled water (5)	0.0	0.0
MO	Raw extract (1)	0.0	0.0
	Un-optimized AgNPs (2)	11.0	19.0
	Optimized AgNPs (3)	11.0	12.0
	1mM $AgNO_3$ (4)	10.0	0.0
	Distilled water (5)	0.0	0.0
CA	Raw extract (1)	0.0	0.0
	Un-optimized AgNPs (2)	9.0	12.0
	Optimized AgNPs (3)	8.0	11.0
	1mM $AgNO_3$ (4)	0.0	7.0
	Distilled water (5)	0.0	0.0
	Raw extract (1)	0.0	0.0
	Un-optimized AgNPs (2)	9.0	9.0

NE	Optimized AgNPs (3)	8.0	12.0
	1mM $AgNO_3$ (4)	0.0	8.0
	Distilled water (5)	0.0	0.0
	Raw extract (1)	0.0	9.0
	Un-optimized AgNPs (2)	11.0	10.0
BL	Optimized AgNPs (3)	10.0	10.0
	1mM $AgNO_3$ (4)	0.0	4.0
	Distilled water (5)	0.0	0.0
	Raw extract (1)	0.0	9.0
UG	Un-optimized AgNPs (2)	11.0	11.0
	Optimized AgNPs (3)	8.0	13.0
	1mM $AgNO_3$ (4)	0.0	8.0
	Distilled water (5)	0.0	0.0
	Raw extract (1)	0.0	7.0
	Un-optimized AgNPs (2)	9.0	12.0
UZ	Optimized AgNPs (3)	10.0	11.0
	1mM $AgNO_3$ (4)	0.0	8.0
	Distilled water (5)	0.0	0.0
	Raw extract (1)	0.0	8.0
	Un-optimized AgNPs (2)	10.0	10.0
XXY	Optimized AgNPs (3)	12.0	9.0
	1mM $AgNO_3$ (4)	0.0	9.0
	Distilled water (5)	0.0	0.0

CHAPTER FIVE

5.0 DISCUSSION AND CONCLUSION

5.1 Discussion

This research seeks to identify optimal conditions that are required for the production of silver based nanoparticles from Goatweed (GwNP), Ugu leaf (UgNP), Bitter leaf (BLNP), Neem leaf (NeNP), Uziza leaf (UzNP), Sweet Potato leaf (PoNP), Comelina leaf (CoNP), Cassava leaf (CaNP), Moringa leaf and Independence leaf (*Chromolaena odorata*) (XXYNP) which were chosen randomly. The silver (Ag) nanoparticles (AgNPs) were produced from 10 mMol concentration which was quite small as required. Particle size plays an influential role in the antibacterial properties of silver nanoparticles, with smaller particles exhibiting improved activities (Burt *et al*., 2004; Pal *et al*., 2007). However, it must be noted that the smaller nanoparticles have a tendency to agglomerate in a media with high electrolyte content resulting in a loss of antibacterial effectiveness (Burt *et al*., 2004).

The optimum conditions for the production of goatweed (GwNP) (pH 8.0, temperature 35 ^{0}C and time of 24 hours) had a predicted yield of 1.6149, which was higher than that produced by the Independence leaf (*Chromolaena odorata*) (XXYNP), at its predicted optimum conditions (pH 8.0, temperature of 35 degree Celsius and a time of 72 hours) and predicted yield of 1.4053. Uziza leaf (UzNP) at its predicted optimum conditions (pH 8.0, temperature of 35 degree Celsius and a time of 72 hours) and predicted yield of 0.9350, and Neem leaf (NeNP), at its predicted optimum conditions (pH 8.0, temperature of 35 degree Celsius and a time of 72 hours) and predicted yield of 0.5373 respectively. These were lower than that produced by cassava Leaf (CaNP), at its predicted optimum conditions (pH 8.0, temperature of 35 degree Celsius and a time of 72 hours) and predicted yield of 1.6418. Also, Comelina leaf (CoNP), Moringa leaf (MoNP), Bitter leaf (BLNP), Potato leaf (PoNP) and Ugu leaf (UgNP) with predicted yields of 1.6485, 1.8356, 1.8543, 2.0977 and 1285.13 respectively at the same optimum conditions (pH 8.0, temperature of 35 degree Celsius and a time of 72 hours). The study also demonstrated that among other parameters measured, time was a factor of great significance. This is because it takes a lot of time for the molecules of the leaf extracts to conjugate with the molecules of silver nitrate. As a result, the longer the time of incubation, the more probable yield is obtained.

The antimicrobial activities of GwNP, MoNP, UgNP, CaNP, CoNP, PoNP, UzNP, NeNP, BLNP and XXYNP demonstrated that the nanoparticles had antimicrobial properties. The BLNP, XXYNP, MoNP and UzNP silver nanoparticles have been reported to have antibacterial activity against *Bacillus subtilis, Klebsiella pneumonia, E.coli, Pseudomonas aeruginosa* and *Staphylococcus aureus*. (Ramya and Silvia, 2012). On the other hand, Siddiqi, et al., (2018) has proposed that the biologically synthesized nanoparticles from PoNP and CoNP recorded considerable antibacterial activity against various pathogenic organisms such as *Staphylococcus aureus, Streptococcus pyogenes, Salmonella typhi, Klebsiella pneumoniae* and *Vibrio cholerae* using agar well diffusion method. In his research, the synthesized silver nanoparticles showed highest antibacterial activity against all the pathogens except for *Vibro cholerae.*

Nanoparticles show antimicrobial activity against a range of bacteria. Among the various nanoparticles, silver nanoparticles exhibit broad inhibitory behaviour towards at least 650 species of microbes or more, and more importantly against antibiotic resistant bacterial strains (Jeong *et al*., 2005, 2010, 2012; Rai *et al*., 2012; Marambio-Jones et al., 2009, 2010, 2012). In one of the findings, it was revealed that silver nanoparticles showed superior antibacterial activity against *E. coli* and *S. aureus* when compared to gold nanoparticles (Amin *et al*., 2009). Gram positive bacteria (*Staphylococcus aureus, Staphylococcus epidermidis* though not used in this study,) and Gram negative bacteria (*Escherichia coli, Salmonella typhi, Pseudomonas aeruginosa, Proteus vulgaris*) has already been tested and NPs show great activity against them. The silver nanoparticles showed high activity against *Salmonella typhi* followed by *Staphylococcus epidermidis, Staphylococcus aureus, Pseudomonas aeruginosa, Proteus vulgaris, E.coli,* and least activity was against *Klebsiella pneumoniae* (Kim *et al.,* 2007).

It has also been reported that medically, small concentration of silver nanoparticles are harmless to human cells and cidal to majority of viral cells and bacterial cells. Silver nanoparticles (AgNPs) reduce toxicity of the cell without affecting its antibacterial efficacy (Karimzadeh and Mansour, 2010). Silver Nano particles show high antibacterial activity because of their finely honed surface and are small enough to penetrate through the membrane of the cell to disturb the intracellular processes. Silver nanoparticles show higher antibacterial effect due to their formation of free radicals on its surface (Kim *et al*., 2007). The mechanisms of these antimicrobial activities was suggested by Zewde *et al*. (2016)

which ranged from formation of pits in cell wall, disruption of cell membrane via free radical formation by nanoparticles and inhibition of respiratory enzymes by free oxygen species produced by silver nanoparticles and silver ion, and binding of silver nanoparticles with soft basic residues within the cell, e.g., DNA. Depending upon their size, shape, and composition, nanoparticles are capable of penetrating the cell membrane and influencing the intracellular processes (Zewde et al, 2016).

Also, it is worthy of note that the activity of silver nanoparticles are broad spectrum.

5.2 Conclusion and Recommendation

Biological synthesis of nanoparticles is a novel and effective approach of nanoparticles synthesis. The microorganisms or plant biomass involved serve as reducing agents which are environmentally benign and non-toxic and has significant advantages over other processes since it takes place at relatively ambient temperature and pressure. Biological synthesis of nanoparticles is thus effective and economic approaches which even control the size and shape of the nanoparticles (Narayanan and Sakthivel 2010).

The potential benefits of nanotechnology in biomedical and industrial applications have become widely accepted and are the most promising sector for the generation of new applications in medicine.

It is now clear that silver nanoparticles possess a strong antibacterial and antiviral activity, highlighted by several studies. Silver nanoparticles have the ability to interact with various microorganisms (such as bacteria) and also impact both the growth of and mature bacterial biofilms and, therefore, could be used as broad spectrum antimicrobials. The antibacterial effect appears to be conferred by their ultra-small size and increased surface area, through which they destroy the membrane, cross the body of the microbe and create intracellular damage. Due to the structural difference in the composition of the cell walls of Gram-positive and Gram-negative organisms, AgNPs have significantly less effect on the growth of Gram-positive bacteria. The Gram-negative bacteria have a layer of lipopolysaccharides on the outside, and present below a thin (7 to 8 nanometers) layer of peptidoglycan. Although lipopolysaccharides are composed of lipids covalently bound to polysaccharides, there is a lack of rigidity of the overall structural envelope. The negative charges on the lipopolysaccharides are attracted to the weak positive charge of AgNPs. On the other hand, the cell wall of Gram-positive bacteria is mainly composed of a thick layer (20 to 80

nanometers) of peptidoglycan consisting of linear polysaccharidic chains cross-linked by short peptides to form a three-dimensional rigid structure. The stiffness and the extensive cross-linking not only reduce the bacterial cell wall anchoring sites for AgNPs but also render the wall itself more difficult to penetrate. However, the same features that make AgNPs attractive, at the same time raise important issues such as the toxicity and environmental safety. Siver nanoparticles antibacterial effects have been described in detail, but their mechanism of action is still unclear. A multifaceted mechanism against microorganisms seems to be due to nanoparticle interactions with the bacterial surfaces, as well as to their particular structure. Defining AgNPs' mechanism of action is, nowadays, a priority for biomedical research and more research on the bioactivity and biocompatibility of AgNPs is necessary.

Understanding the kinetics of dissolution that lead to transformations of AgNPs in the presence of specific inorganic ligands is crucial to determining their antimicrobial activity and overall toxicity in the environment. Silver ions (Ag+), released by AgNPs, are likely to interact with chloride (Cl^-) which is often present in bacterial growth media and exhibits a strong affinity for oxidized silver. High concentrations of chloride ions in the routinely used media can cause precipitation of Ag ions as AgCl, thus masking the contribution of dissolved silver to AgNPs antibacterial effect. This consideration should influence the choice of the medium to be used when evaluating antimicrobial effects and more studies are needed to investigate the contribution of AgCl to the observed antibacterial activity of AgNPs. The studies on the combined use of AgNPs with other antimicrobial agents can help reduce the problem of toxicity and to avoid the potential for development of resistance and, above all, strongly enhance the microbicidal effect. The broad spectrum of bioactivity of AgNPs makes them promising agents not only to fight infections, but in many other biomedical areas.

5.3 Contribution to Knowledge

As an inference from this work my contribution to knowledge is that the efficacy of silver nanoparticles produced is enhanced when the environmental factors that control the production of nanoparticle like temperature, time of incubation and pH (*pondus dehydroium*) be taken into consideration. A control over these factors aforementioned is the optimization process, and when applied produces better results and high efficacy antimicrobials. I therefore, recommend optimization for every antimicrobial produced.

References

Abhishek, K., Sanyog, J., and Uttan, C. B. (2013). Green and rapid synthesis of anticancerous silver nanoparticles by *Saccharomyces boulardii* and insight into mechanism of Nanoparticle synthesis. *BioMed res Intl*; 1-8.

Ahmad, A., Mukherjee, P., Senapati, S., Mandal, D., Khan, M. I., Kumar, R., and Sastry, M (2003). Extracellular biosynthesis of silver nanoparticles using the fungus *Fusarium oxysporum*. *Col Surf. B Bio*; **28:**313-318.

Amin, R. M., Mohamed, M. B., Ramadan, M. A., Verwanger, T., Krammer, B. (2009). Rapid and sensitive microplate assay for screening the effect of silver and gold nanoparticles on bacteria. *Nanomed (Lond*); 637- 643.

Asghari, S., Johari, S. A., Lee, J. H., Kim, Y. S., Jeon, Y. B., Choi, H. J., Moon, M. C., and Yu, I. J. (2012). Toxicity of various silver nanoparticles compared to silver ions in DapHnia magna. *J. Nanobiotechnol;* 10: 14.

Atul. R., Ingole, S. R. T., Khati, N. T., Atul, V., Wankhade, D., and Burghate, K. (2010). Green synthesis of selenium nanoparticles under ambient condition. *Chalco Let;* **7**: 485-489.

Buchannan, R. E. and Gibbon, N.E. (1974). *Bergy's Manual of Determinative Bacteriology.* Williams and wilkins Co.: Baltimore, U.S.A.

Burt, J., Gutierrez-Wing, C., Miki-Yoshida, M., Jose-Yacaman, M. (2004). Nobel-Metal Nanoparticles Directly Conjugated to Globular Proteins. *Langmuir*. **20**:11778-11783.

Catauro, M., Rein, M., and De Gaaetano, F. D. (2005), Marotta A, Sol–gel processing of drug delivery materials and release kinetics. *J Mater Sci Mater Med*; **16(3)**: 261-265.

Cheesbrough, M. (2009). D*istrict Laboratory Practice in Tropical Countries Part 2. Second Edition*. Cambridge University Press. Pp 132-141.

Chitravadivu C, Manian S Kalachelvi K (2009). Qualitative analysis of Selected Medicinal Plants, Tamilnadu, India. *Mid. East J. Sci. Res*.**4:** 144-146.

Ciulei (1964). Practical Manuals on the Industrial Utilization of Medicinal and Aromatic plants, University of Bucharest, Romania. 67 (17): 5159 - 5172

Colvin, V. L. S., Michel, C., and Alivisatos, A. (1994) Light emitting diodes made from cadmium selenide nanocrystals and a semiconducting polymer. *Nat*; **370**: 354-357.

Chrisopher, T.J., Christopher, M. J., Andrew, K. B., Susan, F., and Karin, C. (2016). Stay Green traits to improve wheat adaptation in well watered and water limited environment. Jornal of Experimental botany. 67 (17): 5159 - 5172

Duran, N. M. P., Alves, O. L., De Souza, G. I. H. and Esposito, E. (2011). Mechanistic aspects of biosynthesis of silver nanoparticles by several *Fusarium oxysporum* strains. *J Nanobiotechnol*; **3**: 8-14.

Garima, S. R. B., Kunal, K., Ashish, R. S. and Rajendra, P. S. (2011). Biosynthesis of silver nanoparticles using *Ocimum sanctum* (Tulsi) leaf extract and screening its antimicrobial activity. *J Nanopart Res*; **13**: 2981-2988.

Grier, N., (1968). Silver and its compounds. In: Block, SS., Ed., Disinfection, Sterilization and Preservation, Lee and Febiger, Philadephia. 375 – 398.

Harekrishna, D. K. B., Gobinda, S. P., Priyanka, S. and Sankar, P. D. (2009) Green synthesis of silver nanoparticles using latex of *JatropHa curcas. Colliod surface A;* **39(3)**: 134-139.

Hurst, S. J (2011). Biomedical Nanotechnology, Methods in molecular biology. *JOUR;* 1(13): 726

Husseiny, M., Aziz, M. A. E., Badr, Y., and Mahmoud, M. A. (2006). Biosynthesis of gold nanoparticles using *Pseudomonas aeruginosa*. *Spectro Acta;* Part A. **67**: 1003-1006.

Jeong, S., Yeo, S. and Yi, S. (2005). The effect of filler particle size on the antibacterial properties of compounded polymer/silver fibres. *J. Mater. Sci*. **40:** 5407-5411.

Jha, A., Prasad, K, Prasad, K, Kulkarni, A. R. (2009). Plant system: nature's nano-factory. *Colloids Surf. B Biointerf*; **73**: 219-223.

Ju-Nam, Y., and Lead J. R. (2008). Manufactured nanoparticles: An overview of their chemistry, interactions and potential environmental implications. *Sci. Total Environ;* **400(1)**: 396-414.

Jung, J. O. H., Noh, H., Ji, J., and Kim, S. (2006). Metal nanoparticle generation using a small ceramic heater with a local heating area. *J Aero Sci*; **37**: 1662-1670.

Karimzadeh, R., and Mansour, N. (2010). The Effect of Concentration on the Thermo-Optical Properties of Colloidal Silver Nanoparticles, *Opt. Laser Technol;* **42**: 783.

Kaviya, S. S. J. and Viswanathan, B. (2011). Green Synthesis of silver nanoparticles using *Polyalthia longifolia* Leaf extract along with D-Sorbitol. *J Nanotechnol*; p. 1-5.

Kim, Y., Song, M. Y., Park, J. D., Song, K. S., Ryu, H. R., Chung, Y. H., Chang, H. K., Lee, J. H., Oh, K. H., Kelman, B. J., Hwang, I. K. and Yu, I. J. (2010). Sub chronic oral toxicity of silver nanoparticles. *Part. Fibre Toxicol;* **7**: 20.

Kim, J. S., Kuk, E., Yu, K. N., Kim, J. H., Park, S. J. and Lee, H. J. (2007). Antimicrobial effects of silver nanoparticles. Nanomedicine: *Nanotechnol Biol Med*; **3(1)**: 95-101.

Lee, H. Y. L., Chen, K., Hsu, A. R., Xu, C., Xie, J., Sun, S. and Chen, X. (2008). PET/MRI dualmodality tumor imaging using arginine-glycine-aspartic (RGD) – conjugated radiolabeled iron oxide nanoparticles. *J Nucl Med*; **49**:1371-1379.

Liu, P. Z. (2009). Silver nanoparticle supported on halloysite nanotubes catalyzed reduction of 4-nitropHenol (4-NP). *Appl Surf Sci*; **225**: 3989-3993.

Marambio-Jones, C. and Hoek, E. M. V. (2010). A review of the antibacterial effects of silver nanomaterials and potential implications for human health and the environment. *J Nanopart. Res*; **12**:1531-1551.

McAuliffe, M. and Perry, M. J. (2007). Are nanoparticles potential male reproductive toxicants? A literature review. *Nanotoxicol;* **1**: 204-210.

Mohamed, S. H., Hansi, P. D. and Kavitha, T. (2010). Antimicrobial activity and pHytochemical analysis of selected Indian folk medicinal plants. *Intl J PHarm Sci Res;* **1(10)**:430-434.

Morones, J., Elechiguerra, J. L., Camacho, A., Holt, K., Kouri, J. B., Ramirez, J. T. and Yacaman, M. J. (2005). The bactericidal effect of silver nanoparticles. *Nanotechnol;* **16**: 2346-2353. --

Mukherjee, P. A. A., Mandal, D. S., Senapati, S., Sainkar, R., Khan, M. I., Parishcha, R., Ajaykumar, P. V., Alam, M., Kumar, R. and Sastry, M. (2001). Fungus-mediated synthesis of silver nanoparticles and their immobilization in the mycelial matrix: a novel biological approach to nanoparticle synthesis. *Nano Let;* **1**: 515-519.

Narayanan, K. B., and Sakthivel, N. (2010). Biological synthesis of metal nanoparticles by microbes. *Adv. Colloid Interface Sci;* **156(1-2)**: 1-13.

Oliveira, M. U., Zanchet, D. and Zarbin, A. (2005). Influence of synthetic parameters on the size, structure, and stability of dodecanethiol-stabilized silver nanoparticles. *J Col Interf Sci;* **292**: 429-435.

Pal, S., Tak, Y. K., and Song, J. M. (2007). Does the antibacterial activity of silver nanoparticles depend on the shape of the nanoparticle? A study of the Gram-negative bacterium *Escherichia coli*. *Appl Environ Microbiol.* **73**: 1712-20.

Panyala, N., Pena-Mendez, E. M., and Havel, J. (2008). Silver or silver nanoparticles: a hazardous threat to the environment and human health. *J. Appl. Biomed.* **6**: 117-129.

Parashar, R. and Sharma, B. (2009). Parthenium leaf extract mediated synthesis of silver nanoparticles: a novel approach towards weed utilization. *Dig J Nanopart Biostr;* **4**:45-50.

Raaman, N., (2006). Phytochemical techniques.

Rai, M. K., Deshmukh, S., Ingle, A. and Gade, A. (2012) Silver nanoparticles: the powerful nanoweapon against multidrug-resistant bacteria. *J Appl Microbiol*; **112:** 841-852.

Ramya, M. and Sylvia, S. M. (2012). Green Synthesis of Silver Nanoparticles. *Intl J PHarm Med Bio Sci;* **1**(1):54-61.

Yousaf, H., Mehmood, A., Ahmad, K. S. and Raffi. M., (2020). Green Synthesis of Silver nanoparticles and their application as an alternative antibacterial and antioxidant agent. Material Science and Engineering 112 (1)

Roe, D., Karandikar, B., Bonn-Savage, N., Gibbins, B. and Roullet, J-B. (2008). Antimicrobial surface functionalization of plastic catheters by silver nanoparticles. *J. Antimicrob. Chemoth*; **61**: 869.

Saxena, M., Saxena, J., Nema, R., Singh, D and Gupta, A. (2016). Journal of Pharmacognosy and phytochemistry. 1(6): 1 – 68.

Senapati, S. (2005). *Biosynthesis and immobilization of nanoparticles and their applications*. University of pune, India.

Shahverdi, A. R., Minaeian, S., Shahverdi, H. R., Jamalifar, H. and Nohi, A. A. (2007). Rapid synthesis of silver nanoparticles using culture supernatants of Enterobacteriaceae: A novel biological approach. *Proc Biochem*; **42**:919-923.

Sharma, V. K. Y., Rajah A., and Lin, Y. (2009). Silver nanoparticles: green synthesis and their antimicrobial activities. *Adv Col Intl Sci*; **145**: 83-96.

Sondi, I., and Salopek-Sondi, B (2004). Silver nanoparticles as antimicrobial agent: a case study on *E. coli* as a model for Gram-negative bacteria. *J Col Intl Sci;* **275**: 177-182.

Tsuji, T. I., K., Watanabe, N. and Tsuji, M. (2002). Preparation of silver nanoparticles by laser ablation in solution: influence of laser wavelength on particle size. *App Surf Sci;* **202:** 80-85.

Vaidyanathan, R., Gopalram, S, Kalishwaralal, K, Deepak, V, Pandian, S. R., Gurunathan, S. (2010). Enhanced silver nanoparticle synthesis by optimization of nitrate reductase activity. *Col Surf B Biointerf;* **75**: 335-341.

Xu, Z. P, Lu, G. Q., and Yu, A. B. (2006). Inorganic Nanoparticles as Carriers for Efficient Cellular Delivery. *Chem Eng Sci;* **61**: 1027-1040.

Yin, Y. L., Zhong, Z., Gates, B. and Venkateswaran, S. (2002). Synthesis and characterization of stable aqueous dispersions of silver nanoparticles through the Tollens process. *J Mater Chem;* **12**: 522-527.

Zewde, B., Ambaye, A., Stubbs, J., and Dharmara, R. (2016) A Review of Stabilized Silver Nanoparticles – Synthesis, Biological Properties, Characterization, and Potential Areas of Applications. *J S M Nanotechnol Nanomed;* **4(2)**: 1043.

APPENDIX: STATISTICAL ANALYSIS

———— 31/03/2018 10:45:21 AM ————————————————————

Results for: Worksheet 2

Box-Benken Design

Factors: 3 Replicates: 1
Base runs: 15 Total runs: 15
Base blocks: 1 Total blocks: 1

Center points: 3

Design Table

Run	Blk	A	B	C
1	1	-1	-1	0
2	1	1	-1	0
3	1	-1	1	0
4	1	1	1	0
5	1	-1	0	-1
6	1	1	0	-1
7	1	-1	0	1
8	1	1	0	1
9	1	0	-1	-1
10	1	0	1	-1
11	1	0	-1	1
12	1	0	1	1
13	1	0	0	0
14	1	0	0	0
15	1	0	0	0

Response Surface Regression: Gw versus Time, pH, Temperature

Analysis of Variance

Source	DF	Adj SS	Adj MS	F-Value	P-Value
Model	9	0.331722	0.036858	2.69	0.144
Linear	3	0.216762	0.072254	5.28	0.052
Time	1	0.000666	0.000666	0.05	0.834
pH	1	0.061250	0.061250	4.48	0.088
Temperature	1	0.154846	0.154846	11.32	0.020
Square	3	0.043336	0.014445	1.06	0.445
Time*Time	1	0.000327	0.000327	0.02	0.883
pH*pH	1	0.028702	0.028702	2.10	0.207
Temperature*Temperature	1	0.011407	0.011407	0.83	0.403
2-Way Interaction	3	0.071624	0.023875	1.75	0.273

Time*pH	1	0.000930	0.000930	0.07	0.805
Time*Temperature	1	0.057121	0.057121	4.18	0.096
pH*Temperature	1	0.013572	0.013572	0.99	0.365
Error	5	0.068407	0.013681		
Lack-of-Fit	3	0.056547	0.018849	3.18	0.248
Pure Error	2	0.011861	0.005930		
Total	14	0.400129			

Model Summary

S	R-sq	R-sq(adj)	R-sq(pred)
0.116968	82.90%	52.13%	0.00%

Coded Coefficients

Term	Effect	Coef	SE Coef	T-Value	P-Value	VIF
Constant		1.1747	0.0675	17.39	0.000	
Time	-0.0183	-0.0091	0.0414	-0.22	0.834	1.00
pH	0.1750	0.0875	0.0414	2.12	0.088	1.00
Temperature	0.2782	0.1391	0.0414	3.36	0.020	1.00
Time*Time	0.0188	0.0094	0.0609	0.15	0.883	1.01
pH*pH	0.1763	0.0882	0.0609	1.45	0.207	1.01
Temperature*Temperature	-0.1112	-0.0556	0.0609	-0.91	0.403	1.01
Time*pH	0.0305	0.0153	0.0585	0.26	0.805	1.00
Time*Temperature	-0.2390	-0.1195	0.0585	-2.04	0.096	1.00
pH*Temperature	0.1165	0.0582	0.0585	1.00	0.365	1.00

Regression Equation in Uncoded Units

Gw = 3.33 + 0.0235 Time - 1.527 pH + 0.127 Temperature + 0.000016 Time*Time
+ 0.0882 pH*pH
- 0.00222 Temperature*Temperature + 0.00064 Time*pH - 0.000996 Time*Temperature
+ 0.0117 pH*Temperature

Response Surface Regression: Mo versus Time, pH, Temperature

Analysis of Variance

Source	DF	Adj SS	Adj MS	F-Value	P-Value
Model	9	0.168796	0.018755	4.98	0.046
Linear	3	0.139443	0.046481	12.33	0.010
Time	1	0.022578	0.022578	5.99	0.058
pH	1	0.116162	0.116162	30.81	0.003
Temperature	1	0.000703	0.000703	0.19	0.684
Square	3	0.021186	0.007062	1.87	0.252
Time*Time	1	0.010470	0.010470	2.78	0.156
pH*pH	1	0.001552	0.001552	0.41	0.549
Temperature*Temperature	1	0.007728	0.007728	2.05	0.212

2-Way Interaction	3	0.008167	0.002722	0.72	0.581
Time*pH	1	0.003080	0.003080	0.82	0.407
Time*Temperature	1	0.003364	0.003364	0.89	0.388
pH*Temperature	1	0.001722	0.001722	0.46	0.529
Error	5	0.018849	0.003770		
Lack-of-Fit	3	0.014971	0.004990	2.57	0.292
Pure Error	2	0.003878	0.001939		
Total	14	0.187645			

Model Summary

S	R-sq	R-sq(adj)	R-sq(pred)
0.0613983	89.96%	71.87%	0.00%

Coded Coefficients

Term	Effect	Coef	SE Coef	T-Value	P-Value	VIF
Constant		1.6160	0.0354	45.59	0.000	
Time	0.1063	0.0531	0.0217	2.45	0.058	1.00
pH	0.2410	0.1205	0.0217	5.55	0.003	1.00
Temperature	-0.0187	-0.0094	0.0217	-0.43	0.684	1.00
Time*Time	0.1065	0.0532	0.0320	1.67	0.156	1.01
pH*pH	0.0410	0.0205	0.0320	0.64	0.549	1.01
Temperature*Temperature	-0.0915	-0.0458	0.0320	-1.43	0.212	1.01
Time*pH	-0.0555	-0.0277	0.0307	-0.90	0.407	1.00
Time*Temperature	0.0580	0.0290	0.0307	0.94	0.388	1.00
pH*Temperature	-0.0415	-0.0207	0.0307	-0.68	0.529	1.00

Regression Equation in Uncoded Units

Mo = -0.62 - 0.0058 Time + 0.013 pH + 0.1254 Temperature + 0.000092 Time*Time
+ 0.0205 pH*pH
- 0.00183 Temperature*Temperature - 0.00116 Time*pH + 0.000242 Time*Temperature
- 0.00415 pH*Temperature

Response Surface Regression: Ug versus Time, pH, Temperature

Analysis of Variance

Source	DF	Adj SS	Adj MS	F-Value	P-Value
Model	9	2001305	222367	1.52	0.336
Linear	3	732023	244008	1.67	0.288
Time	1	366135	366135	2.50	0.175
pH	1	0	0	0.00	1.000
Temperature	1	365888	365888	2.50	0.175
Square	3	537094	179031	1.22	0.393
Time*Time	1	168994	168994	1.15	0.332
pH*pH	1	169091	169091	1.15	0.332

Temperature*Temperature	1	168950	168950	1.15	0.332
2-Way Interaction	3	732188	244063	1.67	0.288
Time*pH	1	0	0	0.00	1.000
Time*Temperature	1	732188	732188	5.00	0.076
pH*Temperature	1	0	0	0.00	1.000
Error	5	732208	146442		
Lack-of-Fit	3	732208	244069	4.80136E+08	0.000
Pure Error	2	0	0		
Total	14	2733513			

Model Summary

S	R-sq	R-sq(adj)	R-sq(pred)
382.677	73.21%	25.00%	0.00%

Coded Coefficients

Term	Effect	Coef	SE Coef	T-Value	P-Value	VIF
Constant		2	221	0.01	0.994	
Time	428	214	135	1.58	0.175	1.00
pH	0	0	135	0.00	1.000	1.00
Temperature	428	214	135	1.58	0.175	1.00
Time*Time	428	214	199	1.07	0.332	1.01
pH*pH	-428	-214	199	-1.07	0.332	1.01
Temperature*Temperature	428	214	199	1.07	0.332	1.01
Time*pH	-0	-0	191	-0.00	1.000	1.00
Time*Temperature	856	428	191	2.24	0.076	1.00
pH*Temperature	-0	-0	191	-0.00	1.000	1.00

Regression Equation in Uncoded Units

Ug = 1492 - 133.7 Time + 2996 pH - 642 Temperature + 0.371 Time*Time - 214 pH*pH
+ 8.56 Temperature*Temperature - 0.00 Time*pH + 3.57 Time*Temperature
- 0.0 pH*Temperature

Fits and Diagnostics for Unusual Observations

Obs	Ug	Fit	Resid	Std Resid	
5	2	430	-428	-2.24	R
8	1713	1285	428	2.24	R

R Large residual

Response Surface Regression: Ca versus Time, pH, Temperature

Analysis of Variance

Source	DF	Adj SS	Adj MS	F-Value	P-Value
Model	9	0.369151	0.041017	63.97	0.000
Linear	3	0.358522	0.119507	186.37	0.000
Time	1	0.003280	0.003280	5.12	0.073

pH	1	0.351961	0.351961	548.88	0.000
Temperature	1	0.003280	0.003280	5.12	0.073
Square	3	0.005804	0.001935	3.02	0.133
Time*Time	1	0.005215	0.005215	8.13	0.036
pH*pH	1	0.000785	0.000785	1.22	0.319
Temperature*Temperature	1	0.000003	0.000003	0.00	0.947
2-Way Interaction	3	0.004826	0.001609	2.51	0.173
Time*pH	1	0.000289	0.000289	0.45	0.532
Time*Temperature	1	0.000441	0.000441	0.69	0.445
pH*Temperature	1	0.004096	0.004096	6.39	0.053
Error	5	0.003206	0.000641		
Lack-of-Fit	3	0.003002	0.001001	9.78	0.094
Pure Error	2	0.000205	0.000102		
Total	14	0.372357			

Model Summary

S	R-sq	R-sq(adj)	R-sq(pred)
0.0253226	99.14%	97.59%	86.98%

Coded Coefficients

Term	Effect	Coef	SE Coef	T-Value	P-Value	VIF
Constant		1.3273	0.0146	90.79	0.000	
Time	0.04050	0.02025	0.00895	2.26	0.073	1.00
pH	0.41950	0.20975	0.00895	23.43	0.000	1.00
Temperature	0.04050	0.02025	0.00895	2.26	0.073	1.00
Time*Time	0.0752	0.0376	0.0132	2.85	0.036	1.01
pH*pH	0.0292	0.0146	0.0132	1.11	0.319	1.01
Temperature*Temperature	-0.0018	-0.0009	0.0132	-0.07	0.947	1.01
Time*pH	-0.0170	-0.0085	0.0127	-0.67	0.532	1.00
Time*Temperature	-0.0210	-0.0105	0.0127	-0.83	0.445	1.00
pH*Temperature	0.0640	0.0320	0.0127	2.53	0.053	1.00

Regression Equation in Uncoded Units

Ca = 1.63 - 0.00032 Time - 0.169 pH - 0.0343 Temperature + 0.000065 Time*Time
+ 0.0146 pH*pH
- 0.000037 Temperature*Temperature - 0.000354 Time*pH -
0.000087 Time*Temperature
+ 0.00640 pH*Temperature

Fits and Diagnostics for Unusual Observations

Obs	Ca	Fit	Resid	Std Resid	
10	1.4730	1.4985	-0.0255	-2.01	R

11 1.1450 1.1195 0.0255 2.01 R

R Large residual

Response Surface Regression: Co versus Time, pH, Temperature

Analysis of Variance

Source	DF	Adj SS	Adj MS	F-Value	P-Value
Model	9	0.394159	0.043795	4.04	0.069
Linear	3	0.373703	0.124568	11.48	0.011
Time	1	0.000002	0.000002	0.00	0.990
pH	1	0.348613	0.348613	32.14	0.002
Temperature	1	0.025088	0.025088	2.31	0.189
Square	3	0.006098	0.002033	0.19	0.901
Time*Time	1	0.004448	0.004448	0.41	0.550
pH*pH	1	0.001041	0.001041	0.10	0.769
Temperature*Temperature	1	0.000170	0.000170	0.02	0.905
2-Way Interaction	3	0.014359	0.004786	0.44	0.734
Time*pH	1	0.013806	0.013806	1.27	0.310
Time*Temperature	1	0.000420	0.000420	0.04	0.852
pH*Temperature	1	0.000132	0.000132	0.01	0.916
Error	5	0.054240	0.010848		
Lack-of-Fit	3	0.051677	0.017226	13.44	0.070
Pure Error	2	0.002563	0.001281		
Total	14	0.448399			

Model Summary

S	R-sq	R-sq(adj)	R-sq(pred)
0.104153	87.90%	66.13%	0.00%

Coded Coefficients

Term	Effect	Coef	SE Coef	T-Value	P-Value	VIF
Constant		1.3487	0.0601	22.43	0.000	
Time	-0.0010	-0.0005	0.0368	-0.01	0.990	1.00
pH	0.4175	0.2088	0.0368	5.67	0.002	1.00
Temperature	0.1120	0.0560	0.0368	1.52	0.189	1.00
Time*Time	-0.0694	-0.0347	0.0542	-0.64	0.550	1.01
pH*pH	0.0336	0.0168	0.0542	0.31	0.769	1.01
Temperature*Temperature	0.0136	0.0068	0.0542	0.13	0.905	1.01
Time*pH	-0.1175	-0.0587	0.0521	-1.13	0.310	1.00
Time*Temperature	0.0205	0.0102	0.0521	0.20	0.852	1.00
pH*Temperature	-0.0115	-0.0058	0.0521	-0.11	0.916	1.00

Regression Equation in Uncoded Units

Co = -0.46 + 0.0203 Time + 0.126 pH - 0.001 Temperature - 0.000060 Time*Time
+ 0.0168 pH*pH
    + 0.00027 Temperature*Temperature - 0.00245 Time*pH + 0.000085 Time*Temperature
    - 0.0011 pH*Temperature

Fits and Diagnostics for Unusual Observations

Obs	Co	Fit	Resid	Std Resid	
9	1.2130	1.1018	0.1112	2.14	R
12	1.5200	1.6313	-0.1113	-2.14	R

R Large residual

Response Surface Regression: Po versus Time, pH, Temperature

Analysis of Variance

Source	DF	Adj SS	Adj MS	F-Value	P-Value
Model	9	0.015260	0.001696	16.96	0.003
Linear	3	0.013336	0.004445	44.45	0.000
Time	1	0.005000	0.005000	50.00	0.001
pH	1	0.007688	0.007688	76.88	0.000
Temperature	1	0.000648	0.000648	6.48	0.052
Square	3	0.000799	0.000266	2.66	0.159
Time*Time	1	0.000427	0.000427	4.27	0.094
pH*pH	1	0.000283	0.000283	2.83	0.154
Temperature*Temperature	1	0.000028	0.000028	0.28	0.620
2-Way Interaction	3	0.001125	0.000375	3.75	0.094
Time*pH	1	0.000484	0.000484	4.84	0.079
Time*Temperature	1	0.000625	0.000625	6.25	0.054
pH*Temperature	1	0.000016	0.000016	0.16	0.706
Error	5	0.000500	0.000100		
Lack-of-Fit	3	0.000252	0.000084	0.68	0.642
Pure Error	2	0.000248	0.000124		
Total	14	0.015760			

Model Summary

S	R-sq	R-sq(adj)	R-sq(pred)
0.01	96.83%	91.12%	70.87%

Coded Coefficients

Term	Effect	Coef	SE Coef	T-Value	P-Value	VIF
Constant		2.00800	0.00577	347.80	0.000	
Time	0.05000	0.02500	0.00354	7.07	0.001	1.00

pH	0.06200	0.03100	0.00354	8.77	0.000	1.00
Temperature	0.01800	0.00900	0.00354	2.55	0.052	1.00
Time*Time	0.02150	0.01075	0.00520	2.07	0.094	1.01
pH*pH	-0.01750	-0.00875	0.00520	-1.68	0.154	1.01
Temperature*Temperature	-0.00550	-0.00275	0.00520	-0.53	0.620	1.01
Time*pH	0.02200	0.01100	0.00500	2.20	0.079	1.00
Time*Temperature	0.02500	0.01250	0.00500	2.50	0.054	1.00
pH*Temperature	0.00400	0.00200	0.00500	0.40	0.706	1.00

Regression Equation in Uncoded Units

Po = 1.590 - 0.00708 Time + 0.1195 pH + 0.0006 Temperature + 0.000019 Time*Time
- 0.00875 pH*pH - 0.000110 Temperature*Temperature + 0.000458 Time*pH
+ 0.000104 Time*Temperature + 0.00040 pH*Temperature

Response Surface Regression: Uz versus Time, pH, Temperature

Analysis of Variance

Source	DF	Adj SS	Adj MS	F-Value	P-Value
Model	9	0.110970	0.012330	43.03	0.000
Linear	3	0.089922	0.029974	104.61	0.000
Time	1	0.000145	0.000145	0.50	0.509
pH	1	0.089465	0.089465	312.23	0.000
Temperature	1	0.000312	0.000312	1.09	0.344
Square	3	0.008897	0.002966	10.35	0.014
Time*Time	1	0.000196	0.000196	0.69	0.446
pH*pH	1	0.003061	0.003061	10.68	0.022
Temperature*Temperature	1	0.006449	0.006449	22.51	0.005
2-Way Interaction	3	0.012151	0.004050	14.14	0.007
Time*pH	1	0.008742	0.008742	30.51	0.003
Time*Temperature	1	0.001056	0.001056	3.69	0.113
pH*Temperature	1	0.002352	0.002352	8.21	0.035
Error	5	0.001433	0.000287		
Lack-of-Fit	3	0.001148	0.000383	2.69	0.283
Pure Error	2	0.000285	0.000142		
Total	14	0.112402			

Model Summary

S	R-sq	R-sq(adj)	R-sq(pred)
0.0169273	98.73%	96.43%	83.09%

Coded Coefficients

Term	Effect	Coef	SE Coef	T-Value	P-Value	VIF

Constant	0.69467	0.00977	71.08	0.000	
Time	0.00850	0.00425	0.00598	0.71	0.509	1.00
pH	0.21150	0.10575	0.00598	17.67	0.000	1.00
Temperature	-0.01250	-0.00625	0.00598	-1.04	0.344	1.00
Time*Time	0.01458	0.00729	0.00881	0.83	0.446	1.01
pH*pH	0.05758	0.02879	0.00881	3.27	0.022	1.01
Temperature*Temperature	0.08358	0.04179	0.00881	4.74	0.005	1.01
Time*pH	-0.09350	-0.04675	0.00846	-5.52	0.003	1.00
Time*Temperature	-0.03250	-0.01625	0.00846	-1.92	0.113	1.00
pH*Temperature	-0.04850	-0.02425	0.00846	-2.87	0.035	1.00

Regression Equation in Uncoded Units

Uz = 1.060 + 0.01666 Time - 0.058 pH - 0.0611 Temperature + 0.000013 Time*Time
+ 0.02879 pH*pH + 0.001672 Temperature*Temperature - 0.001948 Time*pH
- 0.000135 Time*Temperature - 0.00485 pH*Temperature

Response Surface Regression: Ne versus Time, pH, Temperature

Analysis of Variance

Source	DF	Adj SS	Adj MS	F-Value	P-Value
Model	9	0.032021	0.003558	10.64	0.009
Linear	3	0.029584	0.009861	29.50	0.001
Time	1	0.001404	0.001404	4.20	0.096
pH	1	0.023762	0.023762	71.07	0.000
Temperature	1	0.004418	0.004418	13.21	0.015
Square	3	0.000822	0.000274	0.82	0.536
Time*Time	1	0.000772	0.000772	2.31	0.189
pH*pH	1	0.000009	0.000009	0.03	0.878
Temperature*Temperature	1	0.000044	0.000044	0.13	0.731
2-Way Interaction	3	0.001615	0.000538	1.61	0.299
Time*pH	1	0.001332	0.001332	3.98	0.102
Time*Temperature	1	0.000240	0.000240	0.72	0.435
pH*Temperature	1	0.000042	0.000042	0.13	0.737
Error	5	0.001672	0.000334		
Lack-of-Fit	3	0.001359	0.000453	2.90	0.267
Pure Error	2	0.000313	0.000156		
Total	14	0.033693			

Model Summary

S	R-sq	R-sq(adj)	R-sq(pred)
0.0182848	95.04%	86.11%	33.38%

Coded Coefficients

Term	Effect	Coef	SE Coef	T-Value	P-Value	VIF
Constant		0.4547	0.0106	43.07	0.000	
Time	0.02650	0.01325	0.00646	2.05	0.096	1.00
pH	0.10900	0.05450	0.00646	8.43	0.000	1.00
Temperature	0.04700	0.02350	0.00646	3.64	0.015	1.00
Time*Time	-0.02892	-0.01446	0.00952	-1.52	0.189	1.01
pH*pH	0.00308	0.00154	0.00952	0.16	0.878	1.01
Temperature*Temperature	-0.00692	-0.00346	0.00952	-0.36	0.731	1.01
Time*pH	0.03650	0.01825	0.00914	2.00	0.102	1.00
Time*Temperature	-0.01550	-0.00775	0.00914	-0.85	0.435	1.00
pH*Temperature	-0.00650	-0.00325	0.00914	-0.36	0.737	1.00

Regression Equation in Uncoded Units

Ne = -0.175 - 0.00042 Time + 0.016 pH + 0.0207 Temperature - 0.000025 Time*Time
+ 0.00154 pH*pH - 0.000138 Temperature*Temperature + 0.000760 Time*pH
- 0.000065 Time*Temperature - 0.00065 pH*Temperature

Response Surface Regression: BL versus Time, pH, Temperature

Analysis of Variance

Source	DF	Adj SS	Adj MS	F-Value	P-Value
Model	9	0.139929	0.015548	6.65	0.025
Linear	3	0.092735	0.030912	13.22	0.008
Time	1	0.002665	0.002665	1.14	0.335
pH	1	0.087990	0.087990	37.63	0.002
Temperature	1	0.002080	0.002080	0.89	0.389
Square	3	0.024402	0.008134	3.48	0.107
Time*Time	1	0.001596	0.001596	0.68	0.446
pH*pH	1	0.013984	0.013984	5.98	0.058
Temperature*Temperature	1	0.007298	0.007298	3.12	0.138
2-Way Interaction	3	0.022792	0.007597	3.25	0.119
Time*pH	1	0.015376	0.015376	6.58	0.050
Time*Temperature	1	0.007396	0.007396	3.16	0.135
pH*Temperature	1	0.000020	0.000020	0.01	0.929
Error	5	0.011690	0.002338		
Lack-of-Fit	3	0.010006	0.003335	3.96	0.208
Pure Error	2	0.001685	0.000842		
Total	14	0.151620			

Model Summary

S	R-sq	R-sq(adj)	R-sq(pred)

0.0483537 92.29%   78.41%   0.00%

Coded Coefficients

Term	Effect	Coef	SE Coef	T-Value	P-Value	VIF
Constant		1.5687	0.0279	56.19	0.000	
Time	0.0365	0.0182	0.0171	1.07	0.335	1.00
pH	0.2097	0.1049	0.0171	6.13	0.002	1.00
Temperature	0.0323	0.0161	0.0171	0.94	0.389	1.00
Time*Time	0.0416	0.0208	0.0252	0.83	0.446	1.01
pH*pH	0.1231	0.0615	0.0252	2.45	0.058	1.01
Temperature*Temperature	-0.0889	-0.0445	0.0252	-1.77	0.138	1.01
Time*pH	0.1240	0.0620	0.0242	2.56	0.050	1.00
Time*Temperature	0.0860	0.0430	0.0242	1.78	0.135	1.00
pH*Temperature	-0.0045	-0.0023	0.0242	-0.09	0.929	1.00

Regression Equation in Uncoded Units

BL = 3.49 - 0.0315 Time - 0.867 pH + 0.0959 Temperature + 0.000036 Time*Time
+ 0.0615 pH*pH
    - 0.00178 Temperature*Temperature + 0.00258 Time*pH + 0.000358 Time*Temperature
    - 0.00045 pH*Temperature

Fits and Diagnostics for Unusual Observations

Obs	BL	Fit	Resid	Std Resid	
1	1.6390	1.5899	0.0491	2.03	R
4	1.7870	1.8361	-0.0491	-2.03	R

R Large residual

Response Surface Regression: xxy versus Time, pH, Temperature

Analysis of Variance

Source	DF	Adj SS	Adj MS	F-Value	P-Value
Model	9	0.639836	0.071093	6.95	0.023
Linear	3	0.563931	0.187977	18.37	0.004
Time	1	0.023112	0.023112	2.26	0.193
pH	1	0.530450	0.530450	51.83	0.001
Temperature	1	0.010368	0.010368	1.01	0.360
Square	3	0.027309	0.009103	0.89	0.507
Time*Time	1	0.004785	0.004785	0.47	0.524
pH*pH	1	0.023336	0.023336	2.28	0.191

Temperature*Temperature	1	0.000092	0.000092	0.01	0.928
2-Way Interaction	3	0.048597	0.016199	1.58	0.304
Time*pH	1	0.013924	0.013924	1.36	0.296
Time*Temperature	1	0.012769	0.012769	1.25	0.315
pH*Temperature	1	0.021904	0.021904	2.14	0.203
Error	5	0.051170	0.010234		
Lack-of-Fit	3	0.016604	0.005535	0.32	0.815
Pure Error	2	0.034566	0.017283		
Total	14	0.691007			

Model Summary

S	R-sq	R-sq(adj)	R-sq(pred)
0.101164	92.59%	79.27%	50.30%

Coded Coefficients

Term	Effect	Coef	SE Coef	T-Value	P-Value	VIF
Constant		0.9060	0.0584	15.51	0.000	
Time	0.1075	0.0538	0.0358	1.50	0.193	1.00
pH	0.5150	0.2575	0.0358	7.20	0.001	1.00
Temperature	-0.0720	-0.0360	0.0358	-1.01	0.360	1.00
Time*Time	0.0720	0.0360	0.0526	0.68	0.524	1.01
pH*pH	0.1590	0.0795	0.0526	1.51	0.191	1.01
Temperature*Temperature	-0.0100	-0.0050	0.0526	-0.09	0.928	1.01
Time*pH	0.1180	0.0590	0.0506	1.17	0.296	1.00
Time*Temperature	-0.1130	-0.0565	0.0506	-1.12	0.315	1.00
pH*Temperature	0.1480	0.0740	0.0506	1.46	0.203	1.00

Regression Equation in Uncoded Units

xxy = 6.33 - 0.0068 Time - 1.418 pH - 0.076 Temperature + 0.000063 Time*Time
+ 0.0795 pH*pH
- 0.00020 Temperature*Temperature + 0.00246 Time*pH - 0.000471 Time*Temperature
+ 0.0148 pH*Temperature

Optimization Plot

Contour Plot of Gw, Mo, and Ug,-Responses vs pH, Time(hrs)

Contour Plot of Gw, Mo and Ug,-Responses vs Temperature, Time(hrs)

Contour Plot of Gw, Mo, and Ug-Responses vs Temperature, pH

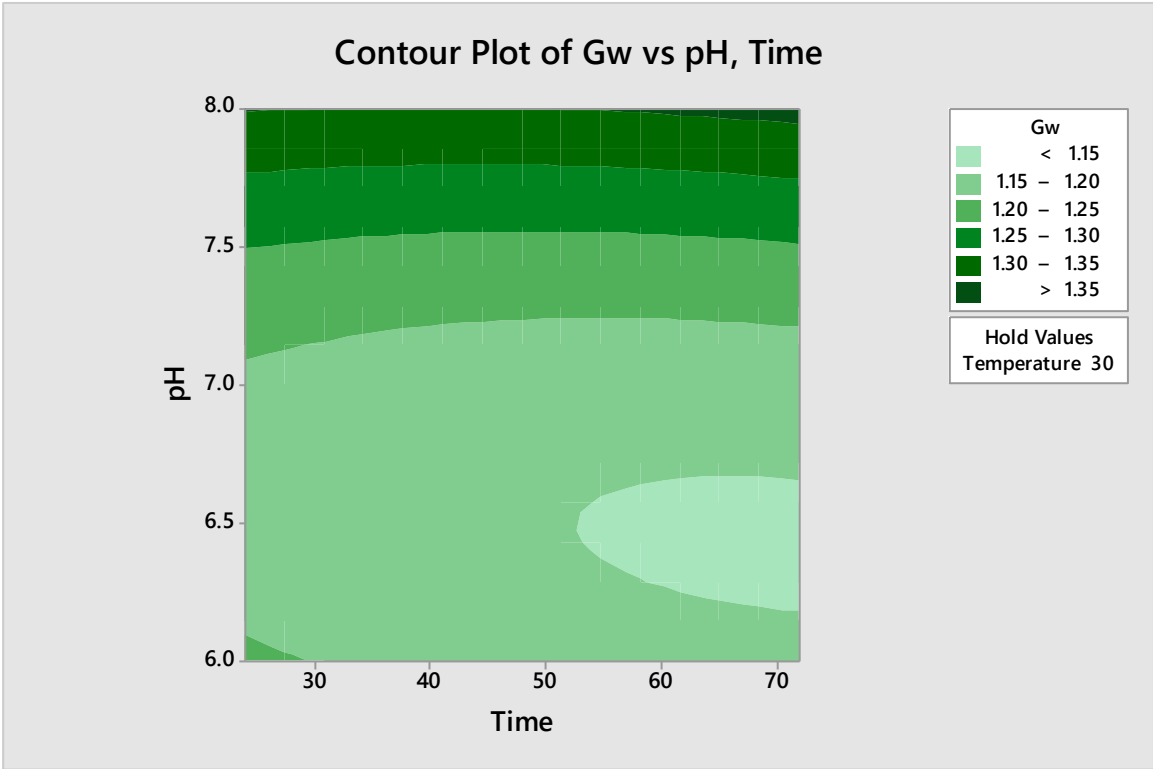
Contour Plot of Gw vs pH, Time
8.0
7.5
7.0
6.5
6.0
pH
30
40
50
60
70
Time
Gw
< 1.15
1.15 – 1.20
1.20 – 1.25
1.25 – 1.30
1.30 – 1.35
> 1.35
Hold Values
Temperature 30

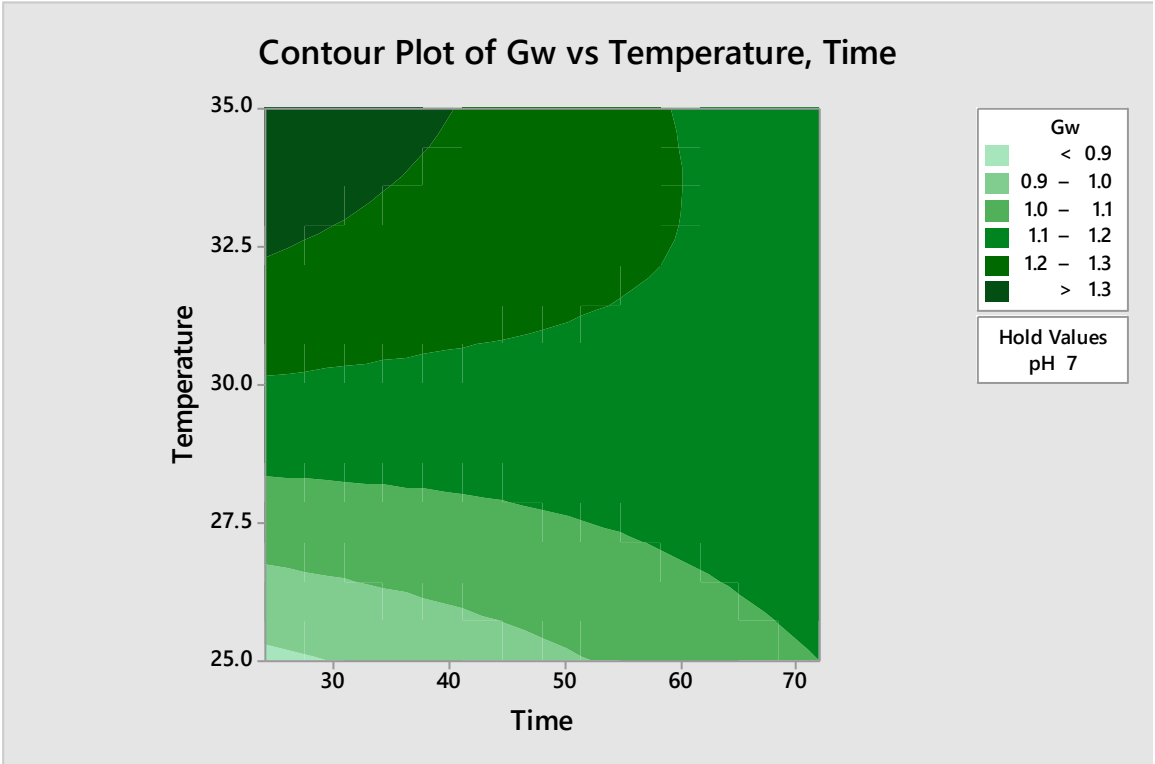
Contour Plot of Gw vs Temperature, Time
35.0
32.5
30.0
27.5
25.0
Temperature
30
40
50
60
70
Time
Gw
< 0.9
0.9 – 1.0
1.0 – 1.1
1.1 – 1.2
1.2 – 1.3
> 1.3
Hold Values
pH 7

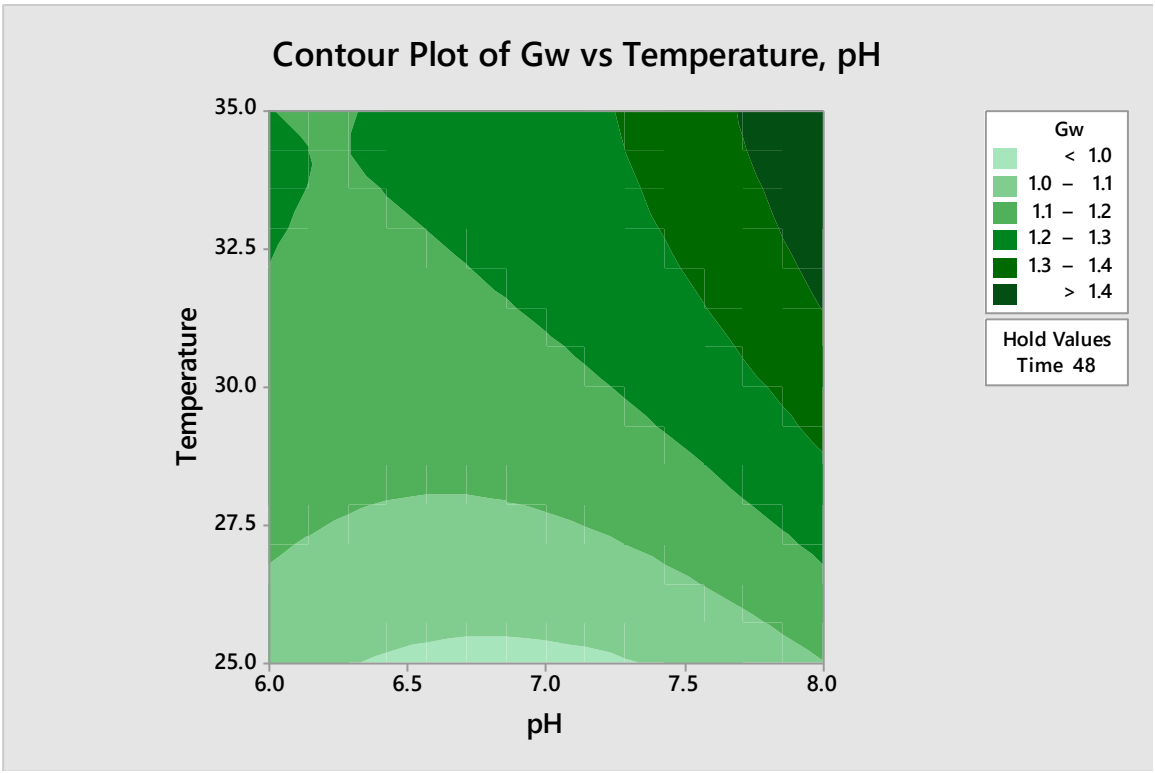
Contour Plot of Gw vs Temperature, pH
Temperature
35.0
32.5
30.0
27.5
25.0
6.0
6.5
7.0
7.5
8.0
pH
Gw
< 1.0
1.0 – 1.1
1.1 – 1.2
1.2 – 1.3
1.3 – 1.4
> 1.4
Hold Values
Time 48

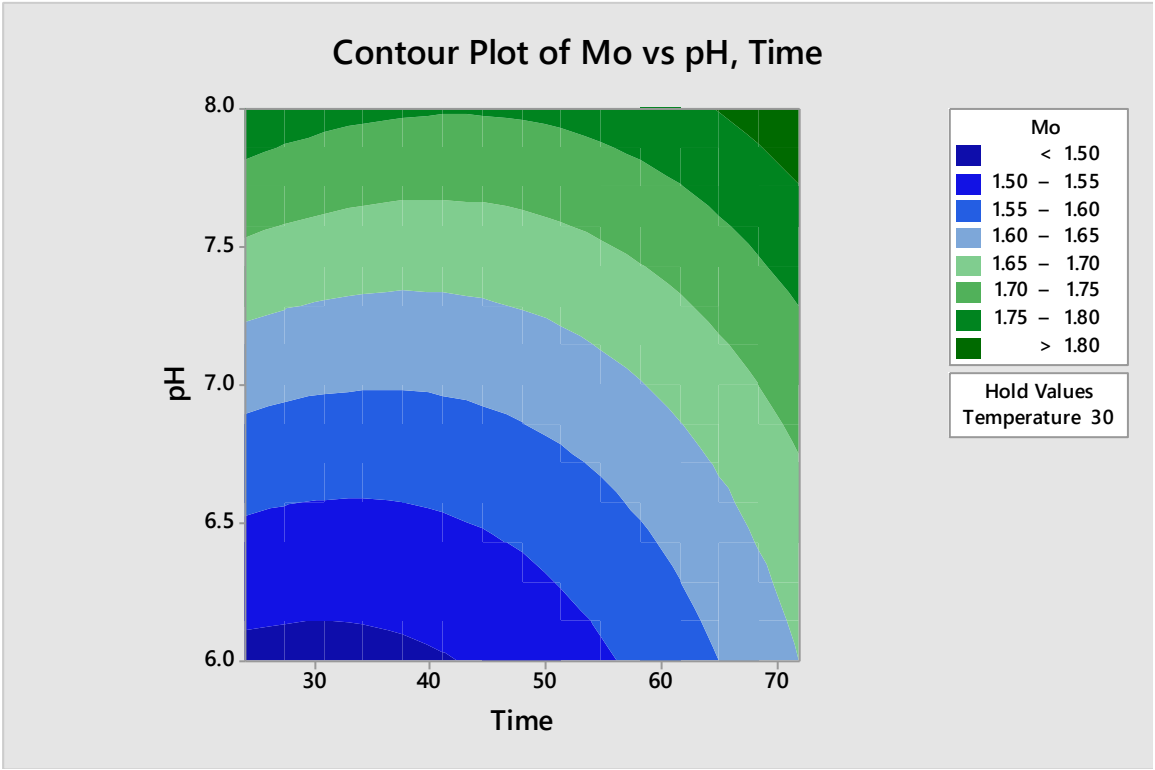
Contour Plot of Mo vs pH, Time
pH
8.0
7.5
7.0
6.5
6.0
30
40
50
60
70
Time
Mo
< 1.50
1.50 – 1.55
1.55 – 1.60
1.60 – 1.65
1.65 – 1.70
1.70 – 1.75
1.75 – 1.80
> 1.80
Hold Values
Temperature 30

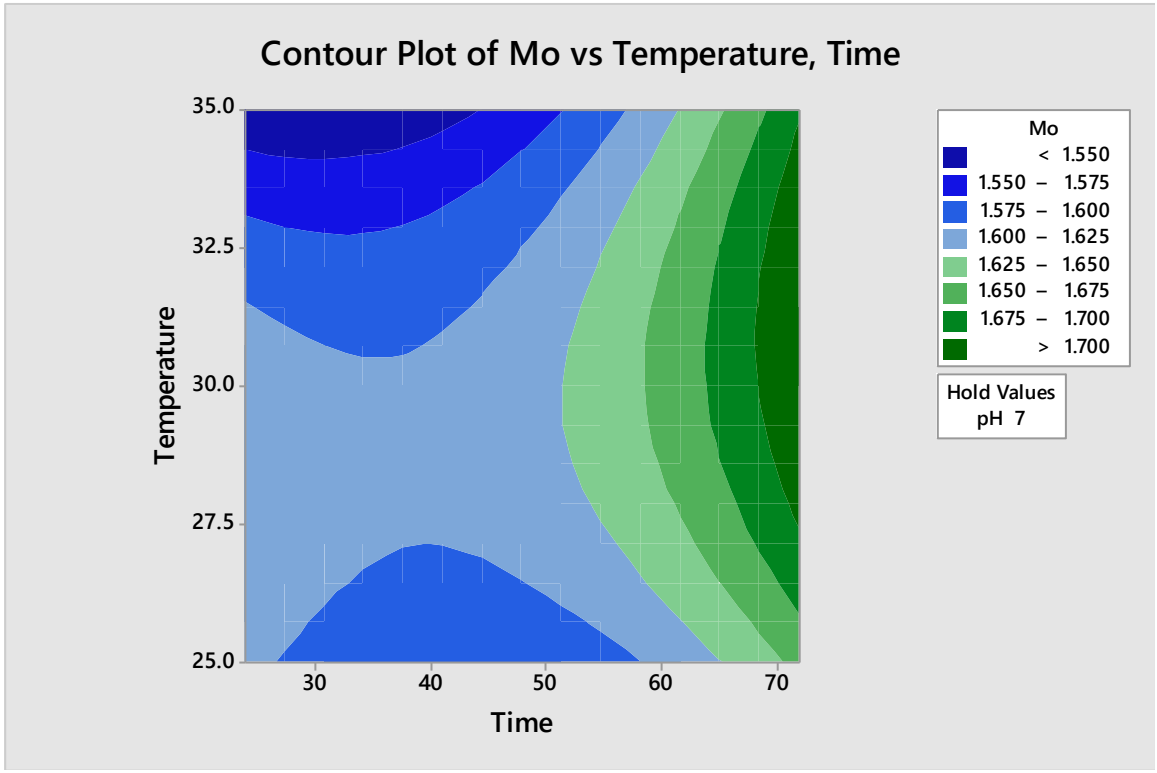
Contour Plot of Mo vs Temperature, Time
Temperature
Time
35.0
32.5
30.0
27.5
25.0
30
40
50
60
70
Mo
< 1.550
1.550 – 1.575
1.575 – 1.600
1.600 – 1.625
1.625 – 1.650
1.650 – 1.675
1.675 – 1.700
> 1.700
Hold Values
pH 7

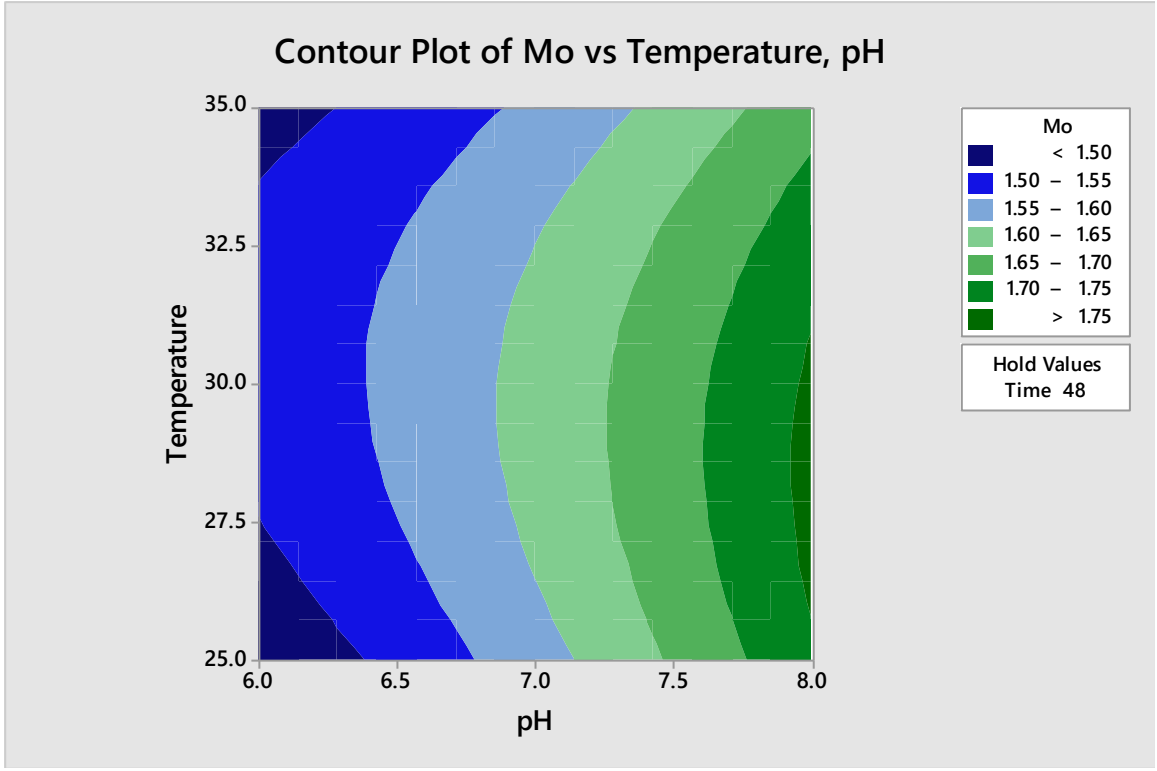
Contour Plot of Mo vs Temperature, pH
Temperature
pH
35.0
32.5
30.0
27.5
25.0
6.0
6.5
7.0
7.5
8.0
Mo
< 1.50
1.50 – 1.55
1.55 – 1.60
1.60 – 1.65
1.65 – 1.70
1.70 – 1.75
> 1.75
Hold Values
Time 48

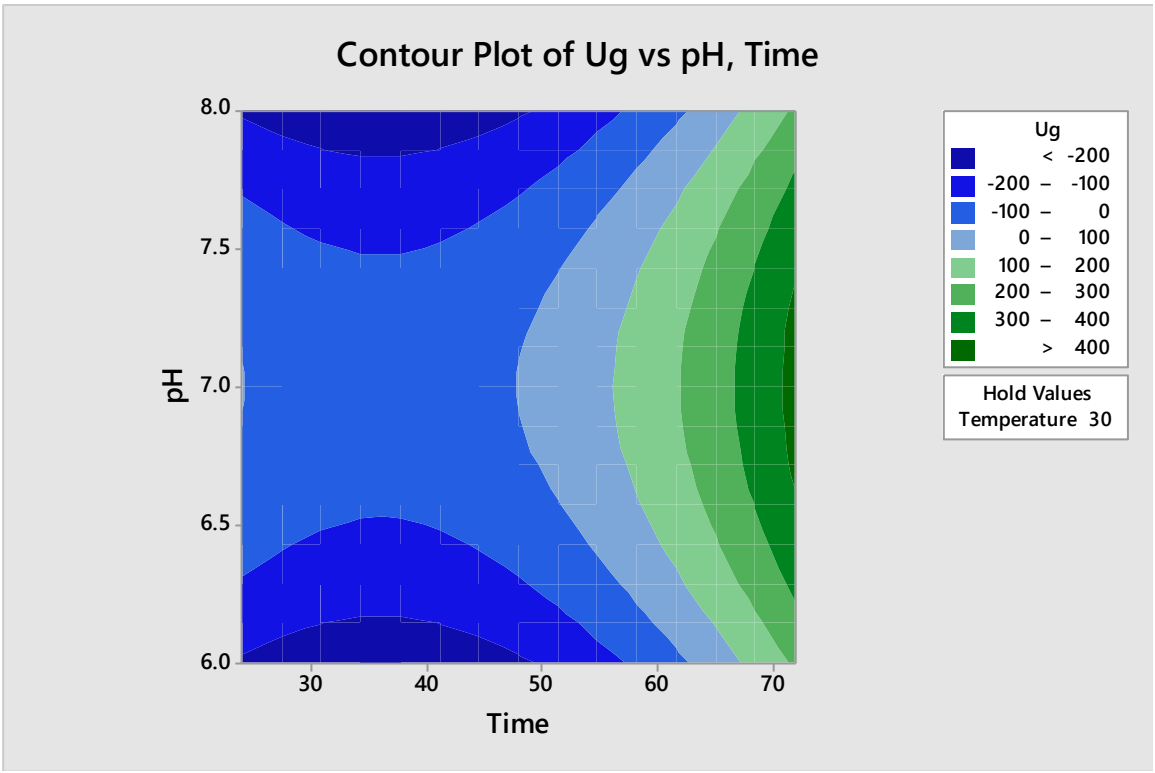
Contour Plot of Ug vs pH, Time
8.0
7.5
7.0
6.5
6.0
pH
30
40
50
60
70
Time
Ug
< -200
-200 – -100
-100 – 0
0 – 100
100 – 200
200 – 300
300 – 400
> 400
Hold Values
Temperature 30

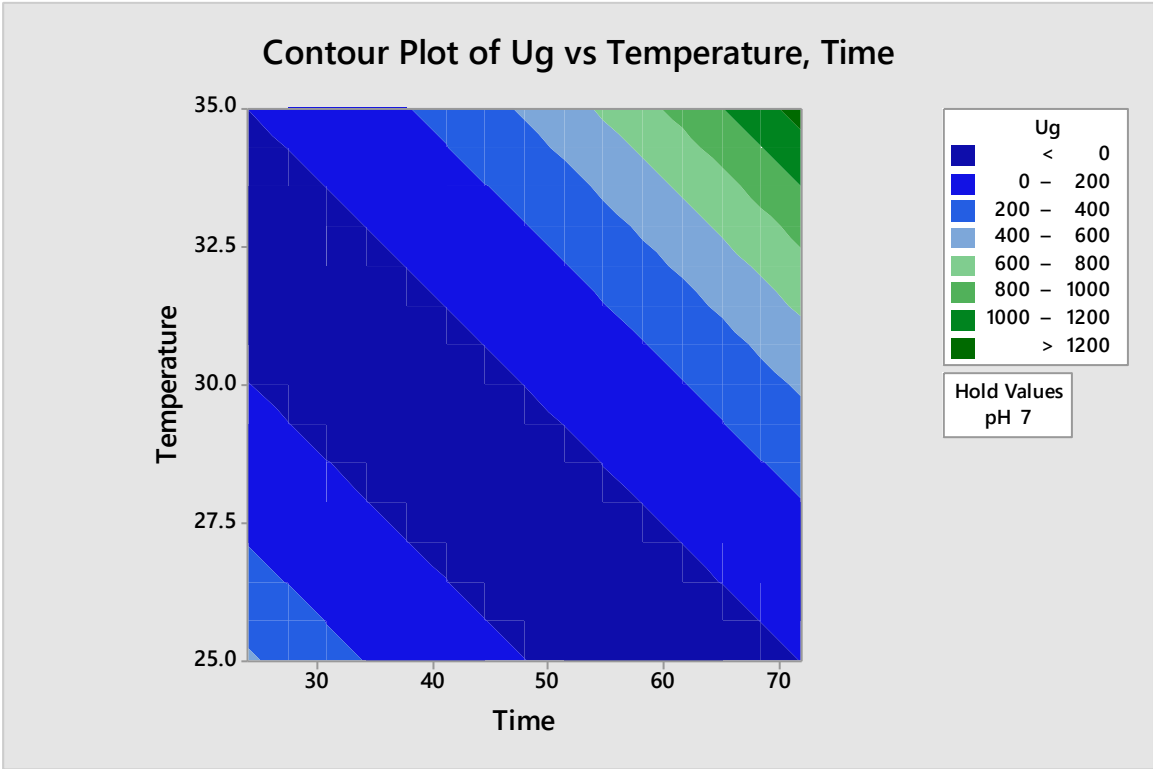
Contour Plot of Ug vs Temperature, Time
35.0
32.5
30.0
27.5
25.0
Temperature
30
40
50
60
70
Time
Ug
< 0
0 – 200
200 – 400
400 – 600
600 – 800
800 – 1000
1000 – 1200
> 1200
Hold Values
pH 7

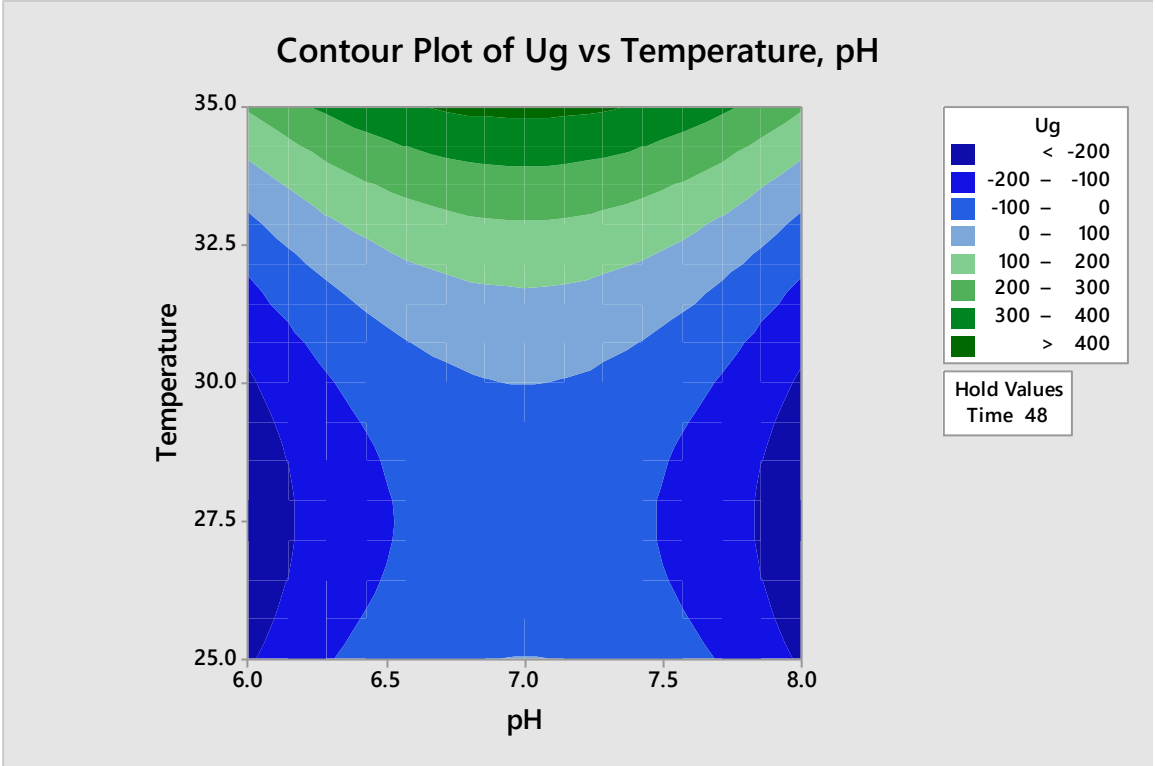
Contour Plot of Ug vs Temperature, pH
Temperature
35.0
32.5
30.0
27.5
25.0
6.0
6.5
7.0
7.5
8.0
pH
Ug
< -200
-200 – -100
-100 – 0
0 – 100
100 – 200
200 – 300
300 – 400
> 400
Hold Values
Time 48

LEAF SAMPLE

158

PLANT EXTRACT AFTER CENTRUFUGATION

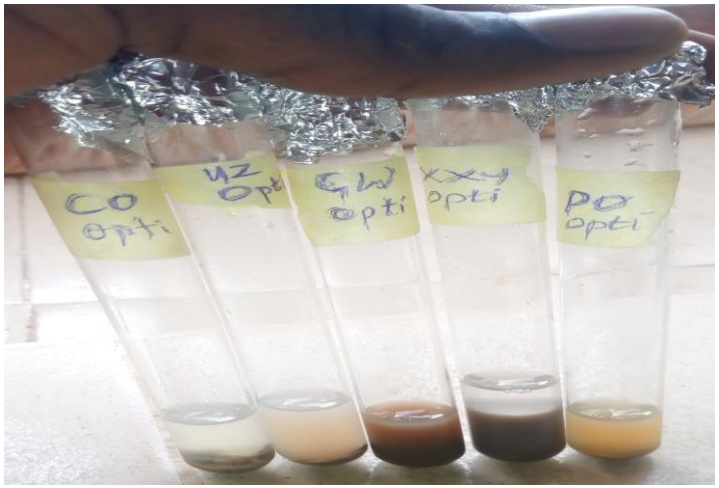

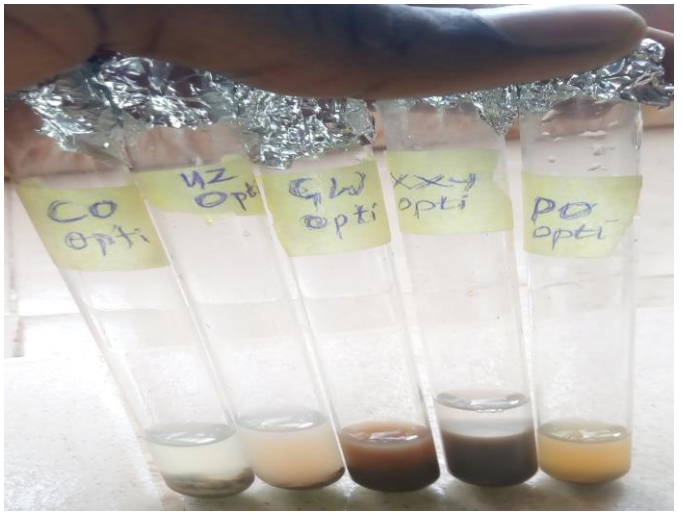

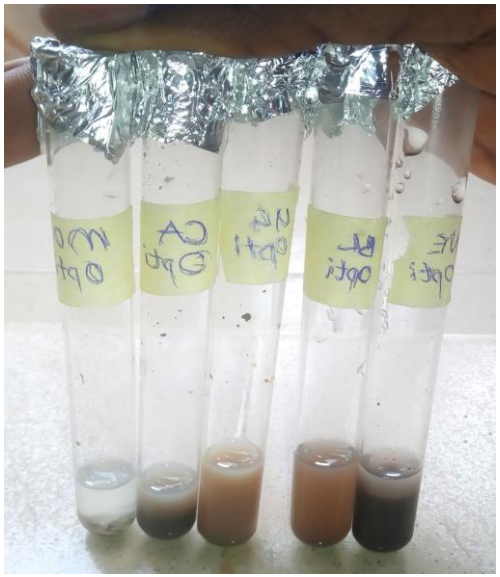

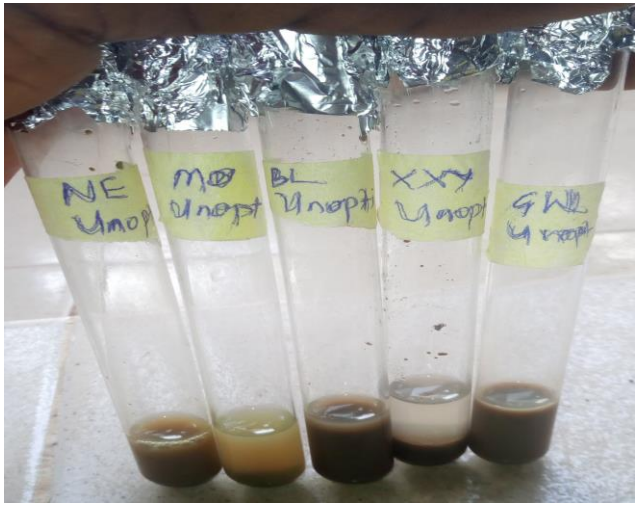

INITIAL COLOR AFTER MIXING

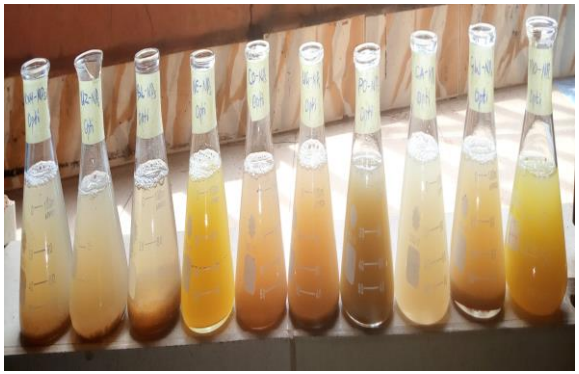

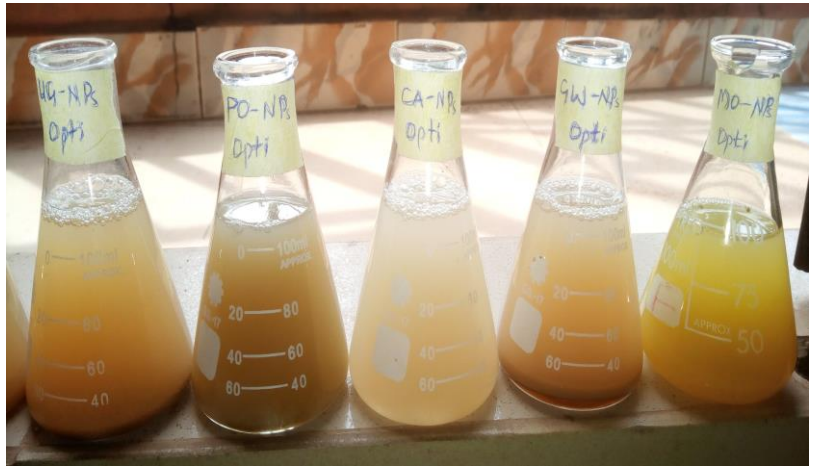


UZ-NPs
Opti
BL-NPs
Opti
NE-NPs
Opti

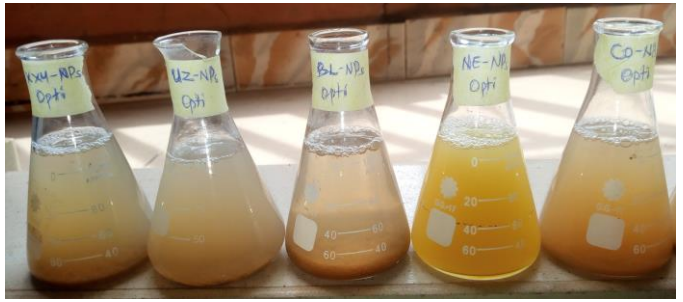
UZ-NPs
Opti
BL-NPs
Opti
NE-NPs
Opti

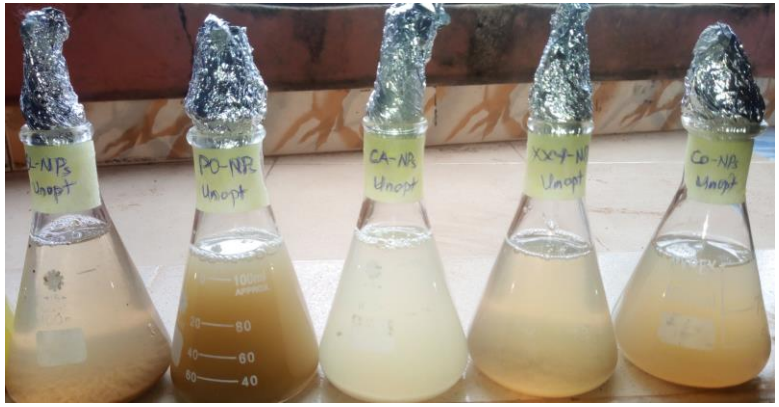
PO-NPs
Unopt
CA-NPs
Unopt
Co-NPs
Unopt


PO-NPs
Unopt
CA-NPs
Unopt
Co-NPs
Unopt


UG-NPs
Unopt
UZ-NPs
Unopt
MO-NPs
Unopt


UG-NPs
Unopt
UZ-NPs
Unopt
MO-NPs
Unopt

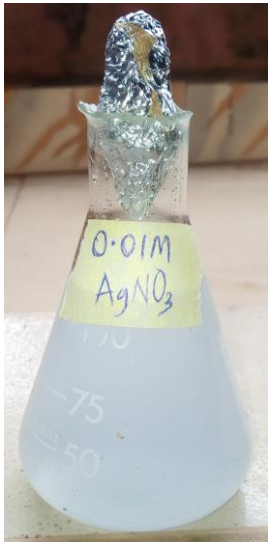
0·01M
$AgNO_3$


0·01M
$AgNO_3$

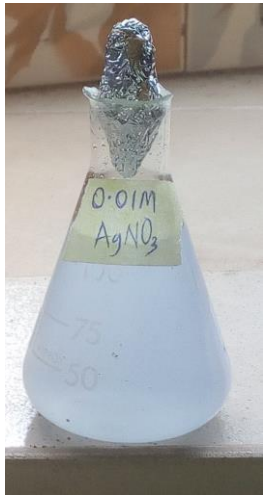
0·01M
$AgNO_3$


UZ-NR
Opti
CO-NR
Opti

ANTIBACTERIAL ACTIVITY

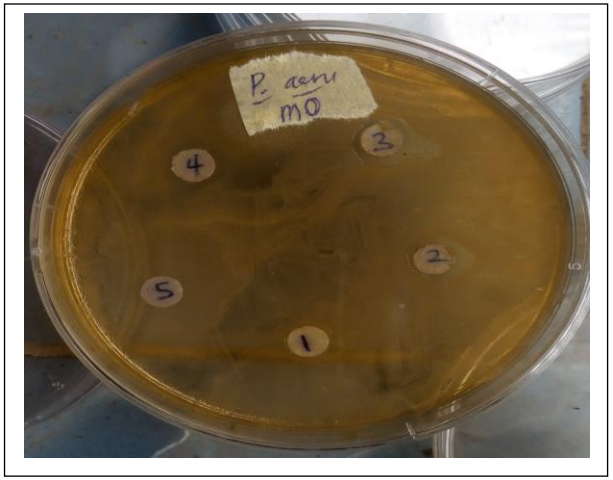

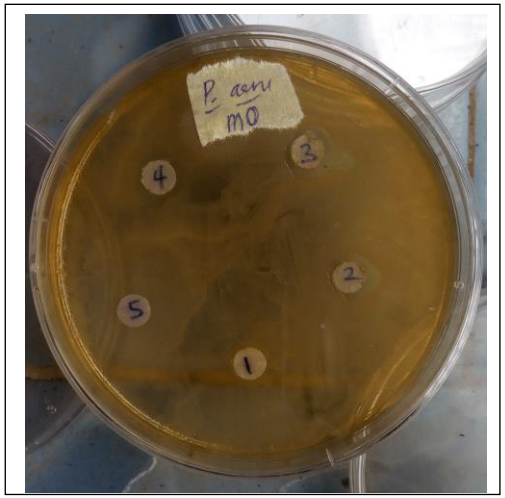

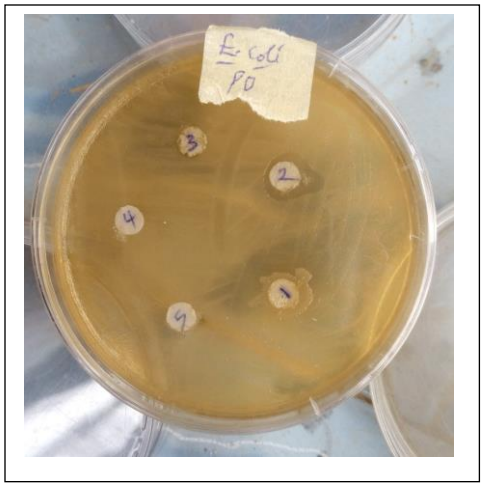
E. coli
PO
3
2
4
1
5

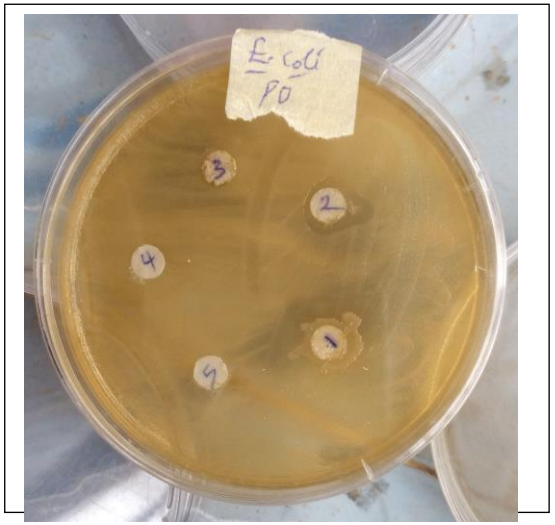
E. coli
PO
3
2
4
1
5

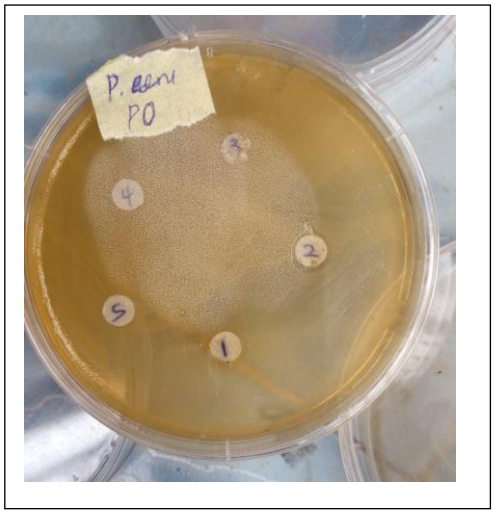
P. aeru
PO
3
4
2
5
1

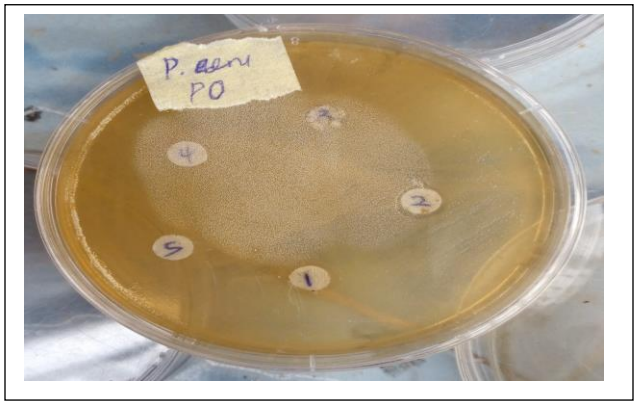
P. aeru
PO
3
4
2
5
1

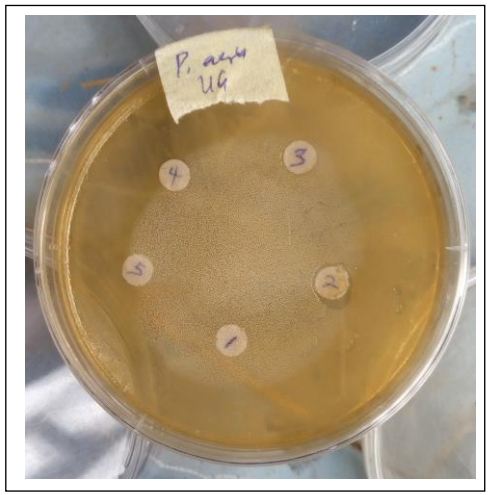
P. aeru
UG
4
3
5
2
1


P. aeru
UG
4
3
5
2
1


E. coli
UG
4
3
5
2
1

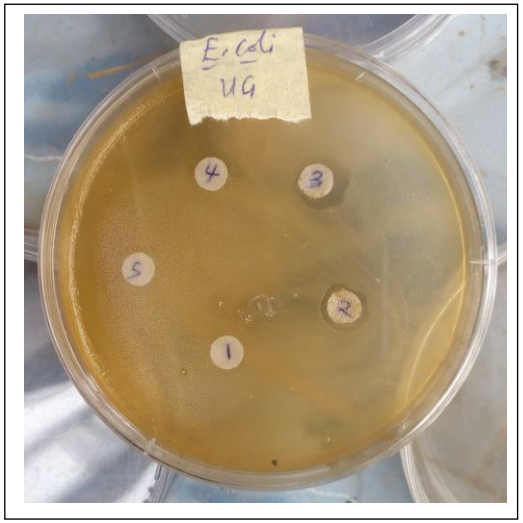
E. coli
UG
4
3
5
2
1

EXTRACTION AND RAW EXTRACT